Master of Science in Civil Engineering

Future projection of climate extremes in Bangladesh: Insights from CMIP6 Multi-Model Ensemble

Submitted by

Fuad Bin Nazrul

191051016

Supervised by

Dr. Md. Rezaul Karim

Professor, Department of Civil and Environmental Engineering,

Islamic University of Technology

Co-supervised by

Dr. Mohammad Kamruzzaman

Senior Scientific Officer,

Farm Machinery and Postharvest Technology Division,

Bangladesh Rice Research Institute

Department of Civil and Environmental Engineering

Islamic University of Technology

Gazipur-1704, Bangladesh

June 2025

Future projection of climate extremes in Bangladesh: Insights from CMIP6 Multi-Model Ensemble

A dissertation submitted to the Department of Civil and Environmental Engineering (CEE) in partial fulfillment of the requirements for the degree of

MASTER OF SCIENCE (M.Sc.) IN CIVIL ENGINEERING

by

Fuad Bin Nazrul

Student No.: 191051016

June 2025

Recommendation of the Board of Examiners

The thesis titled **"Future projection of climate extremes in Bangladesh: Insights from CMIP6 Multi-Model Ensemble"** submitted by Fuad Bin Nazrul, Student ID 191051016 of Academic Year 2019-2020 has been found as satisfactory and accepted as partial fulfillment of the requirement for the degree of Master of Science in Civil Engineering.

1. ____________________

Dr. Md. Rezaul Karim
Professor
Department of Civil and Environmental Engineering,
Islamic University of Technology (IUT), Board Bazar, Gazipur-1704.

Chairman (Supervisor)

2. ____________________

Dr. Mohammad Kamruzzaman
Senior Scientific Officer
Farm Machinery and Postharvest Technology Division, Bangladesh Rice Research Institute, (BRRI), Gazipur- 1701

Member (Co-supervisor)

3. ____________________

Dr. Shakil Mohammad Rifaat
Professor and Head
Department of Civil and Environmental Engineering,
Islamic University of Technology (IUT), Board Bazar, Gazipur-1704.

Member (Ex-Officio)

4. ____________________

Dr. Amimul Ahsan
Associate Professor
Department of Civil and Environmental Engineering,
Islamic University of Technology (IUT), Board Bazar, Gazipur-1704.

Member

5. ____________________

Dr. Sara Nowreen
Professor
Institute of Water and Flood Management (IWFM),
Bangladesh University of Engineering and Technology (BUET), Dhaka-1000

Member (External)

Declaration of Candidate

It is hereby declared that this thesis has not been submitted elsewhere for the award of any Degree or Diploma.

FUAD BIN NAZRUL

Name of Candidate:
Fuad Bin Nazrul
Student No.: 191051016
Academic Year: 2019-2020
Date: 31/07/25

Name of Supervisor:
Dr. Md. Rezaul Karim
Professor
Department of Civil and Environmental Engineering (CEE), Islamic University of Technology,
Board Bazar, Gazipur 1704.
Date: 31/7/25

31.07.2025

Name of Co-supervisor:
Dr. Mohammad Kamruzzaman
Senior Scientific Officer
Farm Machinery and Postharvest Technology Division,
Bangladesh Rice Research Institute, Gazipur-1701.
Date: 31.07.2025

Dedication

This thesis is dedicated to my beloved parents, family, teachers, and friends, whose unwavering support and encouragement have been my greatest strength.

I extend my deepest gratitude to my esteemed supervisor, Professor Dr. Md. Rezaul Karim, and my co-supervisor, Dr. Mohammad Kamruzzaman, for their invaluable guidance and mentorship throughout this journey.

This work is a humble token of appreciation for all who stood by me, inspired me, and believed in my abilities as I pursued my goals to the very end.

Acknowledgements

Glory and praise be to Almighty Allah, the Almighty, for granting me the strength, perseverance, and courage to successfully complete my M.Sc. thesis. Verily, there is no strength except with Allah.

I would like to express my heartfelt gratitude and appreciation to my thesis supervisor, Prof. Dr. Md. Rezaul Karim, and co-supervisor, Dr. Mohammad Kamruzzaman, for their generous guidance, invaluable advice, and unwavering support throughout the course of this study. I am also deeply thankful to Prof. Dr. Sara Nowreen, Prof. Dr. Shakil Mohammad Rifaat, and Associate Prof. Dr. Amimul Ahsan, who graciously took the time to review my thesis and provide their insightful feedback.

Finally, I am deeply grateful to my beloved parents, Md. Nazrul Islam and Rezina Afrose, as well as to my elder brother and sister-in-law, for their unwavering love, care, and encouragement. Their constant support has been the foundation of my strength throughout this journey. I am profoundly grateful to my well-wishers, especially Mussadik Hossain, Daud Nabi Hridoy, Sultan Al Shafian, Md. Habibur Rahman Bejoy Khan, Mohammad Zunaid Bin Harun, Niaz Ahmed, Farhan Anjum Badhon, Anika Tahsin Nabila, and Tahmeed Ahmed, whose patience and love have been a source of comfort and motivation during challenging times.

Table of Contents

List of Figures

List of Tables

List of Abbreviations

Abbreviation	**Full Form**
AI	Artificial Intelligence
ANN	Artificial Neural Network
ArcGIS	Geographic Information System Software
BMA	Bayesian Model Averaging
BMD	Bangladesh Meteorological Department
CC	Correlation Coefficient
CDD	Consecutive Dry Days (precipitation <1 mm)
CDF	Cumulative Distribution Function
CMIP5	Coupled Model Intercomparison Project Phase 5
CMIP6	Coupled Model Intercomparison Project Phase 6
CRU	Climatic Research Unit
CSDI	Cold Spell Duration Index
CWD	Consecutive Wet Days (precipitation 1 mm)
DTR	Diurnal Temperature Range
ECMWF	European Centre for Medium-Range Weather Forecasts
ELM	Extreme Learning Machine
ERA5	Fifth Generation ECMWF Reanalysis
ETCCDI	Expert Team on Climate Change Detection and Indices
GCM	Global Climate Model (or General Circulation Model)
GHG	Greenhouse Gas
IPCC	Intergovernmental Panel on Climate Change
ML	Machine Learning
MME	Multi-Model Ensemble

MS Excel	Microsoft Excel
NCAR	National Center for Atmospheric Research
NCEP	National Centers for Environmental Prediction
NSE	Nash-Sutcliffe Efficiency
PRCPTOT	Total annual precipitation from wet days
R	R Programming Language
R10mm	Number of days with precipitation 10 mm
R20mm	Number of days with precipitation 20 mm
R95p	Total precipitation from days >95th percentile
R99p	Total precipitation from days >99th percentile
R^2	Coefficient of Determination
RCM	Regional Climate Model
RF	Random Forest
RMSD	Root Mean Square Deviation
rSQM	R package for Simple Quantile Mapping
RX1day	Annual maximum 1-day precipitation
RX5day	Annual maximum consecutive 5-day precipitation
SAM	Simple Arithmetic Mean
SDII	Simple Daily Intensity Index
SPSS	Statistical Package for the Social Sciences
SQM	Simple Quantile Mapping
SSP	Shared Socioeconomic Pathway
SSP1-2.6	Sustainability-focused low-emission scenario
SSP2-4.5	Intermediate emission scenario
SSP5-8.5	High-emission fossil-fueled development scenario

SU	Summer Days (TX > 25°C)
SVM	Support Vector Machine
TN10p	Percentage of days when TN < 10th percentile
TN90p	Percentage of days when TN > 90th percentile
TNn	Annual minimum of daily minimum temperature
TNx	Annual maximum of daily minimum temperature
TX10p	Percentage of days when TX < 10th percentile
TX90p	Percentage of days when TX > 90th percentile
TXn	Annual minimum of daily maximum temperature
TXx	Annual maximum of daily maximum temperature
WSDI	Warm Spell Duration Index

List of Notations

Symbol	Description
$x'_p(t)$	Bias-corrected future projections at day t
$F()$	Cumulative distribution function (CDF) of the daily data
$F^{-1}()$	Cumulative distribution function (CDF) of the daily inverse data
$\circ$	Degree
$S(t)$	Ensemble mean at time t
$p.sim$	Future projections simulations
$x_p(t)$	Initial future projections at day t
obs	Observed daily data
mm	Millimeter
%	Percent
$P_n(t)$	Projection output from the n-th GCM at time t
$r.sim$	Retrospective simulations
$\sum$	Summation
t	Time period
N	Total number of GCMs used

Abstract

Bangladesh is increasingly vulnerable to extreme climate events, which are significant threats to the environmental and social resilience. This study investigates future changes in climate extreme indices over Bangladesh (including temperature and precipitation extremes) based on ETCCDI (Expert Team on Climate Change Detection and Indices) indices. For the assessment of future temperature and precipitation extremes, a Multi-Model Ensemble approach was carried out for 18 bias-corrected Global Climate Models (GCMs) of the Coupled Model Intercomparison Project Phase 6 (CMIP6). Projections were made for near future (2015–2044), mid future (2045–2074), and far future (2075–2100) scenarios, following the Shared Socioeconomic Pathways (SSPs) SSP1-2. 6, SSP2-4. 5, and SSP5-8. 5 (bias-corrected) and validated against the fifth generation of ECMWF Re-Analysis (ERA5). A comparison with a historical baseline period (1985–2014) revealed substantial regional disparities in projected climate extremes. By integrating these advanced tools, the research aims to provide a spatially and temporally detailed assessment of future climate extremes, contributing valuable insights to support evidence-based adaptation planning and policy formulation for enhancing climate resilience in Bangladesh. Specially under SSP5-8.5, the results suggest that the period 2075-2100 is expected to experience the highest precipitation and temperature extremes, with an annual maximum temperature (TXx) increase of 5.12°C and an annual minimum temperature (TNn) of 5.49°C. The southwestern region is projected to experience relatively fewer extreme temperature events than other areas, with the most significant warming occurring in the south-to-southeast corridor rather than the lower part of Bangladesh in all future scenarios. Warm spells, like Summer Days (SU), are expected to rise even more up to 84 days with more influence the northeastern region in the very far future. Under all SSPs, Consecutive Dry Days (CDD) are anticipated to reduce substantially, particularly in the north to northwestern part of Bangladesh, due to a pronounced increase in annual total precipitation percentage in the northwest. However, very heavy precipitation days (R20 mm) are projected to increase in the north to northeast, up to approximately 18 days under SSP5-8.5. This study reveals significant spatial differences in temperature and precipitation extreme indices, with a forecasted rise in both the strength and frequency of climate extremes over time.

These insights highlight significant requirements for the development of focused adaptation strategies to enhance resilience in regions vulnerable to emerging climate risks in Bangladesh. The findings emphasize the necessity for climate adaptation policies, including improved flood management, heat adaptation strategies, and climate-resilient agricultural practices. Future research should focus on refining climate model projections and integrating socio-economic factors to develop comprehensive adaptation strategies for Bangladesh’s most vulnerable regions.

Chapter 1
Introduction

1.1 Background

Climate change is one of the greatest global challenges, significantly influencing environmental systems, human livelihoods, and socio-economic stability (Filho, 2015). It amplifies the occurrence and severity of extreme weather events, alters climate patterns, and disrupts ecological and agricultural systems worldwide (Filho, 2015). According to the Climate Risk Index 2025 between 1993 and 2022, extreme weather events claimed over 765,000 lives globally and caused direct economic losses amounting to nearly USD 4.2 trillion (inflation-adjusted), spanning more than 9,400 recorded incidents (Adil et al., 2025). Bangladesh is among the most climate-vulnerable countries globally due to its tropical monsoon climate, low-lying deltaic geography, and high population density (Eckstein et al., 2021). Global center on adaptation states that Bangladesh remains one of the most climate-vulnerable nations, ranking 9th in the World Risk Index 2023 (Karim et al. 2024). In the Climate Risk Index (CRI) 2025 by Germanwatch, Bangladesh is placed 31st globally for the period 1993–2022 (Adil et al. 2025). However, according to the Bangladesh State of Gender Equality and Climate Change Report (UN Women & Ministry of Environment, Forest and Climate Change, 2022) and Climate Change Initiatives of Bangladesh Towards Climate Resilience (Ministry of Environment, Forest and Climate Change, 2023), earlier assessments reveal a more alarming trend: Bangladesh ranked 9th in terms of annual fatalities and 7th overall in the Long-Term Climate Risk Index (CRI) for the period 2000–2019, underscoring its repeated and severe exposure to climate-induced disasters. The intensifying impacts of climate change expose Bangladesh to recurrent extreme events, such as heavy rainfall, floods, droughts, cyclones, and rising temperatures, which pose significant threats to food security, water resources, infrastructure, and public health (Imran et al., 2023.; National Adaptation Plan of Bangladesh (2023-2050), 2022; Paul & Maity, 2023).

Over recent decades, climate extremes have become increasingly severe, and studies predict a continued rise in their frequency and intensity as global temperatures increase (Akter et al., 2024; Hasan et al., 2018). Climate extremes are classified as rare meteorological events that occur at the upper and lower tails of climate variable probability distributions, representing the most severe deviations from historical climate conditions (Zwiers et al., 2013). In temperature distributions, extreme events such as prolonged heatwaves or unusually cold days correspond to the distribution's extremes, while precipitation extremes include both heavy rainfall and drought conditions (Peterson et al., 2008.; Zhang et al., 2011). These extremes have intensified due to global warming, resulting in increased risks of severe weather phenomena, including heatwaves, wildfires, heavy precipitation, floods, and altered hydrological cycles (Seneviratne et al., 2012; Ummenhofer & Meehl, 2017).

Global surface temperature records indicate that the decade from 2011 to 2020 was, on average, 1.09°C warmer than the pre-industrial period (1850–1900), with an uncertainty range of 0.95–1.20°C (IPCC, 2021). In 2023, global surface temperatures reached record highs, with an estimated global average near-surface temperature 1.45°C (±0.12°C) above pre-industrial levels (WMO, 2024). In Bangladesh, these rising temperatures have been accompanied by increasing climate extremes. Research has documented an increasing frequency and intensity of extreme rainfall events, with more heavy precipitation days and a significant reduction in consecutive dry days (Basher et al., 2018; Hasan et al., 2018; Khan et al., 2020; Mallick et al., 2022a). Temperature-related indices indicate a distinct warming trend, with both maximum temperatures (T_{max}) and minimum temperatures (T_{min}) rising at an accelerating rate, further exacerbating regional climate variability (Islam et al., 2021; Mallick et al., 2022a; Rahman et al., 2024).

Extreme climate events in Bangladesh have led to catastrophic consequences, including record-breaking heatwaves and devastating flash floods. The Flood Forecasting and Warning Center (FFWC) reported that in June 2022, over 94% of Sunamganj and more than 84% of Sylhet were submerged by flash floods, illustrating the increasing threats posed by climate extremes (UNICEF Bangladesh, 2022 ;URL: https://www.ffwc.gov.bd). Future climate change is expected to exacerbate these hazards, affecting nearly all socio-economic sectors, including agriculture, water supply, and public infrastructure (Islam et al., 2024; Islam et al., 2021; Rahman et al., 2023). Back in 2010 the Insurance Development and Regulatory Authority (IDRA) estimates that Bangladesh lost 0.5 to 1% annually of its Gross Domestic Product (GDP) due to climate-induced natural disasters, underscoring the economic vulnerability of the country (General Economics Division, 2020). The current loss in GDP is 1.3% which may increase up to 2% in the end of 2050 (National Adaptation Plan of Bangladesh (2023-2050), 2022).

Observational climate data sources used to study extreme weather and climate events include conventional meteorological observations, satellite-based datasets, and atmospheric reanalysis datasets (Gao et al., 2018; Wang et al., 2023; Xu et al., 2022). Among these, (Dee et al., 2011; L. Gao et al., 2018; Gao et al., 2018; Hersbach et al., 2020; Nazrul et al., 2025 Kistler et al., 2001.). Reanalysis datasets widely used in climate research include NCEP-NCAR (Dai et al., 2001; Kalnay et al., 2018; Saha et al., 2010), CFSR and CFSv2 (Roundy et al., 2014; Saha et al., 2014; Yuan et al., 2011), Japan's JRA-25 and JRA-55 (Harada et al., 2016; Kobayashi et al., 2014), and (Branković & Molteni, 2004; Dee et al., 2011; Hersbach et al., 2020; van Oldenborgh et al., 2005). ERA5 (ECMWF's fifth-generation reanalysis), one of the latest datasets, features advanced 4DVAR analysis and broader data assimilation, making it the most accurate for representing atmospheric and surface conditions (Albergel et al., 2018; B. Bell et al., 2021; Hersbach et al., 2020; Lavers et al., 2022; Olauson, 2018; Tarek et al., 2020; Urraca et al., 2018). ERA5 has been widely adopted in climate studies specific to Bangladesh due to its high accuracy in temperature and rainfall trend analysis, confirming its utility for extreme climate studies (Ali et al., 2024; Islam & Cartwright, 2020; Koutavarapu et al., 2021; Tabassum et al., 2024).

Future climate projections rely on Global Climate Models (GCMs), which are critical tools for assessing both historical and future climate conditions (Jihan et al., 2025). GCMs play a pivotal role in the Intergovernmental Panel on Climate Change (IPCC) assessment reports, providing essential insights into long-term climate changes (Donat et al., 2020; Lorenz et al., 2016; Parker, 2024; Seneviratne & Hauser, 2020; Stocker, 2011). Among these, the Coupled Model Intercomparison Project Phase 6 (CMIP6) is the latest framework for future climate projections, incorporating improved spatial resolutions, enhanced process representations, and new socioeconomic emission pathways, known as the Shared Socioeconomic Pathways (SSPs) (Alamgir et al., 2019; Chen et al., 2022; Mesgari et al., 2022). CMIP6 integrates SSPs to analyze future climate changes based on different levels of greenhouse gas emissions, societal responses, and economic trajectories (Almazroui et al., 2020; Kamruzzaman et al., 2024; Shiru et al., 2022; Tian et al., 2021; Yildiz et al., 2024, IPCC, 2021).

To reduce uncertainties in climate projections, Multi-Model Ensembles (MMEs) have gained popularity, combining multiple GCM outputs to enhance projection reliability (Kim et al., 2024; Kumar et al., 2013; Palmer et al., 2005; Sansom et al., 2021; Tebaldi & Knutti, 2007). The ensemble approach ensures that averaged projections provide more robust climate assessments than individual models alone, particularly in regions like Bangladesh, where climate variability is high (Bhattacharjee et al., 2023; Fahad et al., 2018; Kamruzzaman et al., 2023a & 2023b; Khan et al., 2020b; Akter et al., 2024).

This study evaluates future extreme climate conditions in Bangladesh by using the ETCCDI indices, taking into account the CMIP6 multi-model ensemble (MME) projections after bias-correction, focusing on precipitation and temperature patterns for the near (2015–2044), mid (2045–2074), and far (2075–2100) futures under the SSP1-2.6, SSP2-4.5, and SSP5-8.5 scenarios. In contrast to past studies that focused mostly on temporal trends in the mean climate trends or at specific sites, the present work presents a detailed and spatially explicit assessment of climate extremes across Bangladesh, addressing critical knowledge gaps in regional climate projection research. By leveraging high-resolution climate data and multi-model ensemble projections, this study offers valuable insights into future climate risks and supports the development of adaptation strategies to enhance climate resilience in Bangladesh's most vulnerable regions.

1.2 Novelty and contribution to the Research Gap

Different General Circulation Models (GCMs) utilize varying physical parameterizations, numerical schemes, and initial conditions, leading to uncertainties in climate projections. Despite advancements in global climate modeling, CMIP6-based projections remain underutilized in South Asia, including Bangladesh, limiting high-resolution climate assessments essential for understanding future climate risks. Most previous studies on Bangladesh's climate extremes have focused on mean values or observed trends, with limited projections using multi-model ensembles (MMEs). While some studies have employed high-resolution Regional Climate Models (RCMs) from CMIP3 and CMIP5, they primarily analyzed specific regions or a limited number of extreme climate indices, failing to capture national-scale climate variability. Additionally, while ETCCDI (Expert Team on Climate Change Detection and Indices) indices have been used, they were often applied to localized areas or station-based observations, overlooking broader spatiotemporal patterns. The limited application of using CMIP6 models to evaluate future climate extreme events in Bangladesh using ETCCDI indices are presented in Appendix C, Table C1.

This study addresses these gaps by integrating an 18-member bias-corrected CMIP6 MME with ETCCDI indices, offering a spatially and temporally detailed analysis of future climate extremes across SSP1-2.6, SSP2-4.5, and SSP5-8.5 scenarios.

The projections cover three future periods: near (2015–2044), mid (2045–2074), and far future (2075–2100). By employing ERA5 reanalysis data for bias correction, the study enhances projection accuracy, reducing uncertainties associated with raw GCM simulations.

This study not only offers high-resolution projections of temperature and precipitation extremes across Bangladesh but also pinpoints the most vulnerable regions, providing critical insights for evidence-based adaptation planning in climate-sensitive sectors such as food security, water resources, and urban development. By providing a comprehensive spatiotemporal assessment of climate variability, this study provides a methodological bench mark for further studies and highlights the need for sophisticated climate modeling to aid in adaptation planning.

1.3 Objective

This research intends to address the following specific objectives:

1. To assess future extreme climate events, including temperature and precipitation extremes, in Bangladesh.
2. To identify vulnerable regions within Bangladesh that are susceptible to extreme climate events based on temperature shifts and precipitation variations.
3. To assess the future projections of changes and trends of such extremes across SSP 1-2.6, SSP 2-4.5 and SSP 5-8.5.

1.4 Scope of the Study

To accomplish the objectives, the following actions were taken:

1. Collection and validation of ERA5 reanalysis data against observed meteorological station data from the Bangladesh Meteorological Department (BMD).
2. For historical and future forecasts, 18 CMIP6 GCMs were chosen under three SSPs: SSP1-2.6, SSP2-4.5, and SSP5-8.5. Climate extremes for the near (2015–2044), mid (2045–2074), and far (2075–2100) futures are analyzed spatiotemporally.
3. Bias correction and downscaling of GCM outputs using the Simple Quantile Mapping (SQM) method for consistency with ERA5 data.
4. Calculation of 23 ETCCDI indices (13 temperature and 10 precipitation indices) to analyze climate extremes across Bangladesh using Multi-Model Ensemble (MME) and project future extremes with ArcGIS.
5. Identification of regions within Bangladesh vulnerable to temperature and precipitation extremes based on trends and projections of ETCCDI indices.
6. Formulation of recommendations for policymakers to develop effective climate adaptation and resilience strategies targeting identified high-risk areas.

1.5 Conceptual Framework of the study:

The following Figure 1.1 illustrates the flowchart that exhibits the analytical framework of the entire thesis in brief-

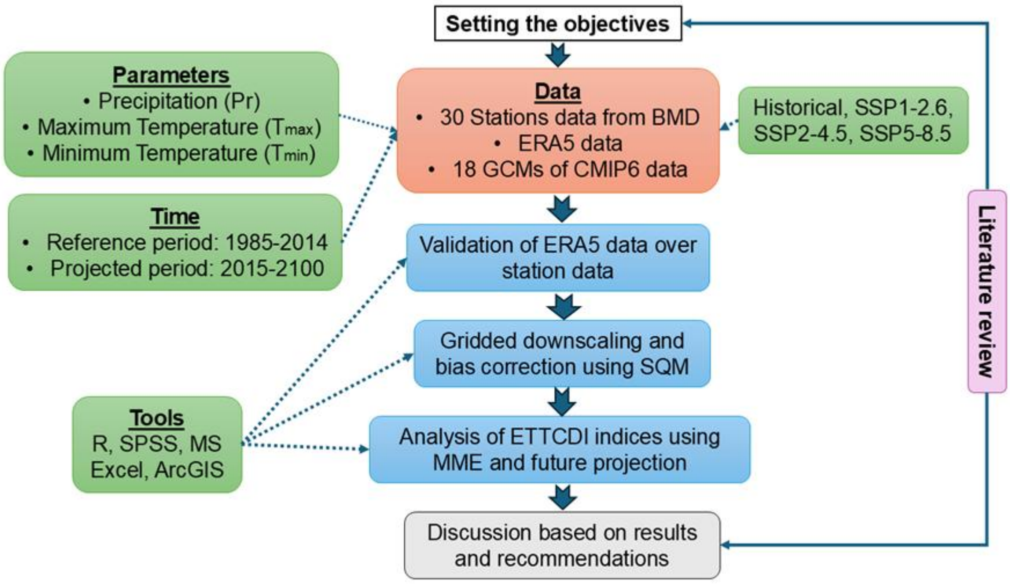

Figure 1.1: Workflow diagram of the study

1.6 Layout of the Thesis

The thesis includes five chapters depicting the literature, the adapted method, the analysis and pre-processing, and the result of the study. The references are also listed within this study.

Chapter 1 This chapter presents the background of the study, research problem, objectives, scope, and contributions of the thesis. It highlights the importance of understanding climate extremes in Bangladesh and outlines the study's motivation to project future climate scenarios using CMIP6 models and ETCCDI indices.

Chapter 2 This chapter reviews relevant literature on climate change impacts, climate extremes, and methodologies for projecting extreme events. Topics include an overview of Global Climate Models (GCMs), the Coupled Model Intercomparison Project Phase 6 (CMIP6), and the Expert Team on Climate Change Detection and Indices (ETCCDI). The chapter also discusses previous studies on climate extremes in Bangladesh and the limitations of existing approaches.

Chapter 3 The study's data sources and methodologies are described in depth in this chapter:

- Data Collection: Description of the ERA5 reanalysis dataset and station data from the Bangladesh Meteorological Department (BMD) for validation.

- CMIP6 GCMs: Selection of 18 GCMs under different SSP scenarios (SSP1-2.6, SSP2-4.5, SSP5-8.5) and data processing.
- Data preparation: Gridded downscaling and bias correction using the Simple Quantile Mapping (SQM) method, and validation of ERA5 data over station data.
- Indices Calculation: Computation of 23 ETCCDI indices to analyze temperature and precipitation extremes.
- Historical and Future Analysis: Use of Multi-Model Ensemble (MME) to analyze historical (1985-2014) and projected (2015-2100) climate extremes under SSP scenarios
- Spatiotemporal Variability: Detailed examination of temperature and precipitation indices across the near future (2015–2044), mid-future (2045–2074), and far future (2075–2100) periods.
- Vulnerable Regions Identification: Identification of regions in Bangladesh most susceptible to extreme climate events based on temperature and precipitation variations.

Chapter 4 This chapter discusses the study's findings in relation to future climate extremes in Bangladesh:

- Projection of future changes in ETCCDI indices for temperature and precipitation extremes across SSP scenarios, along with a discussion on regional disparities in projected climate extremes and their implications for different regions of Bangladesh. Insights into adaptation and resilience strategies for policymakers, focusing on regions identified as high-risk areas.

Chapter 5 This chapter provides a synthesis of the key outcomes, research significance, and acknowledged constraints of the study. It also provides recommendations for future research, including suggestions for refining the methodologies, exploring additional climate models, and conducting further studies on climate resilience in Bangladesh.

Chapter 2
Literature Review

2.1 General

This chapter discussed a literature review on climate extremes, including the mechanisms driving these events, the efficacy of various climate models, the influence of climate and weather patterns, and the socio-economic impacts of climate change on vulnerable regions like Bangladesh. It explores the advantages, limitations, and applications of Global Climate Models (GCMs), particularly CMIP6, in projecting future climate scenarios. The chapter also discusses the use of ETCCDI indices for evaluating temperature and precipitation extremes, the importance of bias-correction in climate projections, and the application of Multi-Model Ensemble (MME) approaches to improve prediction accuracy. Additionally, this review highlights recent studies and guidelines relevant to assessing climate vulnerabilities, identifying gaps in current research, and providing a foundation for evaluating climate resilience strategies tailored to Bangladesh's unique needs.

2.2 Climate Models

Climate models are often used to help us understand and predict changes in the Earth's climate (Ali & Kamraju, 2025). These models simulate physical processes within the climate system by solving equations numerically on a discretized grid (Knutti, 2008). They integrate various components, including the atmosphere, ocean, land surface, cryosphere, hydrological cycle, vegetation dynamics, carbon cycle, and aerosol chemistry, allowing them to capture interactions within the climate system and provide comprehensive future projections (Provenzale, 2014).

An accurate regional and sub-regional prediction of how climate will change is important for the preparation of successful mitigation and adaptation strategies. Complex numerical computer models are essential in predicting changes in phenomena including heavy precipitation, sea ice, permafrost and heat waves (IPCC, 2007). Climate models have evolved over decades, with continuous improvements in their ability to reproduce observed climate features (Flato et al., 2014; Raäisaänen, 2007; Randall et al., 2007).

A climate model is a highly complex system composed of multiple components (Amini, 2019). Testing and verification take place at different levels - from system-level comparison of full model runs with observations to component-level comparison of the individual aspects of the model (Randall et al., 2007.). Model evaluation techniques include standardized tests such as the quasi-biennial workshops on partial differential equations on the sphere and observational case studies conducted under programs like the Atmospheric Radiation Measurement (ARM) Program, EUROpean Cloud Systems (EUROCS), and the Global Energy and Water Cycle Experiment (GEWEX) Cloud System Study (Hourdin et al., 2013, Randall et al., 2007).

Climate models are broadly classified into Global Climate Models (GCMs) and Regional Climate Models (RCMs) (Chen & Ji, 2024). GCMs operate on a global scale, offering insights into broad atmospheric, oceanic, and terrestrial processes, whereas RCMs provide higher-resolution data for localized studies and often use GCM outputs as boundary conditions (Chokkavarapu & Mandla, 2019; Flato et al., 2014; Henderson-Sellers & McGuffie, 2011). Advances in computing power have allowed for higher spatial and vertical resolution in climate models, significantly enhancing their accuracy and usability.

2.2.1 Types of Climate Models

Climate models are broadly categorized into Global Climate Models (GCMs) and Regional Climate Models (RCMs) (Enyew et al., 2024). GCMs simulate climate processes on a global scale, capturing interactions between the atmosphere, ocean, and land surface (Henderson-Sellers & McGuffie, 2011). In contrast, RCMs provide finer-resolution simulations of specific geographic regions, refining global-scale projections for localized climate impacts. RCMs rely on GCM outputs for boundary conditions, offering improved insights into regional climate variations, which are critical for assessing localized climate risks (Randall et al., 2007).

2.2.2 Advances in Climate Modeling

Since the IPCC Third Assessment Report (TAR), significant advances have been made in climate modeling, particularly in resolution, physical parameterizations, and coupling of climate system components (Randall et al., 2007.). Notable improvements include:

- **Enhanced Resolution:** Improved temporal and spatial resolution in atmospheric and ocean components have resulted in better simulation of climate features
- **Comprehensive Physical Processes:** Updates to the realism of model simulations with enhanced representations of cloud microphysics, radiative transfer, aerosols, and land-atmosphere interactions.
- **Interactive Coupling of Climate Components:** Integration of interactive carbon cycle models, aerosol chemistry, and ocean circulation dynamics allows for more robust climate projections.

These advancements have strengthened model confidence, particularly in simulating large-scale temperature and precipitation patterns, though uncertainties remain in aspects such as cloud feedback and regional precipitation extremes (Randall et al., 2007).

2.2.3 Uncertainties in Climate Projections

Despite advancements, climate models face challenges in representing small-scale processes and internal variability. Differences in numerical schemes, parameterization techniques, and initial conditions contribute to uncertainties in climate projections. The lack of a universally recommended approach for GCM selection further complicates model evaluation (Randall et al., 2007). Key sources of uncertainty include:

- **Model Structure and Parameterization:** There is diversity among the models in terms of cloud cover, radiation, and convection, which affects climate sensitivity estimates.
- **Initial Conditions and Boundary Forcing:** Differences in input data, such as greenhouse gas concentrations and land-use changes, impact projections. Natural Climate Variability: Internal climate variability, such as the El Niño-Southern Oscillation (ENSO), complicates long-term projections.

To address these uncertainties, multi-model ensembles (MMEs) have emerged as a preferred approach. (Palmer et al., 2005; Pierce et al., 2009)

Climate models undergo rigorous evaluation through system-level and component-level assessments. The IPCC relies on intercomparison projects, such as the Coupled Model Intercomparison Project (CMIP), to benchmark model performance against observed climate data (Randall et al., 2007). Evaluation methods include:

- **Historical Climate Simulations:** The comparison of model output with historical climate records for purposes of evaluation of accuracy.
- **Extreme Event Simulations:** Testing models against observed extreme weather events to gauge reliability.
- **Sensitivity Analyses:** Examining how the model responds to changes in important parameters, such as greenhouse gas forcing and cloud feedback.

These evaluations enhance confidence in models' ability to project future climate scenarios, although challenges remain in capturing regional climate variations accurately (Randall et al., 2007).

2.2.4 Global Climate Model (GCM)

GCMs are three-dimensional models that simulate interactions between the atmosphere, ocean, land, and ice. These models are categorized as Atmospheric GCMs (AGCMs), which focus on the atmosphere and land surface, and Coupled Atmosphere-Ocean GCMs (AOGCMs), which integrate atmospheric and oceanic processes (Airey & Hulme, 1995; Shell, 2013).

Atmosphere-Ocean General Circulation Models (AOGCMs) are widely used for climate change predictions and show good skill in reproducing extreme temperature events, cold air outbreaks and frost days. Nevertheless, these models tend to exhibit too frequent and too intense extreme precipitation events, and overestimate weak precipitation events (Randall et al., 2007). While models can successfully replicate historical climate patterns, limitations remain, particularly in simulating tropical cyclone intensity and regional precipitation variability.

Figure 2.1 shows how a Global Climate Model (GCM) divides the Earth into a 3D grid to simulate climate processes. It includes horizontal (latitude–longitude) and vertical (height or pressure) layers, allowing for exchanges of heat, moisture, and momentum between grid cells (Balaji et al., 2022; Edwards, 2011). Key physical processes like radiation, precipitation, and ocean-atmosphere interactions are modeled to project climate behavior (Edwards, 2011).

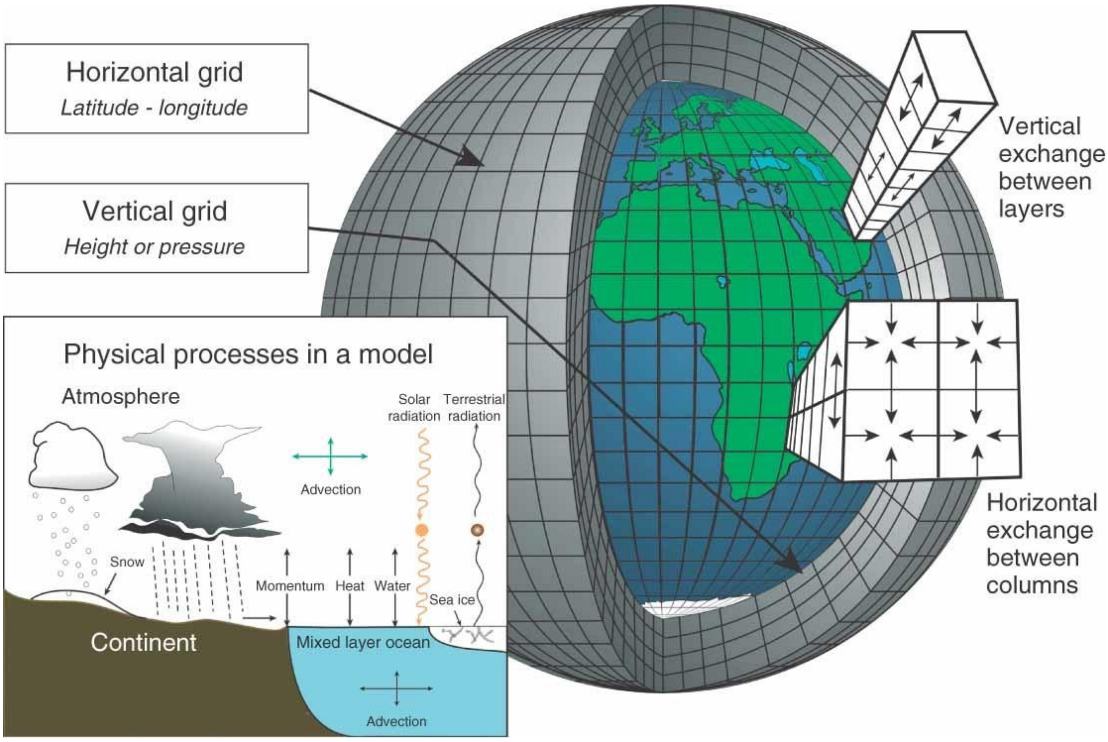

Figure 2.1: Three-Dimensional grid structure and physical processes in a Global Climate Model (GCM) (Balaji et al., 2022; Edwards, 2011)

The selection of GCMs for climate impact studies follows criteria outlined by the Intergovernmental Panel on Climate Change (IPCC). The four key criteria are vintage, resolution, validity, and representativeness (URL: https://www.ipcc-data.org/ddc). These criteria include:

- **Vintage:** Recent GCM simulations incorporate the latest scientific advancements and improved processes, enhancing reliability.
- **Resolution:** Higher spatial and vertical resolutions improve accuracy but do not inherently guarantee better model performance.
- **Validity:** A GCM's ability to replicate present-day climate conditions determines its reliability for future projections.
- **Representativeness:** Using multiple GCMs ensures that a range of possible future climate scenarios is captured (IPCC, 2007).

GCMs also play a crucial role in linking atmospheric and hydrological processes to predict climate and hydrometeorological extremes. However, their spatial resolution often limits their ability to resolve localized features such as precipitation variability. To address this issue, statistical and dynamical downscaling techniques are employed to refine GCM outputs for regional applications (Jayasankar et al., 2018; Shashikanth et al., 2018).

2.2.5 Coupled Model Intercomparison Project (CMIP)

The development of climate models has progressed significantly since the late 1960s and early 1970s, when the first attempts to couple atmospheric and oceanic models were carried out (Bryan, 2006; Manabe & Stouffer, 1988; Stouffer & Manabe, 1999). A major breakthrough in climate modeling occurred with the replacement of slab ocean models by fully coupled ocean-atmosphere models. This advancement was considered one of the most significant in the last two decades, as it allowed for more realistic simulations of climate change patterns, particularly in oceanic regions, and enabled the exploration of transient climate scenarios. It also marked a step toward developing comprehensive Earth-system models that explicitly include chemical and biogeochemical cycles (Trenberth, 1993).

According to World Climate Research Programme (WCRP) early General Circulation Models (GCMs) simulated isolated aspects of the Earth system, such as atmosphere-only or ocean-only models, but did so in three dimensions, incorporating many kilometers of atmospheric height or ocean depth through multiple model layers. The advent of coupled models, specifically Atmosphere-Ocean General Circulation Models (AOGCMs), linked these components, allowing for the simulation of interactions between the land surface, ocean, and atmosphere. AOGCMs can simulate exchanges of heat and freshwater between the land and ocean and the air above, significantly advancing climate system representations. Modern coupled climate models integrate components of the atmosphere, land, ocean, and sea ice to provide a comprehensive representation of the climate system. The atmospheric component, like the ocean, solves the primitive equations of motion with hydrostatic balance, the continuity equation, and predictive equations for temperature and specific humidity. These models often use vertical coordinates such as pressure, terrain-following layers, or a combination of both (Gent, 2013; Petersen et al., 2015).

Coupled models, however, have faced numerous challenges throughout their development. Key issues include the lack of precise knowledge about the ocean's initial state, the potential for minor surface flux imbalances to cause unrealistic drifts in simulations, and the absence of stabilizing feedback mechanisms to correct errors in simulated salinity. Early solutions, such as flux adjustments, introduced empirical corrections to stabilize simulations, although these adjustments were not grounded in physical principles (Manabe & Stouffer, 1988). The National Center for Atmospheric Research (NCAR) was among the first to achieve non-flux-corrected coupled simulations, enabling climate change projections into the 21st century despite persistent drifts in early simulations.

One of the most influential efforts for the development of coupled models is the Coupled Model Intercomparison Project (CMIP). The primary objective of CMIP is to enhance understanding of past, present, and future climate changes arising from both natural variability and responses to radiative forcing. CMIP assesses model performance during historical periods, quantifies the causes of divergence in future projections, and uses idealized experiments to deepen understanding of model responses. Additionally, CMIP explores the predictability of the climate system across various temporal and spatial scales and standardizes the multi-model output for public access. The initiative is overseen by the CMIP Panel and the WGCM Infrastructure Panel (WIP), which coordinate experiments and manage the infrastructure needed for data archiving and dissemination (WCRP). In summary, the evolution of coupled models, from early standalone atmospheric or oceanic models to sophisticated coupled AOGCMs, has revolutionized climate modeling. These improvements have in turn enabled refinement and validation of the world's most sophisticated simulations of the Earth's climate system, including complex feedback regimes among its components, leading to a more robust understanding of climate variability and change.

Climate models, particularly GCMs and RCMs, have evolved into indispensable tools for studying and projecting climate variability and extremes. While they face limitations, ongoing improvements in resolution, computational capacity, and model parameterization enhance their reliability. The CMIP framework plays a vital role in climate model intercomparison, ensuring that projections remain robust and policy relevant. By integrating CMIP6 projections into adaptation and mitigation strategies, nations like Bangladesh can better prepare for climate-induced challenges, ensuring resilience in an increasingly uncertain climate future.

2.3 The future Emission scenarios of CMIP6

The Coupled Model Intercomparison Project Phase 6 (CMIP6) is the most recent global effort to improve climate modelling, by co-ordinating simulations across different Global Climate Models (GCMs) (Enyew et al., 2024). The goal of CMIP6 is to generate a standardized set of climate model simulations that enable researchers to compare projections across different models, assess uncertainties, and analyze future climate trajectories under varying emission scenarios (Carbon Brief, 2019). Ahead of the IPCC AR6, the energy modelling community created the Shared Socioeconomic Pathways (SSPs), which represent different possible futures of society and the economy. A subset of the SSPs were used to characterize CMIP6 climate model experiments, thus extending the range of potential climate outcomes that underpin future emission scenarios associated with different socioeconomic trajectories. These SSPs were developed in collaboration with the energy modeling community to replace the Representative Concentration Pathways (RCPs) used in previous climate projections under CMIP5. The SSPs are categorized based on the challenges they pose to mitigation and adaptation, ranging from low-emission, sustainable scenarios (SSP1-2.6) to high-emission, fossil-fueled development pathways (SSP5-8.5) (Carbon Brief, 2019.).

The following provides a detailed description of these CMIP6 emission scenarios(Carbon Brief, 2019; et al., 2016; O'Neill et al., 2016; URL: https://climate-scenarios.canada.ca/?page=cmip6-overview-notes):

- **SSP1 (Sustainability – Taking the Green Road):** This scenario describes a low-emission pathway where global society gradually evolves toward sustainable outcomes. It places an emphasis on development that is inclusive, the use of low-carbon forms of energy and a decrease in resource intensity, with the expected rise in global temperature at less than 2°C by 2100.
- **SSP2 (Middle of the Road):** This intermediate-emission scenario assumes that global trends in development, technological progress, and climate policies remain close to historical patterns. Moderate mitigation efforts slow

the growth of emissions, leading to a global temperature increase between 2°C and 3°C by 2100.

- **SSP3 (Regional Rivalry – A Rocky Road):** In this high-emissions scenario, the world is divided by nationalism and regional stressors that hinder international collaboration on climate policies. Therefore, there remains a high reliance on fossil fuels, slow pace of technological development, and continued environmental degradation that will result in the predicted increase in the global temperature of over 3.5°C by 2100.
- **SSP4 (Inequality – A Road Divided):** This moderate-to-high-emission scenario depicts a world with increasing social and economic disparities. Wealthier nations adopt clean energy and carbon-neutral policies, whereas poorer countries remain dependent on fossil fuels due to limited resources and technological access. Temperature rise in this scenario is expected to reach approximately 3°C by 2100.
- **SSP5 (Fossil-fueled Development – Taking the Highway):** This worst-case, high-emission scenario assumes that global economic growth continues to be driven by fossil fuels with little regard for climate policies or mitigation strategies. Under this trajectory, greenhouse gas concentrations rise unchecked, leading to a global temperature increase exceeding 4°C by 2100 (Carbon Brief, 2019).

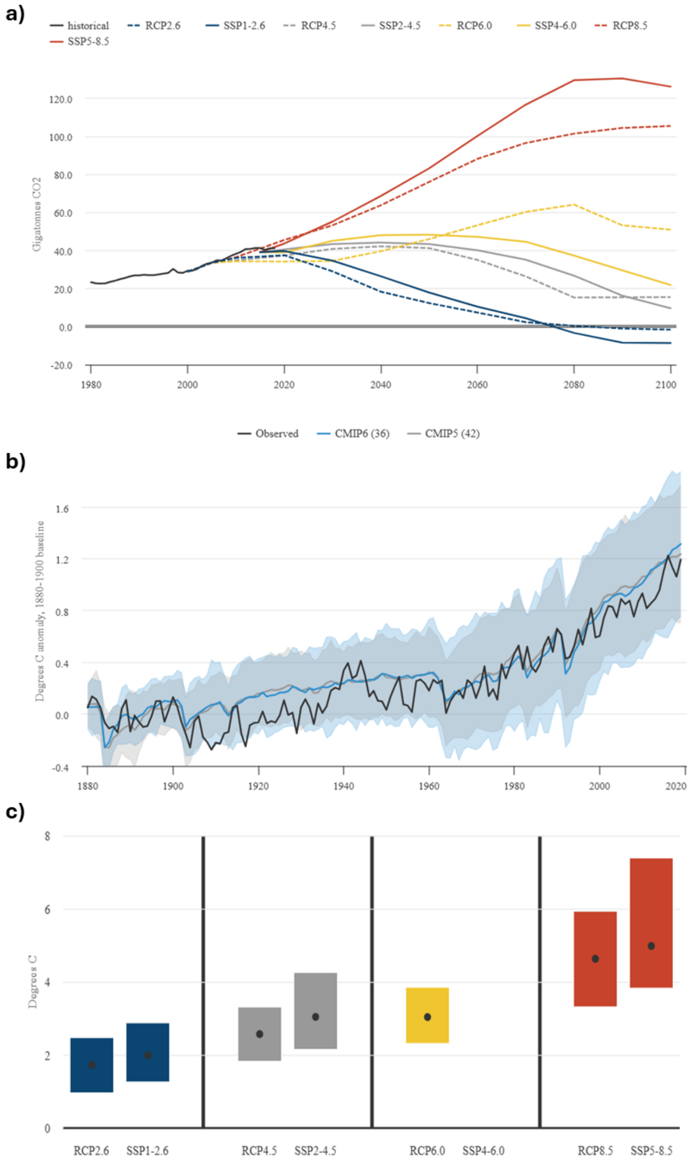

Figure 2.2: Comparison of projected CO_2 emissions in CMIP5 and CMIP6 scenarios (URL: https://www.carbonbrief.org/cmip6-the-next-generation-of-climate-models-explained)

The Figure 2.2 (a-c) compares CO_2 emission trajectories under CMIP5 (RCPs) and CMIP6 (SSPs) scenarios, illustrating the impact of different socioeconomic and policy pathways. According to Zeke Hausfather's findings (URL: https://www.carbonbrief.org/cmip6-the-next-generation-of-climate-models-explained), the SSP1-2.6 scenario in CMIP6 closely mirrors the RCP2.6 pathway, featuring a sharp decline in CO_2 emissions to net-negative levels by 2100, aligned with a <2°C warming limit. Moderate emission scenarios like SSP2-4.5 and SSP4-6.0 represent partial mitigation and global inequality, stabilizing emissions around

20–30 $GtCO_2$ and projecting 2–3°C of warming, while SSP5-8.5 and RCP8.5 follow a high-emission trajectory exceeding 120 $GtCO_2$, associated with >4°C warming by century's end. Despite higher equilibrium climate sensitivity (ECS) values in CMIP6 models, their hindcast performance remains comparable to CMIP5, capturing observed warming trends reasonably well, although both models struggle with the early 20th-century warming (1900–1940). When comparing the rate of warming, both CMIP5 and CMIP6 multi-model means closely track observational records, particularly over the modern period (1970–2019), although CMIP6 shows slightly greater warming estimates. On average, CMIP6 scenarios project around 0.4°C more warming than their CMIP5 counterparts, with SSP1-2.6 yielding ~2.0°C warming compared to 1.7°C under RCP2.6, though differences in scenario structure and model availability (e.g., limited SSP4-6.0 runs) also contribute to this variation. CMIP6 shows slightly higher warming projections (~0.4°C more) than CMIP5 due to higher climate sensitivity but performs similarly in reproducing historical trends. Both models capture recent warming well but struggle with early 20th-century trends. While CMIP6 adds more realistic socioeconomic pathways, its overall accuracy is comparable to CMIP5.

The CMIP6 scenarios provide critical insights into potential climate futures based on global policy choices and socioeconomic developments. These projections inform policymakers, researchers, and stakeholders about the potential impacts of climate change and the urgency of mitigation strategies to limit extreme warming (Enyew et al., 2024). By integrating CMIP6 projections into climate adaptation and mitigation planning, nations like Bangladesh can better prepare for emerging climate risks, such as rising temperatures, increased precipitation variability, and extreme weather events.

2.4 Climate Extreme

Climate change detection has moved away from documentation of changes in monthly and annual averages to be focused now on the analysis of extreme events e.g., heat waves, droughts, floods, and storms (Brönnimannid, 2022; Easterling et al., 2016; Kuglitsch et al., 2009; van der Linden et al., 2015; Wegler & Kuenzer, 2024). Climate extremes refer to infrequent events that occur at the tail ends of the distribution curve of climate variables, as noted by (Zwiers et al., 2013). These events present serious risks to public health, economic resilience, and the integrity of natural and built environments. With ongoing global warming, the frequency and intensity of climate hazards are expected to rise, compounded by increased exposure due to growing populations and infrastructure development and heightened vulnerability from aging infrastructure. Climate extremes rising summer temperature variability combined with a decrease in water resources having an unprecedented impact on ecology, economy and society (Jones, 1999; van der Linden et al., 2015; Xoplaki et al., 2016).

In a normally distributed temperature pattern, extremes such as unusually cold or hot events correspond to the distribution's tails. For precipitation, while it does not conform to a normal distribution, the extremes can still be delineated as light and heavy rainfall occurrences (Peterson et al., 2008; Zhang et al., 2011). Figure 2.3 represents the basic ideas about temperature and precipitation extremes. Climate warming directly amplifies these extremes, increasing the likelihood of abnormal weather events such as heatwaves, wildfires, floods, altered rainfall patterns, and heightened evapotranspiration rates (Seneviratne et al., 2012; Ummenhofer & Meehl, 2017).

According to (Aghakouchak et al., 2020), climate extremes have historically jeopardized human well-being and economic growth globally. Between 1980 and 2017, the United States alone experienced losses exceeding USD 1.537 billion and nearly 10,000 fatalities due to such events. Bangladesh, one of the most climate-vulnerable nations, frequently endures natural disasters, including floods, droughts, tornadoes, and tidal surges (Rahman & Rahman, 2015; Islam, 2023; Rahman et al., 2024). Ranking 7th on the Global Climate Risk Index 2021, Bangladesh faced an estimated annual GDP loss of 1.1% under moderate climate change conditions, which could rise to 2.0% per year under more severe climate scenarios. (Eckstein et al., 2021; General Economics Division, 2018).

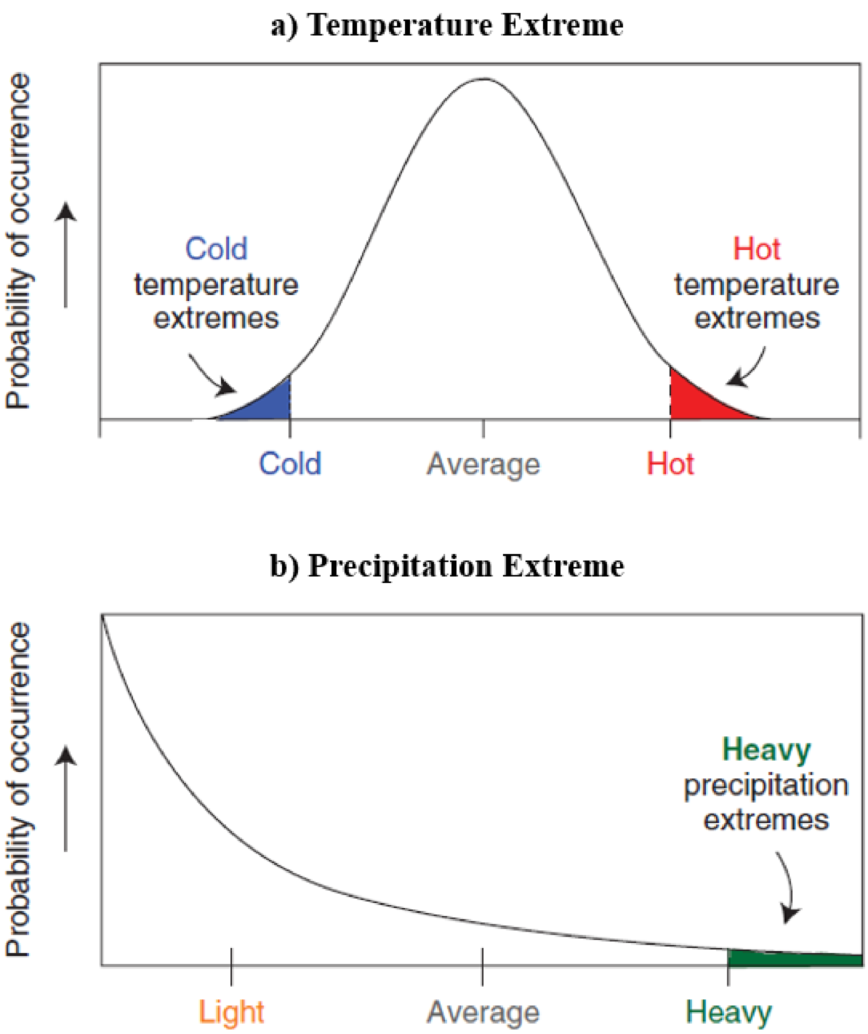

Figure 2.3: Probability distributions of temperature and precipitation extremes. (a) Temperature extremes represented by a normal distribution, showing cold and hot extremes; (b) Precipitation extremes depicted by a skewed distribution, highlighting rare heavy precipitation events (Folland et al., 2001; Houghton, 2001; X. Zhang et al., 2011).

Impacts of variations in frequency and magnitude of extreme weather events are widely recognized. Observational studies indicate amplified changes in total Pr, T_{max} and T_{min} at the distribution's tails. These shifts highlight identifiable trends in certain extreme climatic events, such as temperature and precipitation extremes, underscoring the significant human influence on the climate (Easterling et al., 2016; Meehl et al., 2000).

Extreme climate events can be categorized into two groups (Easterling, 2013):

i. Simple statistical extremes, such as unusually high or low daily temperatures or heavy rainfall, which occur annually.
ii. Complex, event-driven extremes, such as hurricanes, floods, or droughts, which may not recur annually at a given location.

The global mean temperature has risen by approximately 0.6°C since the early 20th century (Nicholls et al., 1996), with a stronger increase in daily minimum temperatures than in maximums, leading to a reduced diurnal temperature range (Easterling et al., 1997). Between 2011 and 2020, global temperatures were 1.09°C warmer than pre-industrial levels (IPCC, 2021). Higher temperatures are linked to more frequent heatwaves and alterations in the global water cycle, manifesting in heavy precipitation events and more intense hurricanes (Babcock et al., 2019; J. E. Bell et al., 2018; Trenberth, 2018).

Land surface precipitation trends show increases in mid-to-high latitudes but declines in the tropics and subtropics (Nicholls et al., 1996). Heavy precipitation events are projected to increase, exacerbating flood risks and triggering landslides, particularly in coastal regions where sea level rise magnifies vulnerability (Aghakouchak et al., 2020; Gariano & Guzzetti, 2016). In Bangladesh, extreme weather in 2023 showcased the nation's vulnerability, with a record-breaking heatwave in May and flash floods in September submerging 94% of Sunamganj and 84% of Sylhet (UNICEF Bangladesh, 2022; URL: https://www.ffwc.gov.bd). Significant sea-level rise in coastal regions, such as Cox's Bazar, where the observed rate (7.8 mm/year) surpasses the global average, further heightens the risks (Hossain & Hossain, 2012).

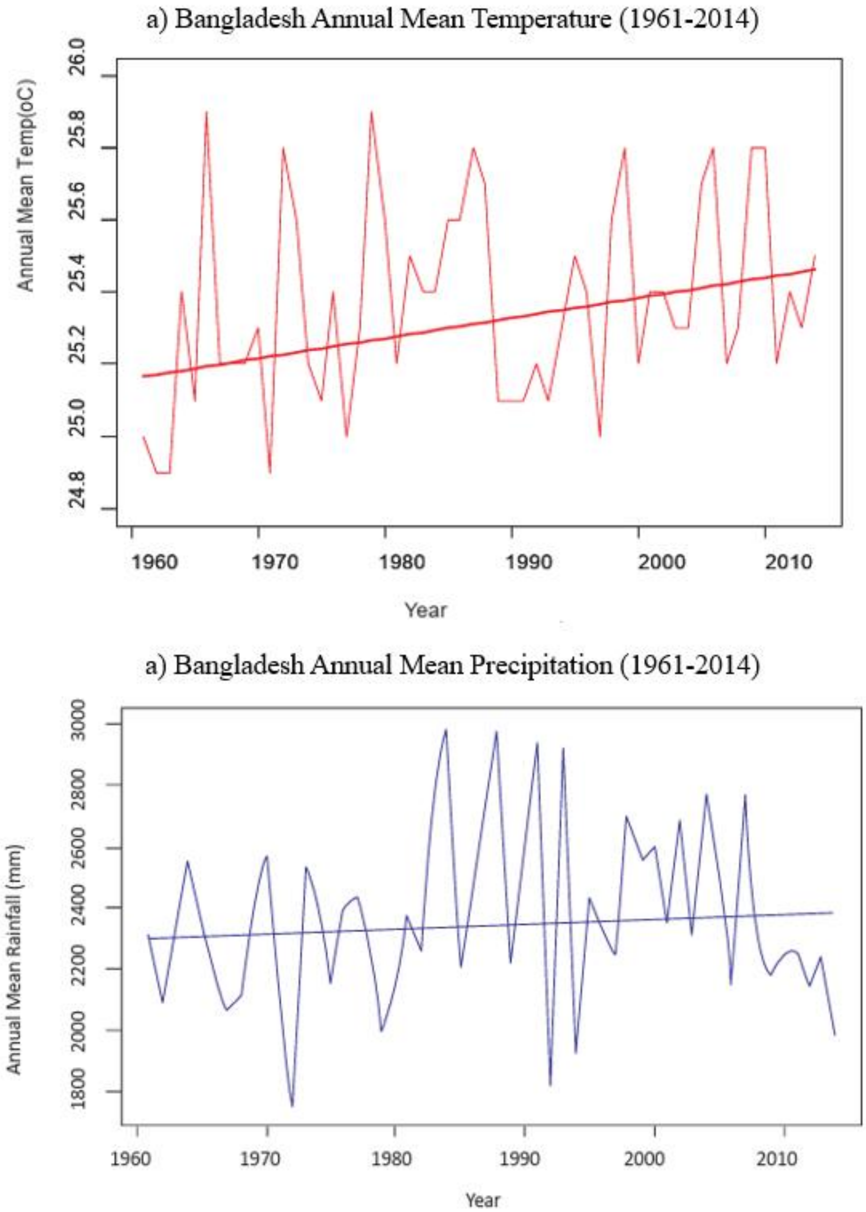

Figure 2.4: Trends in annual mean temperature and precipitation in Bangladesh (1961–2014) based on Sen's slope estimator (Ahmad, 2018)

Figure 2.4 shows trends in annual mean temperature and rainfall in Bangladesh from 1961 to 2014, using Sen's slope estimator (Ahmad, 2018). The mean annual temperature increased by 0.056°C/decade, with regional variations linked to natural hazard vulnerabilities and significant variability in extreme temperatures. Rainfall trends are mixed, though a statistically significant increase was observed at the Srimongal station in the high-rainfall northeast zone. Overall, extreme rainfall indices in Bangladesh exhibit a roughly equal distribution of increasing and decreasing trends (Ahmad, 2018).

Table 2.1: Modified confidence in observed and projected changes of key climate phenomena (Houghton, 2001)

Climate Phenomenon	Observed Change (Late 20th Century)	Projected Change (21st Century)
Maximum temperature rise and increased hot days	Likely	Very likely
Minimum temperature rise with fewer cold and frost days	Very likely	Very likely
Decreased diurnal temperature range	Very likely over most land areas	Very likely
Heat indices increase over land	Likely over many areas	Very likely, over most areas
More frequent intense precipitation events	Likely, especially in Northern Hemisphere mid- to high latitudes	Very likely, over many areas

Table 2.1 presents the confidence levels in observed changes in weather and climate extremes during the late 20th century and projected changes for the 21st century, based on observational data, modeling studies, and expert judgment (Houghton, 2001). The assessment considers the physical plausibility of future changes across commonly used emission scenarios. However, due to limited observational data and insufficient model resolution, there is low confidence in assessing trends or making projections for small-scale phenomena such as thunderstorms, tornadoes, hail, and lightning. Overall, extreme events like heatwaves, heavy precipitation, and droughts are very likely to increase across many regions during the 21st century (Houghton, 2001).

Extreme high-temperature events, such as heatwaves, lead to droughts, while changes in precipitation patterns increase wetness and drought-affected areas globally (Haile et al., 2020). Short-duration episodes of extreme heat or cold can have severe impacts on human health (Changnon et al., 2003; Easterling et al., 2000). Bangladesh's socio-economic sectors, from agriculture to public health, face significant risks due to these changes (Selvaraju & Baas, 2007; Umma et al., 2011). Figure 2.5 illustrates regional assessments of observed changes in hot extremes and heavy precipitation, along with confidence in human influence since the 1950s, as presented in IPCC AR6. Bangladesh falls within the SAS (South Asia) region, which is identified as having a high level of population exposure and impact from these climate extremes. While a clear global trend is not evident due to regional uncertainties and methodological differences, the observed changes consistently indicate intensifying extremes. Where trends are detectable, they point toward a worsening of conditions and increased risks to human well-being (Clarke et al., 2022).

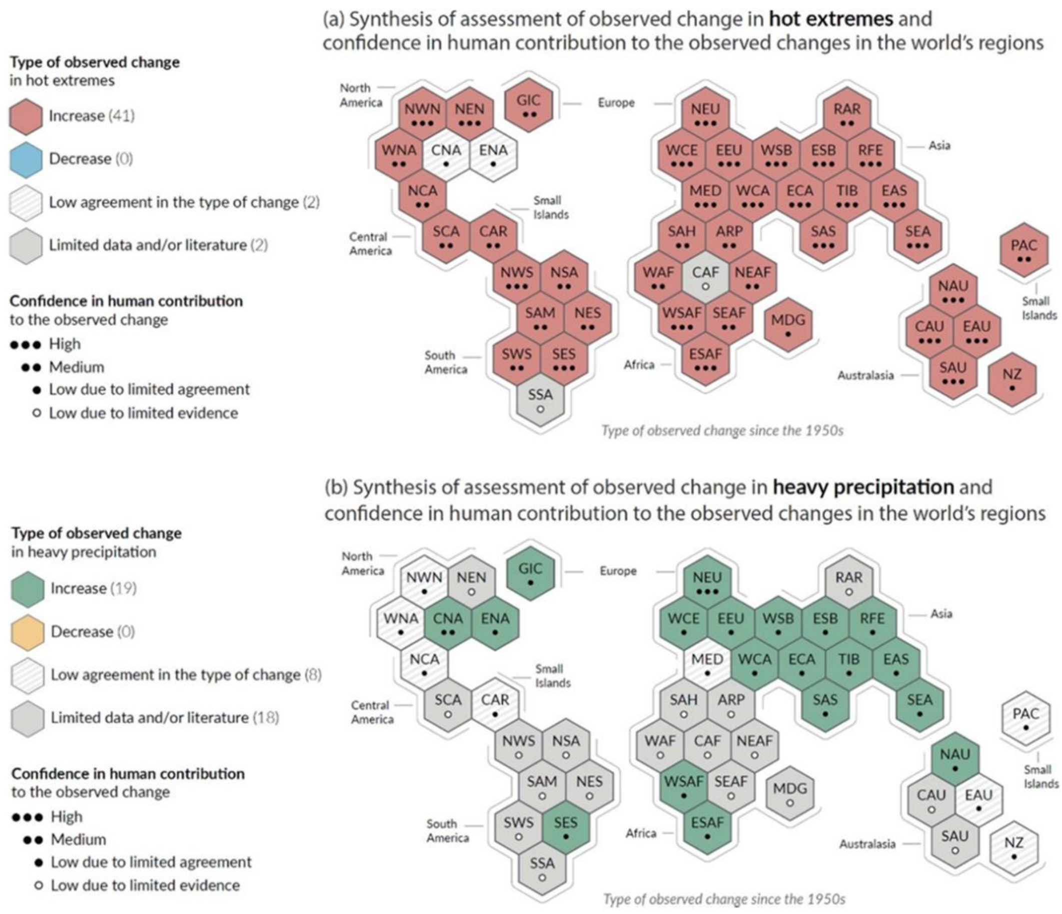

Figure 2.5: Regional assessment of observed changes in (a) Hot extremes and (b) Heavy precipitation with confidence in human influence since the 1950s (Masson-Delmotte et al., 2021; Otto et al., 2021; Clarke et al., 2022; Fyfe, 2021)

In conclusion, climate extremes are not only indicators of a warming world but also catalysts for broader social and economic challenges. These trends underscore the urgent need for effective adaptation strategies and resilience planning.

2.4.1 Climate Extreme Indices

The research into climate extremes has advanced significantly over the last few decades due to international coordinated efforts aimed at compiling, quality-controlling, and analyzing variables that represent extreme climate events (Nicholls & Alexander, 2007; Zwiers et al., 2013). One of the most notable efforts in this regard is led by the Expert Team on Climate Change Detection and Indices (ETCCDI) (Donat et al., 2013). ETCCDI has focused extensively on changes in temperature and precipitation extremes by defining a set of 27 widely recognized indices, which are derived from surface station observations. These indices facilitate the spatiotemporal analysis of climate extremes at global and regional scales, offering valuable insights into shifts in climate variability and extreme weather patterns (Alexander et al., 2006; Frich et al., 2002; Rehana et al., 2022).

Some National Meteorological Services are more and more prepared to share (generally raw) indices, rather than (raw) daily data, rendering climate information available for areas in which historical data are not widely available (Zhang et al., 2011). The ETCCDI framework has consequently enabled the development of standardized global and regional datasets in a comparable manner, enhancing the robustness of climate change research. The 27 ETCCDI indices are grossly classified into four groups according to the approach of their calculations: percentile-based indices, absolute indices, threshold-based indices and others (Abdullah et al., 2022; Yang, 2024). Each of these indices captures a distinct aspect of climate variability and extremes, providing essential tools for climate impact assessments are provided below Table 2.2. (Abdullah et al., 2022; Alexander et al., 2006; Aram et al., 2019; Barry et al., 2018; Behnke et al., 2016; Brown et al., 2010; Donat et al., 2013; Frich et al., 2002; Hajat et al., 2014; Lin et al., 2020; Nicholls & Alexander, 2007; Palme, 2021; Nowreen et al., 2015; Perkins & Alexander, 2013; Rajulapati et al., 2022; Sillmann, et al., 2013a & 2013b; Singh et al., 2025; Sun & Hu, 2023; Yang et al., 2023; Yin & Sun, 2018; Zhang et al., 2011; Klein Tank et al., 2009; URL: http://www.bom.gov.au/climate/pccsp/about-pi-extreme-indices.shtml).

Table 2.2: ETCCDI extreme indices with associated Impacts. (TX = Daily maximum temperature, TN = Daily minimum temperature, TG = Daily mean temperature)

Index	Climatic Factor Represented	Definition	Associated Impacts	Category
FD	Frequency of frost occurrence	Annual count of days when TN < 0°C	Impacts agriculture by affecting crop survival; influences heating energy demand	Threshold-Based
SU	Frequency of warm days	Annual count of days when TX > 25°C	Affects human health due to heat stress; increases cooling energy demand	Threshold-Based
ID	Frequency of cold days	Annual count of days when TX < 0°C	Impacts transportation safety; increases heating energy demand	Threshold-Based
TR	Frequency of warm nights	Annual count of days when TN > 20°C	Affects human health due to lack of nighttime relief from heat; influences energy consumption patterns	Threshold-Based
GSL	Length of the growing season	Annual count of days between first span of at least 6 days with TG > 5°C and first span after July 1st of 6 days with TG < 5C	Influences agricultural planning and crop yields	Other
TXx	Highest daytime temperature	Monthly maximum value of daily maximum temperature	Indicates intensity of heatwaves; affects human	Absolute

			health and infrastructure	
TNx	Highest nighttime temperature	Monthly maximum value of daily minimum temperature	Indicates intensity of warm nights; impacts human health and energy consumption	Absolute
TXn	Lowest daytime temperature	Monthly minimum value of daily maximum temperature	Reflects cold daytime extremes; affects energy demand and agriculture	Absolute
TNn	Lowest nighttime temperature	Monthly minimum value of daily minimum temperature	Reflects cold nighttime extremes; impacts energy demand and crop survival	Absolute
TN10p	Frequency of cold nights	Percentage of days when TN < 10^{th} percentile	Indicates occurrence of cold nights; affects agriculture and energy demand	Percentile-Based
TX10p	Frequency of cold days	Percentage of days when TX < 10^{th} percentile	Indicates occurrence of cold days; impacts energy demand and human health	Percentile-Based
TN90p	Frequency of warm nights	Percentage of days when TN > 90^{th} percentile	Indicates occurrence of warm nights; affects human health and energy consumption	Percentile-Based
TX90p	Frequency of warm days	Percentage of days when TX > 90^{th} percentile	Indicates occurrence of warm days; impacts human health and energy demand	Percentile-Based
WSDI	Duration of warm spells	Annual count of days with at least 6 consecutive days when TX > 90^{th} percentile	Indicates prolonged warm periods; affects human health,	Threshold-Based

			agriculture, and water resources	
CSDI	Duration of cold spells	Annual count of days with at least 6 consecutive days when TN < 10^{th} percentile	Indicates prolonged cold periods; impacts energy demand and agriculture	Threshold-Based
DTR	Variability between day and night temperatures	Monthly mean difference between TX and TN	Affects human health and agricultural practices	Other
Rx1day	Intensity of extreme daily precipitation	Monthly maximum 1-day precipitation	Indicates potential for flash floods; impacts infrastructure and agriculture	Absolute
Rx5day	Intensity of extreme 5-day precipitation	Monthly maximum consecutive 5-day precipitation	Reflects prolonged heavy precipitation; affects flood risk and water management	Absolute
SDII	Average precipitation intensity	Mean precipitation amount on wet days (RR ≥ 1mm)	Indicates rainfall intensity; impacts soil erosion and agriculture	Other
R10mm	Frequency of moderate precipitation days	Annual count of days when precipitation ≥ 10mm	Reflects occurrence of moderate rainfall events; affects agriculture and water resources	Threshold-Based
R20mm	Frequency of heavy precipitation days	Annual count of days when precipitation ≥ 20mm	Reflects occurrence of heavy rainfall events; impacts flood risk and infrastructure	Threshold-Based
Rnmm	Frequency of very heavy precipitation days	Annual count of days when precipitation ≥ user-defined threshold (nn mm)	Indicates occurrence of very heavy rainfall events; affects flood risk and water management	Threshold-Based
CDD	Length of dry spells	Maximum number of consecutive days with precipitation < 1mm	Indicates drought potential; impacts agriculture and water resources	Threshold-Based

CWD	Length of wet spells	Maximum number of consecutive days with precipitation 1mm	Reflects prolonged wet periods; affects agriculture and flood risk	Threshold-Based
R95p	Volume of very wet days	Annual total precipitation from days > 95th percentile	Indicates contribution of very wet days to total precipitation; impacts flood risk and water management	Percentile-Based
R99p	Volume of extremely wet days	Annual total precipitation from days > 99th percentile	Indicates contribution of extremely wet days to total precipitation; affects flood risk and infrastructure	Percentile-Based
PRCPTOT	Total annual precipitation	Annual total precipitation from wet days (RR ≥ 1mm)	Reflects overall precipitation; impacts water resources and agriculture	Other

2.5 Multimodel Ensemble

Various uncertainties in climate model simulations arise from multiple factors, including model resolution, mathematical formulation, initial assumptions, and calibration processes (Kamruzzaman et al., 2021). These uncertainties limit the credible application of climate projections at regional or local scales (Foley, 2010; Kamruzzaman et al., 2021; Khan et al., 2019; Northrop & Chandler, 2014). Addressing these uncertainties is critical for improving the accuracy of climate predictions, particularly for impact assessments and adaptation planning.

Over the past few years, many methods have been developed to deal with uncertainty in climate projections. A commonly adopted method of mitigation of these uncertainties is through multimodel ensembles (MME), which could mitigate model uncertainties by combining multiple GCMs in a single projection (Dey et al., 2022; Tebaldi & Knutti, 2007; Wang et al., 2018). Several studies have demonstrated that the ensemble mean of multiple GCMs provides a more robust representation of future climate than any single GCM (Gharbia et al., 2016; Her et al., 2019; Maher et al., 2021; Raju & Kumar, 2020). However, there is no consensus on the optimal number of GCMs to be used in an MME. For example, studies such as (Deegala et al., 2023; Lee et al., 2024; Mondal et al., 2022; Sahabi-Abed and Selmane, 2023) propose varying criteria for selecting CMIP6 GCMs, often based on factors such as data availability and model performance or skill. This study selects 18 GCMs based on data availability and performance for a more comprehensive ensemble approach.

Beyond simple arithmetic averaging, alternative MME techniques have demonstrated greater robustness in climate projections. Some of these approaches include:

1. **Arithmetic Mean Method (Simple Ensemble Mean):** The arithmetic mean approach in multi-model ensemble (MME) analysis involves a straightforward averaging of outputs from all participating climate models. This is the method most frequently used in climate change studies because it is computationally simple and convenient (Rhymee et al., 2022). An important drawback of this approach is the assumption regarding equal skill of each model (regardless of inter-model differences in skill) which may oversimplify models if institutions have invested in different model configurations and simulation approaches (Latonin et al., 2021). Despite this drawback, the arithmetic mean remains a widely accepted baseline for ensemble projections and comparative studies.

2. **Weighted Ensemble Method:** Weighted ensemble approaches that weigh individual models according to their simulation skill and how interdependent they are, have been employed in several studies (Merrifield et al., 2020; Sanderson et al., 2017; Wu & Levinson, 2021; Zuckerman & Chong, 2017). Despite this, model weighting in climate modelling is not yet a standardised technique. The Intergovernmental Panel on Climate Change (IPCC 2013) has noted that the climate modelers do not have an agreed method to weight models to determine the best estimate of future climate change. It has been found that climate models perform differently for different variables, regions and a part of the climate system under study. Therefore, defining model skill, deriving model weights, and determining the best method to combine model outputs remains a controversial issue.

3. **Bayesian Model Averaging (BMA):** Bayesian Model Averaging (BMA) has been extensively applied to integrate prediction for climate from individual models and to quantify the uncertainty arising from model structure (Huo et al., 2019; Raftery et al., 2005). This statistical approach considers a probabilistic framework to assess and integrate different models, improving uncertainty quantification in ensemble projections (Abbaszadeh et al., 2022; Madadgar & Moradkhani, 2014).
4. **Model Weighting Using Observation Distance Matrix:** Several studies introduced an approach that assigns weights to models based on their performance and interdependence using a model observation distance matrix (Duncan et al., 2017; Sanderson et al., 2017). This method enhances the accuracy of climate projections by accounting for model biases and interdependencies.
5. **Residual-Based or Error-Corrected Ensemble Models:** The residual-based ensemble approaches (e.g., the Residual-based Bagging Tree (RBT) model) downscale MME predictions by post-processing MME output to remove the discrepancies between models and observations through statistical learning on residuals, and have been successfully implemented for ensemble crop and grassland models (Sándor et al., 2023; Tao et al., 2018). These approaches focus on systematically reducing model biases post-simulation, thus enhancing the reliability of climate projections. However, they still depend on the quality and quantity of available observational data and might not fully capture new, emergent climate system behaviors under future emission scenarios.
6. **Machine Learning-Based Approaches:** Recently, State-of-the-art Machine Learning (ML) methods have also been recently established in climate science as they are able to capture the non-linear relationships and multilevel dependencies in climate data (Chen et al., 2023; Materia et al., 2024). ML-based ensemble learning techniques offer a promising alternative to traditional MME methods (Jose et al., 2022). Several studies used ML approaches for the multimodel ensemble. Acharya et al., 2014 employed an Extreme Learning Machine (ELM) on seven GCMs to generate an MME-based estimation of the northeast monsoon rainfall over

South Peninsular India (Wang et al., 2018). Their study found that ELM performed better in capturing seasonal rainfall extremes compared to other MME methods (Wang et al., 2018). Dey et al., (2022) utilized three machine learning algorithms—Artificial Neural Networks (ANN), Random Forest (RF), and Support Vector Machine (SVM)—to develop a multi-model ensemble (MME) system for forecasting climate variables in an Indian river basin. Their results showed that SVM and RF outperformed both the Simple Arithmetic Mean (SAM) method and the ANN-based ensemble approach.

The integration of these advanced techniques in multimodel ensembles provides a more reliable projection framework for assessing future climate change impacts. By leveraging both statistical and machine learning methods, climate scientists can refine uncertainty quantification and improve the precision of localized climate predictions. Future research should continue exploring innovative MME methodologies that combine physics-based model simulations with data-driven approaches to enhance the reliability of climate change projections.

2.6 Reanalysis Data (ERA5)

Reanalysis data products have emerged as vital tools in climate research, aiming to balance two core objectives: achieving high synoptic accuracy by assimilating diverse observational data and producing temporally consistent, spatially continuous datasets for long-term climate analysis (Bengtsson & Shukla, 1988; Soci et al., 2024; Trenberth & Olson, 1988). In Bangladesh, the reliability of observed climate data is often compromised by spatial and temporal inconsistencies, largely due to the irregular distribution of meteorological stations and limited coverage in remote or elevated regions. These limitations hinder comprehensive climate assessments based solely on ground observations. As a result, satellite-based and global reanalysis datasets offer a viable alternative by providing high-resolution, gridded climate variables.

Several widely used reanalysis datasets have been developed over time, including NCEP/NCAR (Cavazos & Hewitson, 2005; Kalnay et al., 2018), CFSR and CFSv2 (Gramcianinov et al., 2020; Liu et al., 2018), JRA-25 and JRA-55 (Ebita et al., 2011; S. Kobayashi et al., 2015), and ECMWF products such as FGGE, ERA-15, ERA-40, ERA-Interim, and ERA5 (Dee et al., 2011; Hersbach et al., 2020; Xu et al., 2022). Among these, ERA5 is the most advanced, offering higher spatial-temporal resolution and improved data assimilation capabilities. Among various global reanalysis products, the ERA5 dataset—developed by the European Centre for Medium-Range Weather Forecasts (ECMWF)—has shown notable performance in representing climatic conditions in Bangladesh. Islam & Cartwright (2020) reported that ERA5 accurately captured rainfall and temperature patterns when validated against observed data. Similarly, Zhai et al. (2020) successfully used ERA5 to forecast drought conditions across South Asia. ERA5 represents the latest generation of ECMWF reanalysis products, succeeding ERA-Interim. It incorporates a broader range of assimilated data, offers enhanced spatial and temporal resolution, and employs an advanced four-dimensional variational assimilation system (4DVAR) (Hersbach et al., 2020). Its improved performance and granularity make it particularly suitable for studies in regions with sparse observational networks, such as Bangladesh.

Given these advantages, ERA5 was selected for the present study to supplement gaps in ground-based meteorological records and to support robust analysis of climatic variables, especially in regions with limited observational infrastructure. The choice aligns with recent studies that have validated its reliability and applicability for hydrometeorological research across South Asia (McNicholl et al., 2022; Singh & Mohanty, 2023; Tarek et al., 2020).

Table 2.3 presents the descriptive statistics and associated biases in precipitation and temperature by comparing observational data with outputs from CMIP5 and CMIP6 model simulations across South Asia. The analysis includes a multi-year average at the monthly time scale to assess the simulation capabilities of both model ensembles (Zhai et al., 2020).

The findings reveal that although both CMIP5 and CMIP6 models deviate from observations, CMIP6 exhibits improved performance, with reduced biases and better representation of seasonal temperature and precipitation. This reflects advancements in model structure, resolution, and updated forcings. Overall, CMIP6 shows enhanced simulation capability, particularly at the monthly scale, supporting its growing use in regional climate assessments across South Asia, particularly Bangladesh

Table 2.3: Descriptive Statistics and Biases of Precipitation and Temperature: ERA5 vs CMIP5/CMIP6 over South Asia for 1986–2005 (Zhai et al., 2020).

Statistical tests	ERA5 vs CMIP5		ERA5 vs CMIP6	
	Precipitation (mm)	Temperature (°C)	Precipitation (mm)	Temperature (°C)
Correlation Coefficient (CC)	0.97	0.98	0.98	0.99
Nash-Sutcliffe efficiency coefficient (NSE)	0.73	0.85	0.94	0.9
Root mean square deviation (RMSD)	9.68	0.24	5.53	0.16
Coefficient of determination (R^2)	0.96	0.99	0.98	0.99
Bias	20.92	-3.33	8.52	-0.18

Chapter 3

Methodology*

3.1 General

This chapter describes the method in this analysis for assessing the future climate extremes over Bangladesh in the context of CMIP6 MME simulations. It details the data sources, including station-based meteorological observations, reanalysis datasets, and bias-corrected global climate model outputs, along with the approaches for data validation, downscaling, and bias correction. The study further describes the selection and analysis of temperature and precipitation extreme indices, the use of statistical and geospatial tools for trend analysis, and the evaluation of climate projections across different SSPs. The methodology ensures a comprehensive assessment of climate variability, enabling robust projections and identification of vulnerable regions for effective climate adaptation planning.

---

*This chapter is part of the following publication:

> Nazrul, F. B., Karim, M. R., Pavan, W., & Kamruzzaman, M. (2025). Future Climate Extremes in Bangladesh: Insights from a Multi-Model Ensemble of CMIP6 Simulations. Earth Systems and Environment, 1-20. https://doi.org/10.1007/s41748-025-00681-4

3.2 Study Area

Bangladesh is a South Asian nation located within the Bengal Delta, bordered by India on the west, north, and northeast, and Myanmar to the southeast, with the Bay of Bengal forming its southern boundary (Nazrul et al., 2025). Geographically, the country extends between 20°34′ to 26°38′ N latitude and 88°01′ to 92°41′ E longitude, covering a total area of 143,998 km^2 (Kamruzzaman et al., 2019). It stretches 625 km from north to south and 305 km from east to west, making it one of the most densely populated and climate-vulnerable countries in the world. With its low-lying topography, nearly half of its surface area lies below the 10 m contour line, making it particularly susceptible to flooding and sea-level rise (Nasreen et al., 2023). The topography of Bangladesh is highly diverse, characterized by a deltaic plain in the central and western regions, sandy beaches and hilly areas in the southeast, and a vast mangrove forest (Sundarbans) in the southwest (Alam & Khan, 2022; Brammer, 2014). The country is positioned at the lowermost reaches of three major river systems: the Ganges–Padma, Brahmaputra–Jamuna, and Surma–Meghna river systems. The presence of 230 rivers, many of which swell unpredictably during monsoon rains, significantly heightens the risk of severe flooding (Rahman et al., 2007; Rahman & Salehin, 2013). Additionally, the inflow of river water from melting Himalayan glaciers in the north, combined with rising sea levels from the Bay of Bengal, further exacerbates climate-induced hazards in Bangladesh.

Bangladesh has a tropical monsoon climate, characterized by significant seasonal variations in temperature, humidity, and rainfall. The country is predominantly covered by floodplains, with only a few hilly regions in the southeastern and eastern parts (Islam et al., 2021). The climate is predominantly characterized by humidity and warmth, accompanied by significant variations in temperature and precipitation throughout the year. The four primary seasons observed in Bangladesh are winter (December–February), which is the driest and coolest period, with average temperatures ranging between 16–20°C and nighttime temperatures dropping to around 10°C (Rahman et al., 2020). In the northern parts, temperatures can fall as low as 5°C (Abdullah et al., 2022). The pre-monsoon season (March–May) is characterized by a hot and humid summer, with maximum temperatures ranging from 38°C to 41°C, making April the hottest month. The monsoon season (June–

September) is the wettest, receiving nearly 70% of the total annual rainfall, with July being the rainiest month, recording up to 498 mm of precipitation (Kamruzzaman et al., 2021). The post-monsoon period (October–November) marks the transition to mild temperatures and moderate humidity levels. Bangladesh's mean annual temperature is approximately 25.71°C, but it varies significantly across regions and seasons (World Bank, 2024). The mean daily relative humidity remains high at 80%, and the evapotranspiration rate is estimated at 3.72 mm/day (Mallick et al., 2022a; Kamruzzaman et al., 2023c). The average monthly precipitation (Pr), maximum temperature (T_{max}), and minimum temperature (T_{min}), obtained from the Bangladesh Meteorological Department (BMD), are presented in Figure 3.1 (URL: https://live6.bmd.gov.bd/).

The annual rainfall in Bangladesh varies between 1,536 mm to 4,124 mm, with a 30-year average of 2,410 mm (Kamruzzaman et al., 2021). The majority of precipitation is accounted for by monsoon rainfall, while the pre-monsoon and post-monsoon seasons contribute to the residual rainfall. However, monthly variability in rainfall is evident, posing challenges for agriculture, water resource management, and disaster preparedness (Jerin et al., 2021). Several climate change projections indicate a significant rise in both temperature and precipitation extremes, leading to more frequent and intense climate-related disasters (Clarke et al., 2022; Dastagir, 2015; Rahman et al., 2023). Observational meteorological data show an increasing trend in maximum and minimum monsoon temperatures at an annual rate of 0.05°C and 0.03°C, respectively. Moreover, studies have recorded a considerable rise in cyclone frequency over the Bay of Bengal, particularly in November and May (Dastagir, 2015).

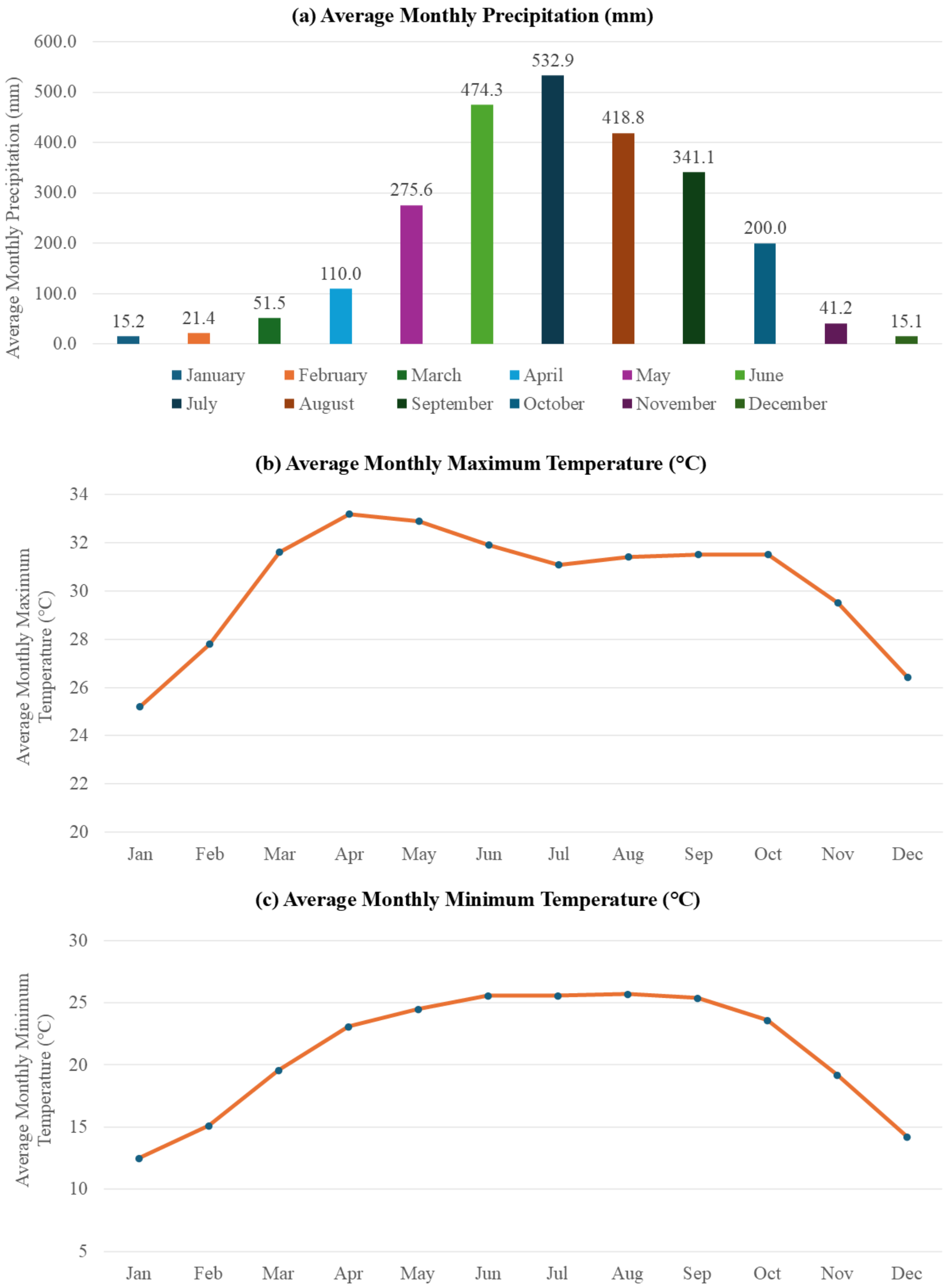

Figure 3.1: Average monthly Pr (mm), Tmax (°C), and Tmin (°C) of Bangladesh from 1985 to 2014.

Bangladesh ranks 7th in the Global Climate Risk Index 2021, placing it among the most vulnerable nations to climate change (Eckstein et al., 2021). The country faces multiple climate hazards, including droughts, which occur every 2.5 years on average (Kamruzzaman et al., 2019). It is also frequently hit by tropical cyclones, leading to massive human and economic losses. The United Nations warns that if sea levels rise by 3 feet within the next 50 years, nearly 25% of Bangladesh's coastline could be submerged, displacing 30 million people (Dastagir, 2015). The observed rate of sea level rise in Cox's Bazar is 7.8 mm per year, which is significantly higher than the global mean rate (Ashrafuzzaman et al., 2022; Sarwar, 2013). Rising sea levels and changing rainfall patterns are increasing salinity in coastal regions, threatening agriculture, fisheries, and drinking water resources. The socio-economic implications of climate change in Bangladesh are severe. Natural disasters in 2007 alone resulted in a loss of 1.8 million tons of rice, affecting the food security of 10 million people. The current annual loss to Bangladesh's gross domestic product (GDP) from climate-induced disasters is estimated at around 1.3 percent, with projections indicating that this could increase to 2% by 2050 and exceed 9% by 2100 under extreme climate scenarios (National Adaptation Plan of Bangladesh (2023-2050), 2022). Between 2000 and 2019, Bangladesh endured 185 extreme weather events, ranking it as the seventh most climate-vulnerable country. In June 2023, a prolonged heatwave pushed temperatures above 40°C. Tropical cyclones have consistently battered coastal areas, causing annual economic losses averaging 0.7% of GDP (International Centre for Climate Change and Development, 2024). Bangladesh has long been on the front lines of climate change, facing repeated impacts from heatwaves, tropical cyclones, floods, and droughts. The most vulnerable populations, especially those reliant on agriculture and fisheries, continue to bear the greatest burden of these climatic disruptions.

The Bangladesh Meteorological Department (BMD) operates 63 weather stations, but only 30 stations with continuous 30-year rainfall records (1976–2005) have been selected for this study due to data availability. The dataset includes historical precipitation, temperature, and extreme weather event records, which are crucial for analyzing climate trends and validating CMIP6 model projections. This study utilizes a high-resolution gridded dataset from ERA5, comprising 193 grid points across Bangladesh. The topographic elevation map of Bangladesh, with 193 ERA5 gridded data points and 30 meteorological observation stations, is shown in Figure 3.2. Table B1 and B2 in Appendix B shows the coordinates of the meteorological stations and ERA5 gridded data points respectively.

Bangladesh's geographical position, low-lying topography, and monsoon-dominated climate make it extremely vulnerable to climate-induced hazards like tropical cyclones, flooding, droughts, and sea-level rise. The combination of rising temperatures, increasing cyclone frequency, and sea-level rise poses a significant threat to livelihoods, infrastructure, and food security. Given these challenges, accurate climate projections are crucial for formulating robust adaptation measures to minimize the adverse effects of climate change on Bangladesh's socio-economic sectors.

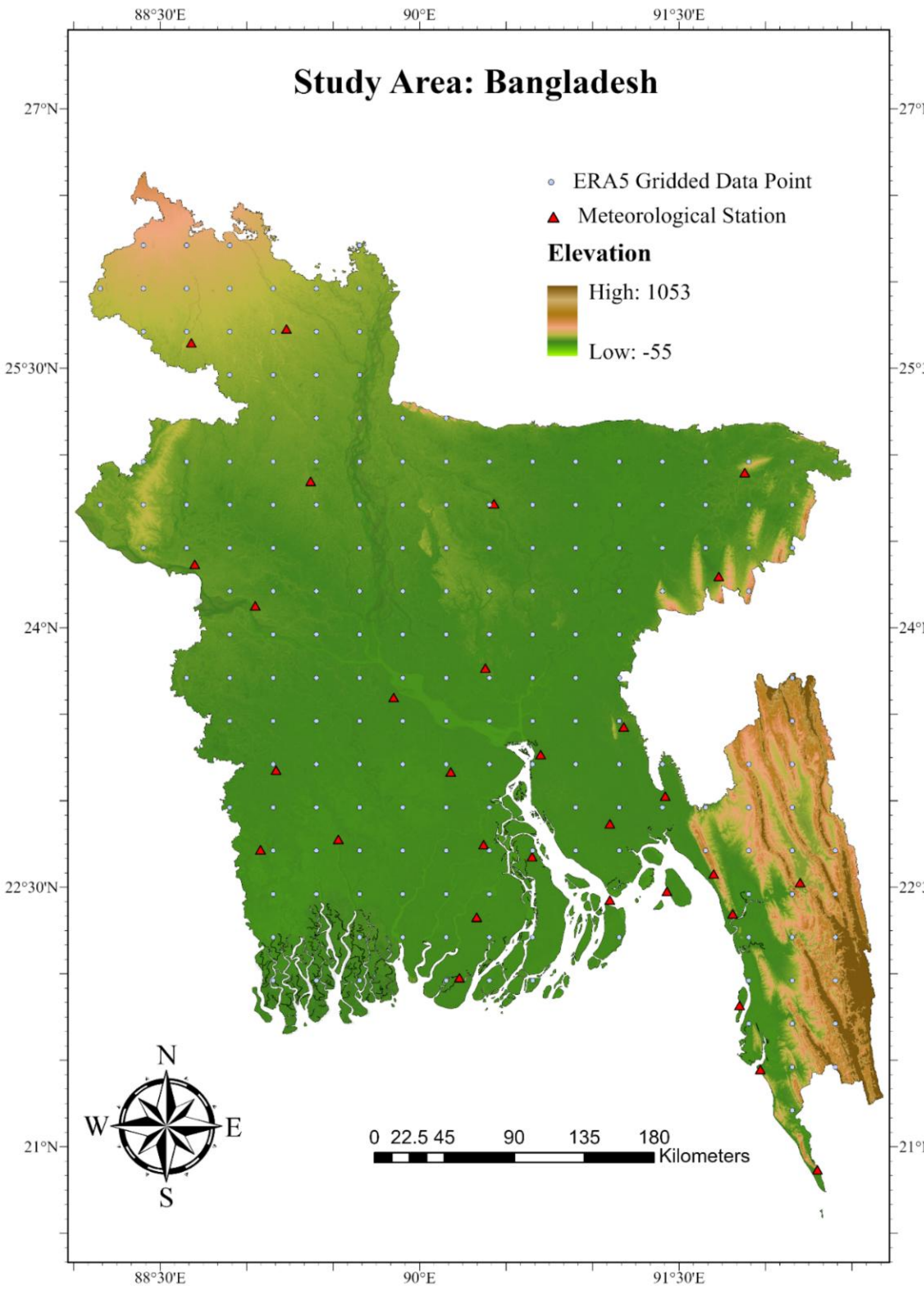

Figure 3.2: Topographic map of Bangladesh

3.3 Data

In this study, three distinct datasets have been utilized: station data, ERA5 reanalysis data, and CMIP6 model data. The CMIP6 dataset comprises 18 climate models, each containing a historical dataset along with three future projections corresponding to different Shared Socioeconomic Pathways (SSPs). Figure 3.3 provides an overview of the datasets employed in this study.

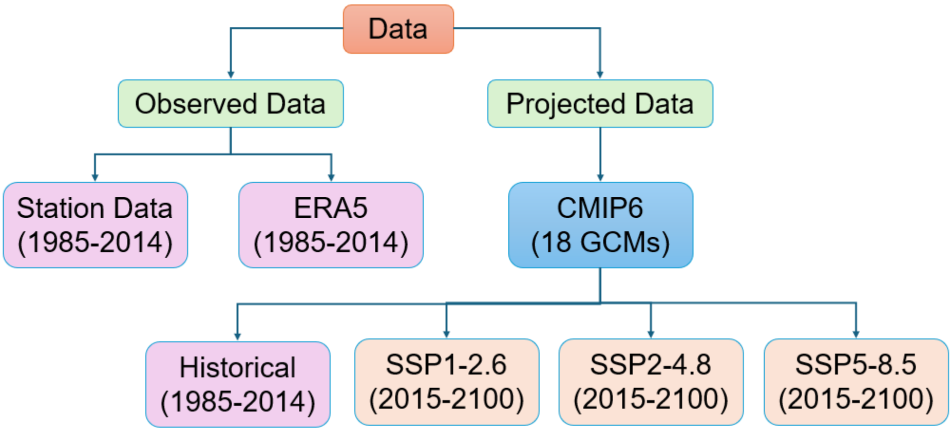

Figure 3.3: Flowchart summarizing the datasets utilized in the Study

3.3.1 Observed Data

This study utilizes the ERA5 reanalysis dataset, obtained from the European Centre for Medium-Range Weather Forecasts (ECMWF) as the observed dataset (Hersbach et al., 2020; URL: https://www.ecmwf.int/en/forecasts/dataset/ecmwf-reanalysis-v5), covering the period from 1985 to 2014. This dataset includes critical climate variables such as Pr (precipitation), T_{max} (maximum temperature), T_{min} (minimum temperature), with a spatial scale of 0.25° x 0.25°, covering 193 grid squares for the studied region. To make agreement of the available data, ERA5 against analyses of 30 meteorological stations located all over Bangladesh were made. We select a 30-year period to minimize the year-to-year variation, which is common practice for the analysis of climate trends.

Station data that used in the present study were obtained from the Bangladesh Meteorological Department (BMD), the government department for meteorological observations in Bangladesh (Nazrul et al., 2025; Kamruzzaman et al., 2023a). When working with observational datasets, missing data and inhomogeneity is a common issue, as station networks are often spatially sparse, and missing records pose challenges in data continuity (Hunziker et al., 2017; Zhang & Thorburn, 2022). Although some data gaps were present in the dataset, the missing values accounted for less than 2% of the total records. To fill in these gaps, interpolation was carried out using the average of the value of the corresponding date from surrounding stations (Jahan et al., 2019; Yang & Hu, 2018). Coordinates of the 30 meteorological stations and 193 grid points used for this study are shown in Appendix B, Tables B1 and B2.

3.3.2 Projected Data

This study used 18 GCMs from CMIP6 to simulate the changes in extreme climatic conditions over the historical (1985–2014) and future (2015–2100) time scales based on temperature and precipitation in near (2015–2044), mid (2045–2074), and far (2075–2100) futures under the SSP1-2.6, SSP2-4.5, and SSP5-8.5 scenarios. The Earth System Grid Federation (ESGF) MetaGrid from Lawrence Livermore National Laboratory (LLNL) (URL: https://aims2.llnl.gov/search/cmip6/) was used to obtain climate model data covering Pr, T_{max}, and T_{min}. The study employs three Shared Socioeconomic Pathways (SSPs): SSP1-2.6, SSP2-4.5, and SSP5-8.5. They refer to greenhouse gas emission and different socio-economic trajectories. SSP1-2.6 seeks to constrain the temperature rise to under 2.0°C by 2100, SSP2-4.5 anticipates a moderate increase of 2.7°C, while SSP5-8.5 characterizes a high-emission trajectory with the maximum projected warming (Nazrul et al., 2025).

To ensure consistency and minimize model bias, the first realization (r1i1p1f1) of each GCM was used in several studies (Babaousmail et al., 2024; Di Virgilio et al., 2022). Since no standardized approach is recommended for GCM selection, and no established guidelines exist for creating a GCM subset (Kamruzzaman et al., 2021), the 18 models were selected based on their data availability. Models containing missing values, incomplete datasets, or irregular time slices were omitted to ensure the reliability of the analysis. The ERA5 dataset, with a grid resolution of 0.25° x 0.25°, was employed for downscaling and bias correction of the GCM outputs. To evaluate the performance of these models, historical observed data from 1985–2014 was used as a benchmark for validation (Nazrul et al. 2025; Kamruzzaman al., 2023a). Table 3.1 presents the essential details of the GCMs, including their developing organizations and spatial resolutions (Deng et al., 2023; Kamruzzaman et al., 2023a and 2023b; Paul & Maity, 2023; Rahman & Islam, 2023). Further details on the selected models are discussed in Chapter 2.

Table 3.1: Lists of the reporting modeling center, data resolution and variant labels for each CMIP6 GCM used (Nazrul et al., 2025).

Modeling center/nation	Name of the GCM	Spatial resolution	Variant label
Australian Community Climate and Earth-System Simulator	ACCESS-CM2	1.87°x1.25°	r1i1p1f1
Australian Community Climate and Earth-System Simulator	ACCESS-ESM1-5	1.87°x1.25°	r1i1p1f1
Canadian Earth System Model	CanESM5	2.8°x2.8°	r1i1p1f1
National Centre for Meteorological Research, France	CNRM-CM6-1	1.4°x1.4°	r1i1p1f1
National Centre for Meteorological Research, France	CNRM-EM2-1	1.4°x1.4°	r1i1p1f1
EC-Earth Consortium	EC-Earth3	0.7°x0.7°	r1i1p1f1
NOAA/ Geophysical Fluid Dynamics Laboratory, USA	GFDL-ESM4	2.0°x2.0°	r1i1p1f1
Institute for Numerical Mathematics, Russia	INM-CM4-8	2.0°x1.5°	r1i1p1f1
Institute for Numerical Mathematics, Russia	INM-CM5-0	2.0°x1.5°	r1i1p1f1
Institut Pierre Simon Laplace, France	IPSL-CM6A-LR	2.5°x1.27°	r1i1p1f1
NIMS-KMA/ South Korea	KACE-1-0-G	1.3°x0.9°	r1i1p1f1
Atmosphere and Ocean Research Institute (The University of Tokyo), National Institute for Environmental Studies, and Japan Agency for Marine-Earth Science and Technology, Japan	MIROC6	1.4°x1.4°	r1i1p1f1

JAMSTEC (Japan Agency for Marine-Earth Science and Technology), AORI (Atmosphere and Ocean Research Institute, The University of Tokyo), NIES (National Institute for Environmental Studies), and R-CCS (RIKEN Center for Computational Science), Japan	MIROC-ES2L	2.8°x2.8°	r1i1p1f1
Max Planck Institute for Meteorology, Germany	MPI-ESM1-2-LR	0.94°x0.94°	r1i1p1f1
Max Planck Institute for Meteorology, Germany	MPI-ESM1-2-HR	1.87°x1.86°	r1i1p1f1
Meteorological Research Institute, Japan	MRI-ESM2-0	1.12°x1.12°	r1i1p1f1
Norwegian Climate Center, Norway	NorESM2-LM	1.0°x1.0°	r1i1p1f1
UK Met Office Hadley Office, UK	UKESM1-0-LL	1.9°x1.3°	r1i1p1f1

3.4 Data Downscaling and Bias Correction

GCMs simulate large-scale climatic conditions but require downscaling for improved spatial resolution. Dynamical downscaling embeds a high-resolution Regional Climate Model (RCM) within a GCM, while statistical downscaling establishes empirical relationships between large-scale predictors and local predictands (Alam, 2011; Chen et al., 2021; Maraun et al., 2010; Zhang & Li, 2021). However, climate models are subject to errors from unrealistic variability, internal climate phase mismatches, and parameterization limitations (Eden et al., 2012; Noguer et al., 1998).

This study applies Simple Quantile Mapping (SQM) for downscaling and bias correction of precipitation (Pr), maximum temperature (T_{max}), and minimum temperature (T_{min}) data over the period 1985–2100, ensuring alignment between modeled and observed distributions (Gudmundsson et al., 2012). The nonparametric empirical approach in SQM effectively reduces systematic biases, outperforms parametric methods, and enhances climate projection reliability (Enayati et al., 2021; Heo et al., 2019). Due to its effectiveness, SQM is widely used for GCM downscaling (Kamruzzaman et al., 2025; Pierce et al., 2015).

The bias correction methodology followed a three-step process as outlined by Kamruzzaman et al., (2019). First, GCM data for the study region was extracted, followed by the quantification of biases. At the final stage, bias correction approaches were utilized and enhanced. The differences between the observed and simulated cumulative distribution functions (CDFs) were calculated over the observation period and used to adjust future simulations at a given percentile (Nazrul et al., 2025).

The bias correction equation used in this study is represented as follows in equation (1):

$$x_p'(t) = x_p(t) + F_{obs}^{-1}(F_{p.sim}\left(x_p(t)\right)) - F_{r.sim}^{-1}(F_{p.sim}\left(x_p(t)\right)) \tag{1}$$

where $F()$ and $F^{-1}()$ denote the cumulative distribution function (CDF) of the daily data and its inverse, respectively and the terms $x_p'(t)$ and $x_p(t)$ refer to the bias-corrected and initial future projections at day t (Nazrul et al. 2025). The subscripts $p.sim, r.sim$, and obs refer to future projections, retrospective simulations, and observed daily data, respectively (Nazrul et al., 2025; Kamruzzaman et al., 2019).

Bias correction was performed using ERA5 grids, ensuring consistency with observed climate conditions. The software package of rSQM (Cho et al., 2016, URL: https://rdrr.io/cran/rSQM/) was used for downscaling GCM simulations.

3.5 Multi-Model Ensemble

This study utilized a Multi-model Ensemble (MME) method was used, and outputs from 18 CMIP6 General Circulation Models (GCMs) (Table 3.1) were averaged to reduce the differences between individual models and improve the robustness of climate projection. The ETCCDI indices (Table 3.2) were computed for the historical period (1985–2014) and for three future scenarios: SSP1-2.6, SSP2-4.5, and SSP5-8.5, across three future timeframes: near future (2015–2044), mid-future (2045–2074), and far future (2075–2100). These indices, derived from MME simulations of Pr, T_{max}, and T_{min}, give the sense of short and long timescale extremes occurring throughout this vast mangrove area, crucial for prospective climate risk appraisal in Bangladesh.

The MME was calculated as an of the median value using the equation (2), and differences between projected and historical periods were analyzed to estimate future climate changes (Nazrul et al., 2025; Kamruzzaman et al., 2023a).

$$S(t) = \frac{1}{N}\sum_{i=n}^{N} P_n(t) \tag{2}$$

Here, $S(t)$ represents the ensemble mean at time t, N indicates the total number of GCMs used during ensemble, and $P_n(t)$ refers to the projection output from the n-th GCM at time t.

In order to further improve the projection scenario, spatial analyses were done also to identify areas in Bangladesh, which are more vulnerable from the effect of climate change. Acknowledging the uncertainty inherent in climate modeling, due to the complexity of the earth's environmental system and challenges in data accessibility, the MME approach was employed to reduce projection uncertainties and offer a comprehensive understanding of climate trends (Nazrul et al., 2025). The projected MME values for future periods were compared to the historical downscaled MME to assess anticipated changes, ensuring a robust evaluation of climate extremes and variability.

3.6 Analysis of the Extreme Climate Indices

In this study, extreme climate indices ETCCDI were analyzed to assess precipitation and temperature extremes across Bangladesh. A total of 23 standardized indices, encompassing percentile-based, threshold-based, absolute, and other types, were employed in this study to capture the occurrence, duration, and severity of extreme events. Total 13 temperature extreme and 10 precipitation extreme indices were used. Table 3.2 shows the selected extreme temperature and precipitation indices. These indices were calculated using daily maximum temperature, minimum temperature, and precipitation data following the methodologies outlined in several studies (Zhang et al., 2004 and 2011; Klein Tank et al., 2009; Yin & Sun, 2018; URL: https://etccdi.pacificclimate.org/list_27_indices.shtml). The use of standardized indices ensures global comparability and allows for consistent detection of trends in climate extremes across regions. To address potential issues such as data inhomogeneity, bias correction techniques and quality control measures were applied prior to the calculation of indices. This approach enables robust and systematic evaluation of historical and projected changes in climate extremes, facilitating the identification of regional vulnerabilities under different emission scenarios.

Table 3.2: Selected extreme temperature indices and precipitation indices (Nazrul et al., 2025).

Indicator name	Indices	ETCCDI definition	Units
Annual maxima of daily maximum temperature	TXx	Annual maxima value of daily maximum temperature	°C
Annual maxima of daily minimum temperature	TNx	Annual maxima value of daily minimum temperature	°C
Annual minima of daily maximum temperature	TXn	Annual minima value of daily maximum temperature	°C
Annual minima of daily minimum temperature	TNn	Annual minima value of daily minimum temperature	°C
Cold nights	TN10p	Percentage of days when daily minimum temperature <10th percentile	%
Cold days	TX10p	Percentage of days when daily maximum temperature <10th percentile	%

Warm nights	TN90p	Percentage of days when daily minimum temperature >90th percentile	%
Warm days	TX90p	Percentage of days when daily maximum temperature >90th percentile	%
Summer days	SU	Annual count when daily maximum temperature >25 °C	d
Tropical nights	TR	Annual count when daily minimum temperature >20 °C	d
Diurnal temperature range	DTR	Annual mean difference between daily max and min temperature	°C
Warm spell duration index	WSDI	Annual number of days with at least 6 consecutive days when Tmax >90th percentile	d
Cold spell duration index	CSDI	Annual number of days with at least 6 consecutive days when Tmin <10th percentile	d
Max 1-day precipitation amount	RX1day	Annual maximum 1-day precipitation	mm
Max 5-day precipitation amount	RX5day	Annual maximum consecutive 5-day precipitation	mm
Very wet days	R95p	Annual total precipitation from days >95th percentile	mm
Extremely wet days	R99p	Annual total precipitation from days >99th percentile	mm
Heavy precipitation days	R10mm	Annual count when precipitation ≥10 mm	d

Very heavy precipitation days	R20mm	Annual count when precipitation ≥20 mm	d
Consecutive dry days	CDD	Maximum number of consecutive days when precipitation <1 mm	d
Consecutive wet days	CWD	Maximum number of consecutive days when precipitation ≥1 mm	d
Total precipitation in wet days	PRCPTOT	Annual total precipitation from days ≥1 mm	mm
Simple daily intensity index	SDII	The ratio of annual total precipitation to the number of wet days (≥1 mm)	mm

3.7 Significance Analysis

The statistical significance of the projected change in precipitation and temperature extremes was examined using the Wilcoxon rank-sum test as a nonparametric counterpart of the two-sample t-test (Nazrul et al. 2025). This approach is well-suited for atmospheric data analysis (Nazrul et al., 2025; Wang et al., 2024; Wilcoxon, 1992) as it does not require the assumption of normality. The analysis compared future projections with the historical baseline at a 95% confidence level, ensuring a robust assessment of significant differences in climate distributions (Nazrul et al., 2025). In addition to strengthening the reliability of detecting climatic trends and enabling thorough variability descriptions for various time-scales, this technique makes less assumptions about the distribution of the data.

3.8 Software and Analytical Tools

This study employed a range of software applications to support data handling, analysis, and visualization. The raw data were organized and processed using Microsoft Excel, while the advanced data processing and the treatment were conducted by R programming language and SPSS sussequestly, which allowed a detailed analysis of the relationships and the testing of the significance (Jihan et al., 2025). Additionally, ArcGIS Pro was utilized for spatial analysis and the creation of visual maps, helping to identify areas within Bangladesh that are particularly vulnerable to climate change impacts.

Chapter 4

Results and Discussion[*]

4.1 General

This chapter presents a comprehensive analysis of the projected changes in temperature and precipitation extremes in Bangladesh based on CMIP6 Multi-Model Ensemble (MME) simulations. The results highlight variations in annual maximum and minimum temperatures, frequency of extreme hot and cold events, and diurnal temperature range, providing insights into future warming trends across different Shared Socioeconomic Pathways (SSPs). Additionally, changes in precipitation extremes, including intensity, frequency, and duration of heavy rainfall and dry spells, are examined to assess potential flood and drought risks. The discussion contextualizes these findings by comparing them with existing literature, evaluating their implications for climate adaptation strategies, and emphasizing the need for sustainable water resource and disaster management policies in response to increasing climate variability.

---

[*]This chapter is part of the following publication:

Nazrul, F. B., Karim, M. R., Pavan, W., & Kamruzzaman, M. (2025). Future Climate Extremes in Bangladesh: Insights from a Multi-Model Ensemble of CMIP6 Simulations. Earth Systems and Environment, 1-20. https://doi.org/10.1007/s41748-025-00681-4

4.2 Observed Data

The ERA5 dataset used as the observational reference in this study, it covers the period 1985–2014. It contains the key climate factors in the area (Pr, T_{max} and T_{min}), with the resolution of 0.25° × 0.25° grid cells, including 193 grid cells across the case study area. To verify the accuracy of the dataset, ERA5 data were agreed with the observations from 30 meteorological stations distributed across Bangladesh. Based on the location and coordinates provided in Appendix B (Tables B1 and B2), the ERA5 grid points demonstrate a well-distributed spatial coverage across the study region. In contrast, the station data reveal noticeable gaps and wider spacing, indicating less uniform coverage compared to the gridded ERA5 dataset.

The Figure 4.1 presents a comparative analysis between ERA5 reanalysis data and station-observed data for Bangladesh over a historical period, focusing on three key climate variables: Pr, T_{max} and T_{min}.

In the case of average monthly precipitation, ERA5 successfully captures the overall seasonal pattern. However, it slightly overestimates rainfall during the peak monsoon months (June to August). Despite this overestimation, the corresponding scatter plot shows a strong correlation between ERA5 and station data, with an R^2 value of 0.9201, indicating good agreement in monthly precipitation distribution.

For average monthly maximum temperature, ERA5 tends to underestimate observed values during the hotter months (April to June), as reflected by the gap between the ERA5 (green line) and station data (purple line). Nevertheless, the R^2 value of 0.9559 demonstrates a strong linear relationship, suggesting that ERA5 still reliably captures maximum temperature trends.

In the case of average monthly minimum temperature, ERA5 and station data align very closely throughout the year. This agreement is further supported by the scatter plot, which yields a very high R^2 value of 0.9907, indicating excellent consistency and reliability of ERA5 in representing minimum temperatures.

Overall, the figure demonstrates that ERA5 reanalysis data aligns well with station-observed data for temperature variables, particularly minimum temperature—and shows a strong correlation for precipitation despite minor seasonal biases. These findings support the suitability of ERA5 as a reliable observational baseline for evaluating and bias-correcting climate model outputs in this study.

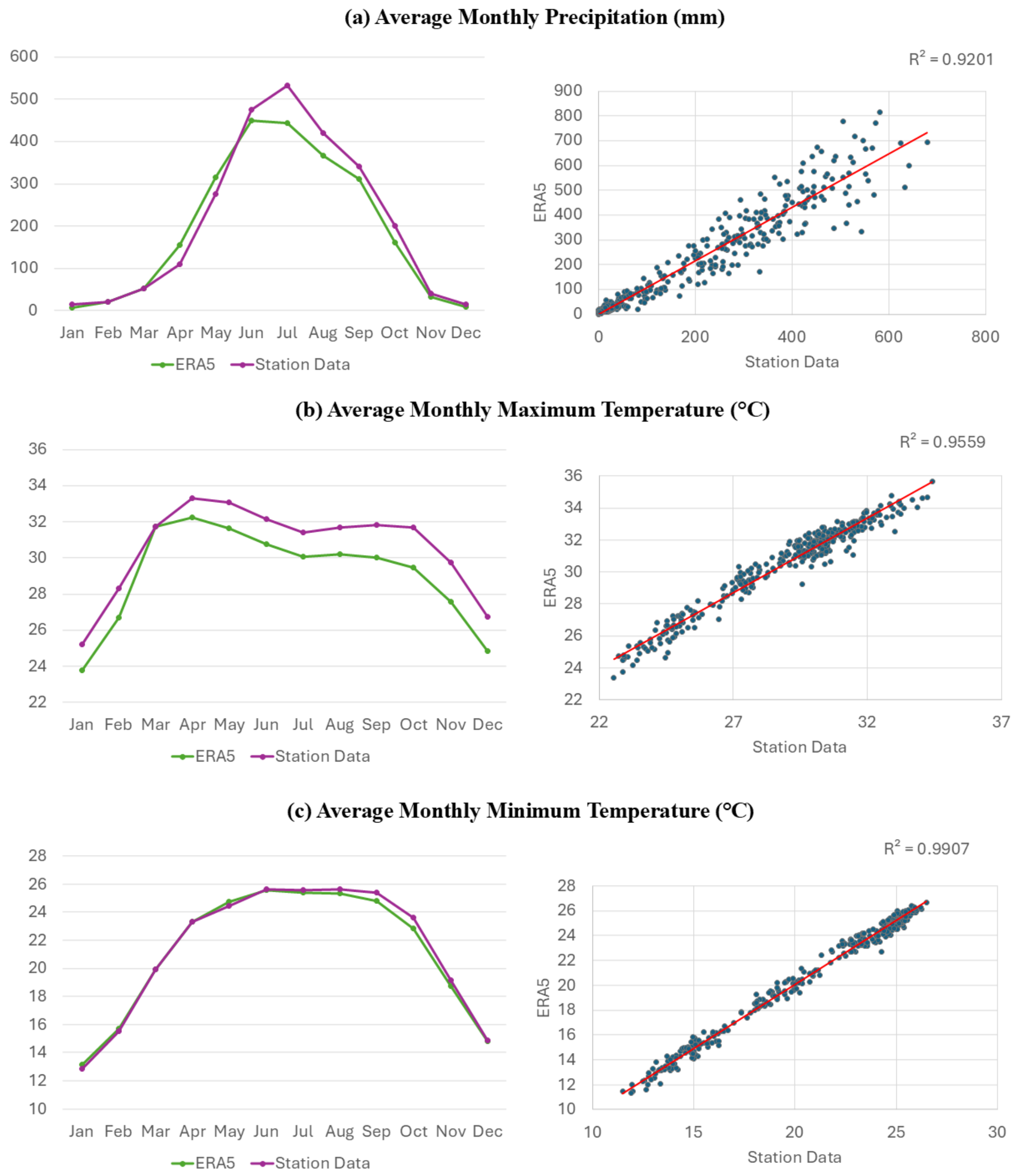

Figure 4.1: Comparison of ERA5 reanalysis data with station observations for (a) Average monthly precipitation, (b) Average monthly maximum temperature, and (c) Average monthly minimum temperature in Bangladesh (1985–2014)

4.3 Reproducibility of the Climate Models

In this study, the reproducibility of climate variables: annual average precipitation, maximum temperature and minimum temperature from 18 CMIP6 GCMs was evaluated for the historical period of 1985–2014 (a total of 30 years). This evaluation was conducted by comparing model outputs with the observed ERA5 dataset for the corresponding period, as illustrated in Figure 4.2.

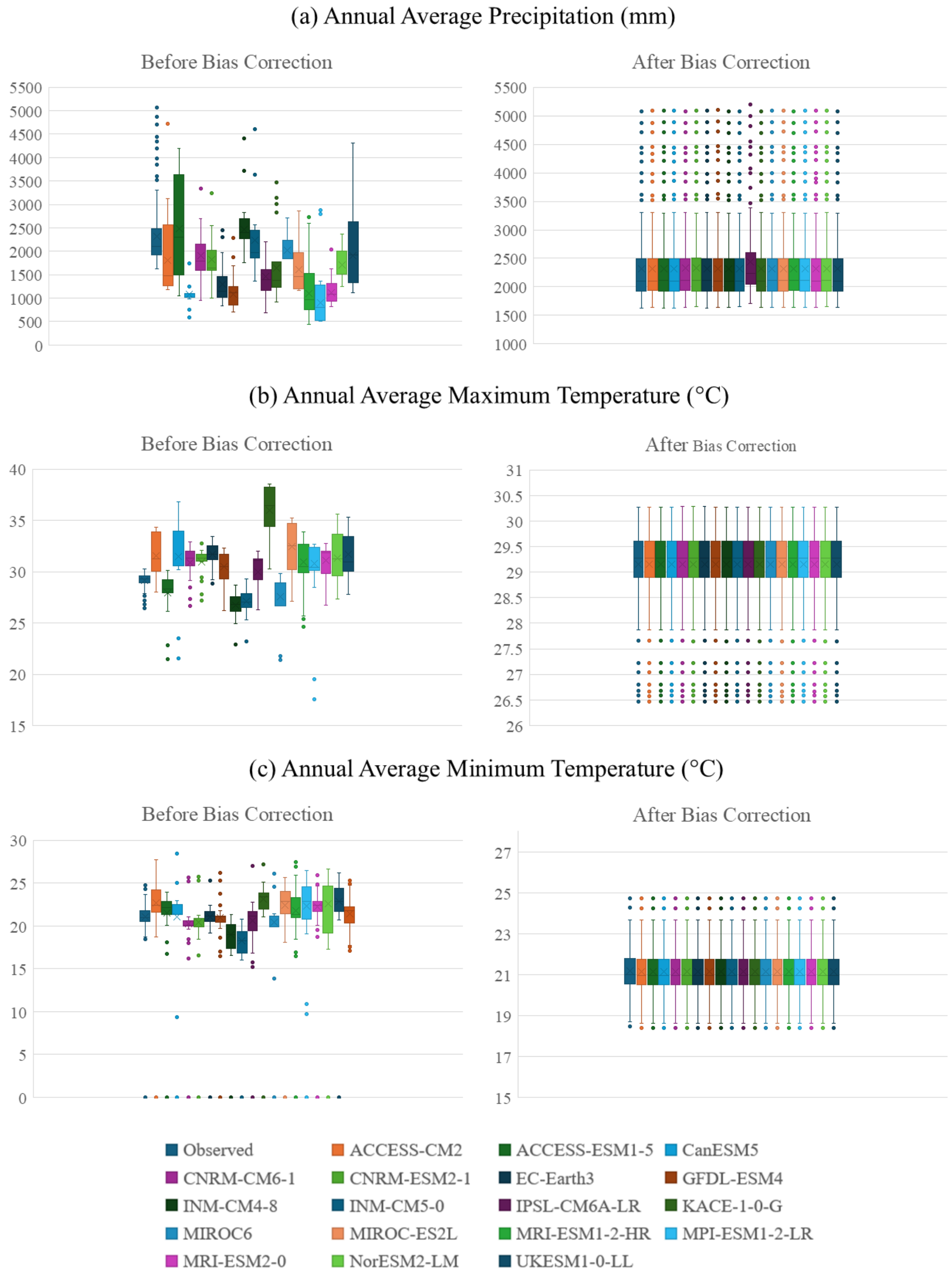

Figure 4.2: Box-and-whisker plots illustrating the improvement of 18 GCMs in (a) Annual average precipitation, (b) Annual average maximum temperature, and (c) Annual average minimum temperature compared to the observed data.

Here, the statistical characteristics such as the median, interquartile range, and mean values of the climate variables from each GCM were compared with the observed dataset to evaluate model performance before (raw) and after bias correction. The bias-corrected GCM outputs were found to reasonably replicate the observed patterns of daily rainfall, as well as minimum and maximum temperatures during the historical period, whereas the raw GCM outputs showed significant deviations from the observed data. The percentage errors before bias correction were 22.81% for precipitation (Pr), 5.50% for maximum temperature (T_{max}), and 3.46% for minimum temperature (T_{min}). After applying bias correction, these errors were significantly reduced to 0.51%, 0.0008%, and 0.20%, respectively.

4.4 Agreement of Climate Models

The evaluation of CMIP6 GCMs, through comparison of bias-corrected and raw outputs against observed records, highlights substantial biases in precipitation and temperature simulations (Figure. 4.3). The Multi-Model Ensemble (MME) in its raw form exhibited cold biases, underestimating T_{max} and T_{min} (Figure 4.3. c,e), post-monsoon and winter months, when the difference was of 1.15–1.56°C and 0.45–1.73°C, respectively. T_{max}, on the other hand, was slightly overestimated during the pre-monsoon and early post-monsoon periods by 0.44–2.17°C and 0.68–2.41°C, respectively, which was in line with those reported by Kamruzzaman et al. (2023a). Similarly, T_{min} was underestimated from April to September by 0.56–2.09°C.

The raw GCM precipitation simulations exhibited considerable dry biases (Figure 4.3.a), particularly underestimating rainfall from June to September by a range of 15.40–162.10 mm/month, 76.51–260.54 mm/month, and 7.85–100.52 mm/month, respectively, while overestimating winter rainfall (December–January) by approximately 5.42–8.00 mm/month consistent with the findings of Kamruzzaman et al., (2024). These biases indicate that unprocessed CMIP6 MME simulations struggle to capture seasonal variations in precipitation and temperature accurately.

To correct these discrepancies, the Simple Quantile Mapping (SQM) bias correction technique was applied, significantly improving the alignment between modeled and observed data (Figure 4.3. b,d,f). After bias correction, the coefficient of determination (R^2) for precipitation improved from 0.74 to 0.99, demonstrating a near-perfect match. A strong similarity was observed in maximum and minimum temperatures, with the R^2 values improving from 0.67 and 0.76, respectively, to nearly 1 after bias correction. Biases in Pr, T_{max} and T_{min} were also reduced, enhancing the accuracy of future climate projections. These improvements highlight the effectiveness of bias correction techniques in refining raw GCM outputs for regional climate assessments. The results summarized in Table 4.1 highlight the overall effectiveness of the bias correction methods employed.

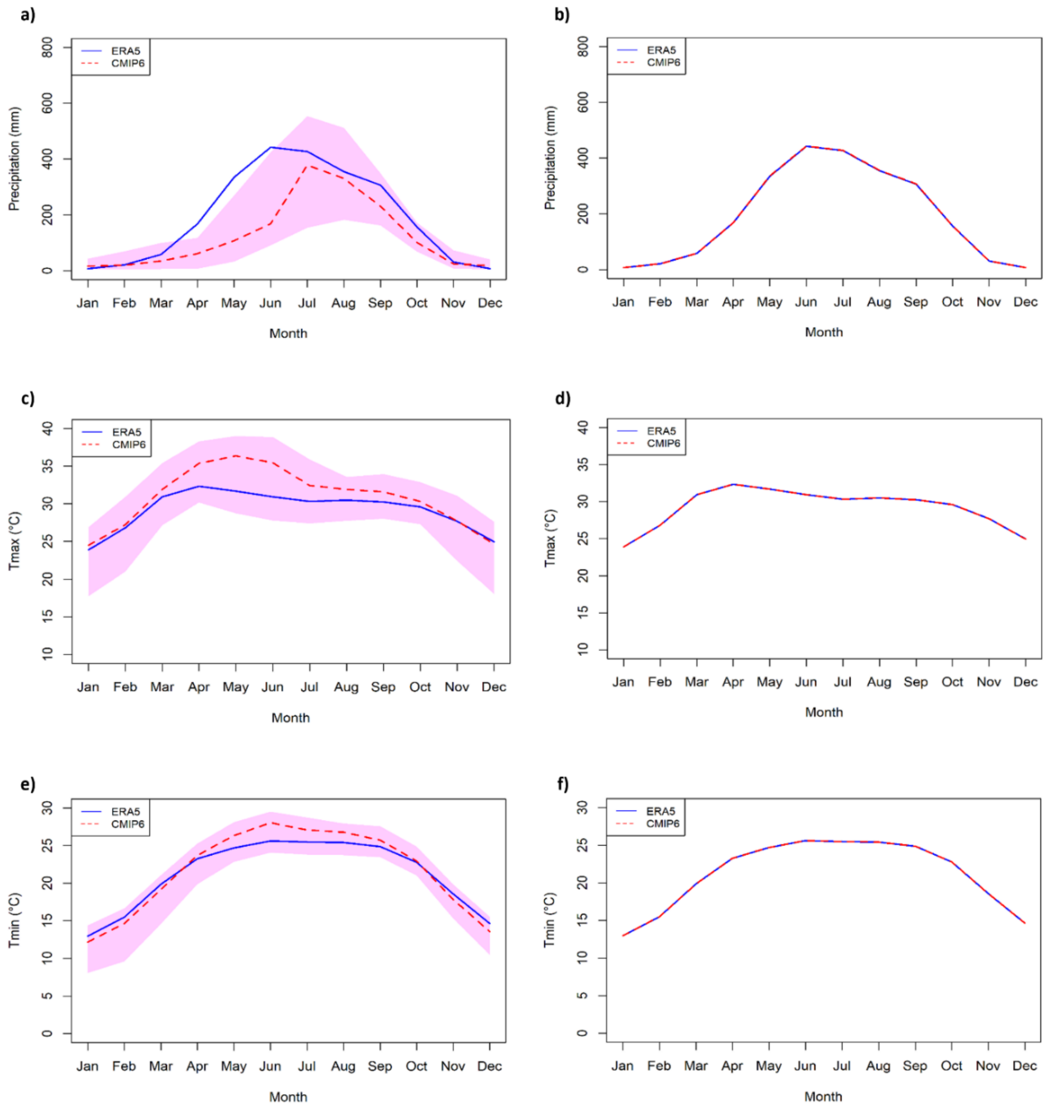

Figure 4.3: Monthly cycles of precipitation (mm), maximum temperature (°C), and minimum temperature (°C) are compared for the historical period (1985–2014) before and after bias correction. Panels (a), (c), and (e) illustrate the original simulations, whereas panels (b), (d), and (f) show the bias-corrected outputs. Uncertainty is represented by the shaded area, corresponding to one standard deviation across the 18 CMIP6 GCMs.

Table 4.1: Statistical comparison of observed data with CMIP6 MME data before and after bias correction for the period 1985–2014.

Parameters	Observed median (ERA5)	Multi Model Ensemble (MME)				
		Before bias correction			After bias correction	
		Median	R^2	Remarks	Median	R^2
Pr	2107.41	1626.65	0.74	Underestimated	2118.22	0.99
T_{max}	29.28	30.89	0.67	Overestimated	29.28	0.99
T_{min}	21.02	21.75	0.76	Overestimated	20.97	0.99

4.5 Evaluation of Bias-Corrected Climate Model Outputs

Figure 4.4 presents the simulated Pr, T_{max}, and T_{min} from the MME median of 18 CMIP6 GCMs, comparing raw bias-corrected data before and after adjustment to ERA5 observations. The findings indicate notable biases in the raw MME outputs, particularly in precipitation and temperature estimates (Figure. 4.4. b, e, h).

The raw mean annual precipitation exhibited a wet bias of up to 25% in the southeastern region, while the northwestern region experienced a dry bias of up to

30% (Figure 4.4. b). Similarly, T_{max} was overestimated in the northern region by up to 3°C while being underestimated by up to 1°C in the south-central and southeastern regions (Figure 4.4. e). Additionally, T_{min} was overestimated by approximately 1.42–5°C across various locations (Figure 4.4. h).

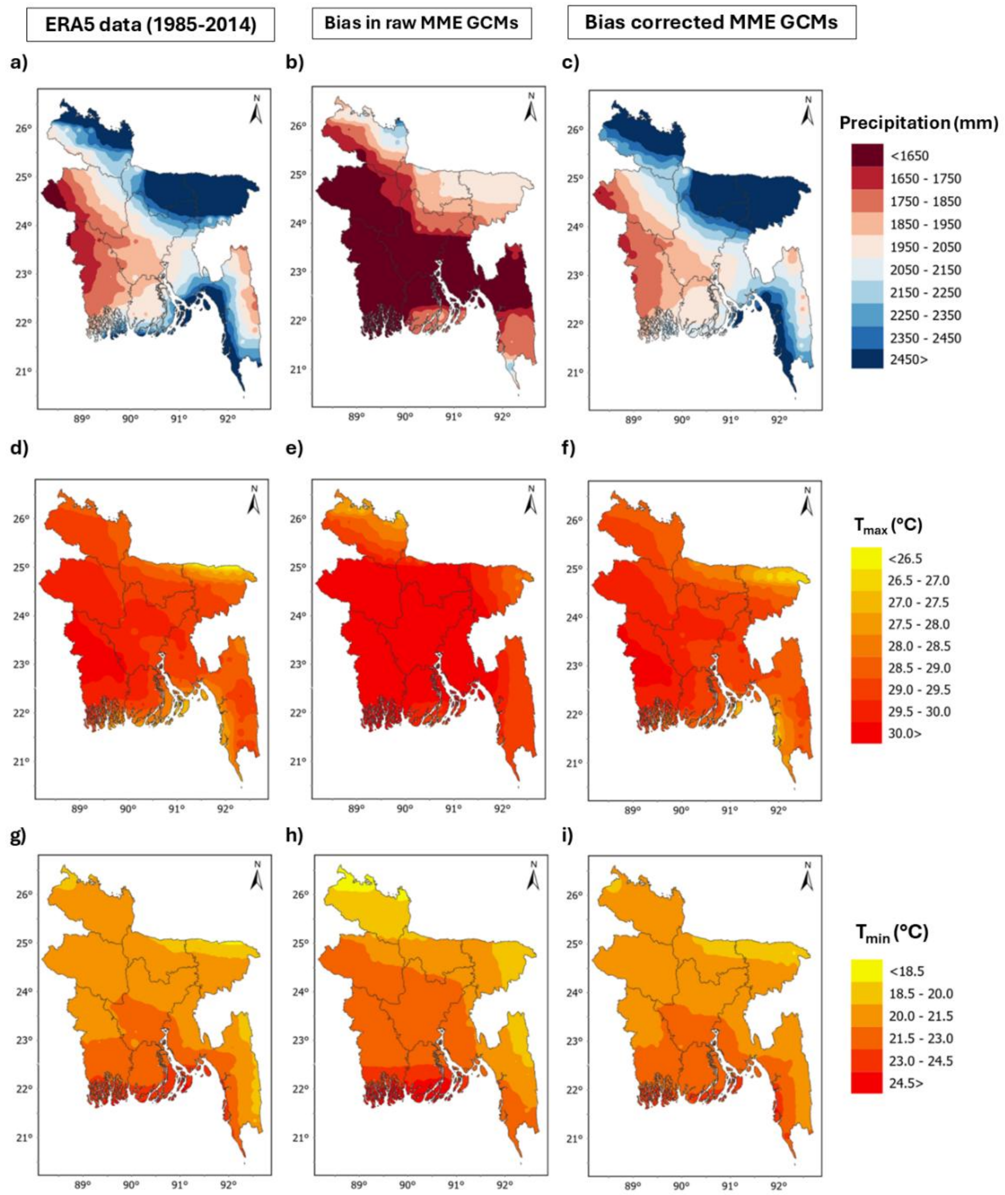

Figure 4.4: Comparison of the ERA5, MME mean before bias correction and after bias correction for the historical period (1985–2014) in terms of (a,b,c) annual precipitation (%), (d,e,f) maximum temperature (°C), and (g,h,i) minimum temperature (°C); The bias is estimated relative to ERA5 data.

To correct these biases, a Simple Quantile Mapping (SQM) technique was applied. After bias correction, precipitation biases were reduced to less than 3 mm/month, while T_{max} and T_{min} biases closely matched the ERA5 observations (Figure. 4.4. c, f, i). The implementation of the quantile mapping (QM) method significantly improved the accuracy of all three climatic variables, ensuring better alignment with observed historical climate data.

4.6 Climate Change of the Parameters

4.6.1 Precipitation

Figure 4.5 illustrates projected precipitation anomalies (%) from 2015 to 2100, using 1985–2014 as the baseline period for different Shared Socioeconomic Pathways (SSPs). The results indicate distinct trends in precipitation changes across scenarios.

For SSP1-2.6 (black line), precipitation anomalies remain consistently positive, suggesting a gradual increase in rainfall throughout the century. The projected increase ranges from 2.5% to 17%, peaking at 20% toward the late 21st century. This trend implies improved water availability, benefiting agriculture and ecosystems, but may necessitate adaptive water resource management.

In contrast, SSP2-4.5 (blue line) exhibits high variability in precipitation anomalies, with no clear long-term trend. The fluctuations indicate periods of increased and decreased precipitation, which could create challenges for flood management and water resource planning.

SSP5-8.5 (red line) projects the highest precipitation anomalies, with increases ranging from 3% to 51%. This scenario suggests a significantly wetter climate compared to the baseline period, with both benefits and risks. While enhanced water availability could support agriculture and hydropower, the increased intensity of rainfall may escalate flood risks and extreme weather events, necessitating robust climate adaptation strategies.

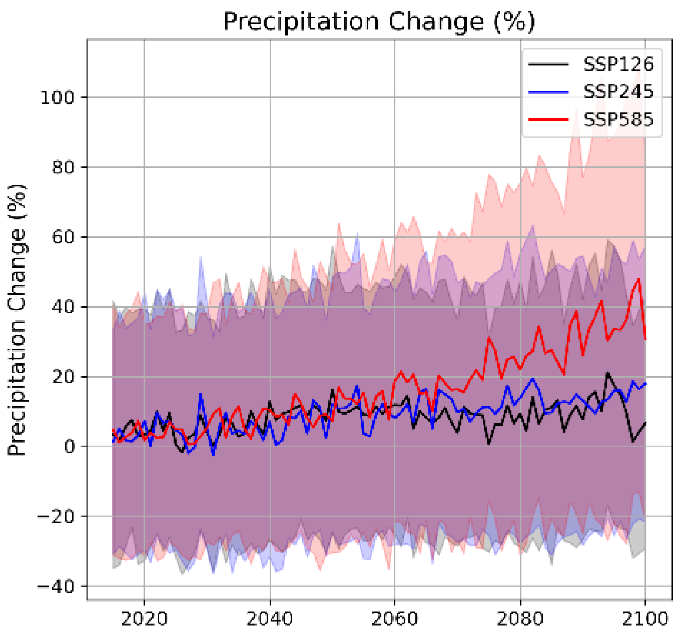

Figure 4.5: Changes in MME mean annual precipitation (%) relative to 1985–2014, with uncertainty shaded (one standard deviation, 18 CMIP6 GCMs).

4.6.2 Maximum Temperature

Figure 4.6 presents maximum temperature (T_{max}) anomalies (°C) from 2015 to 2100, using 1985–2014 as the baseline period, under different SSPs. The findings indicate a steady rise in T_{max} across all scenarios, with varying degrees of warming.

Under SSP1-2.6 (black line), T_{max} anomalies gradually rise, starting at 0.25°C in 2015 and reaching 1.2°C by 2100. This scenario suggests a moderate warming trend, aligning with efforts to limit global temperature rise through low-emission pathways.

For SSP2-4.5 (blue line), the T_{max} anomalies follow an increasing trajectory, with greater fluctuations compared to SSP1-2.6. The T_{max} anomaly starts at 0.23°C in 2015 and reaches 1.85°C by 2100, indicating a higher warming potential with moderate greenhouse gas emissions.

SSP5-8.5 (red line) exhibits the most significant T_{max} increase, with anomalies rising from 0.1°C in 2015 to 3.8°C by 2100. This scenario indicates uncontrolled emissions and substantial warming, posing severe risks for heat stress, agriculture, and overall climate stability.

Overall, the estimated increase in temperatures for all) demonstrates the worsening effect of climate change. This underscores the critical importance of mitigation actions that limit warming and lower climate risks.

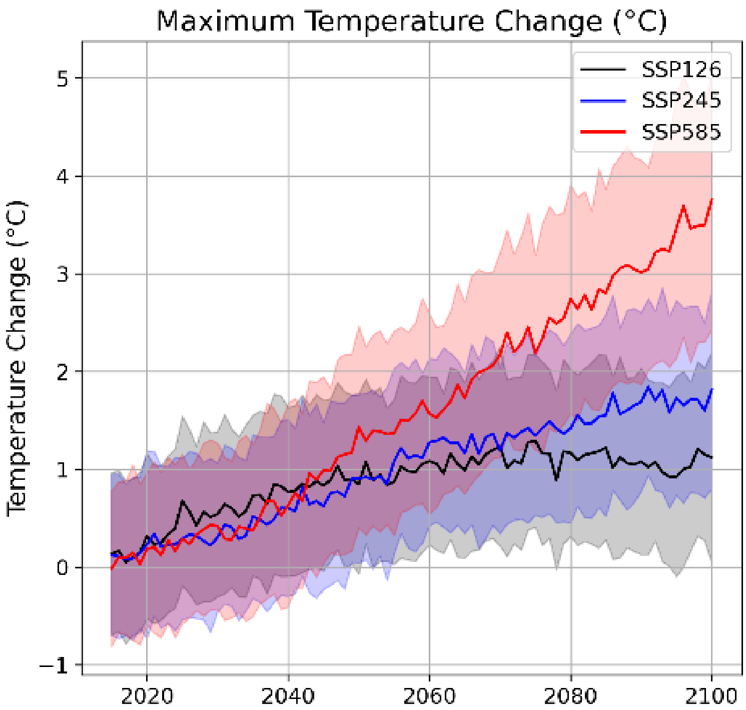

Figure 4.6: Changes in MME mean annual maximum temperature (°C) relative to 1985–2014, with uncertainty shaded (one standard deviation, 18 CMIP6 GCMs).

4.6.3 Minimum Temperature

Figure 4.7 presents projected minimum temperature (T_{min}) anomalies (°C) from 2015 to 2100, using 1985–2014 as the baseline period, under different SSPs. The findings indicate a consistent increase in Tmin across all scenarios, reflecting a long-term warming trend.

Under SSP1-2.6 (black line), T_{min} anomalies gradually increase from 0.4°C in 2015 to 1.16°C by 2100, suggesting moderate warming under a low-emission scenario.

For SSP2-4.5 (blue line), T_{min} anomalies rise more sharply, starting at 0.35°C in 2015 and reaching 2.03°C by 2100, with fluctuations along the trajectory, reflecting a mid-range emission scenario with sustained warming.

SSP5-8.5 (red line) exhibits the highest T_{min} anomalies, with an increase from 0.38°C in 2015 to 4.47°C by 2100, indicating substantial warming and severe climate risks. This scenario suggests increased heat stress, reduced nighttime cooling, and broader impacts on climate stability.

Overall, the rising T_{min} across all SSPs highlights the accelerating impact of climate change, emphasizing the need for adaptive strategies to mitigate long-term temperature increases and associated risks.

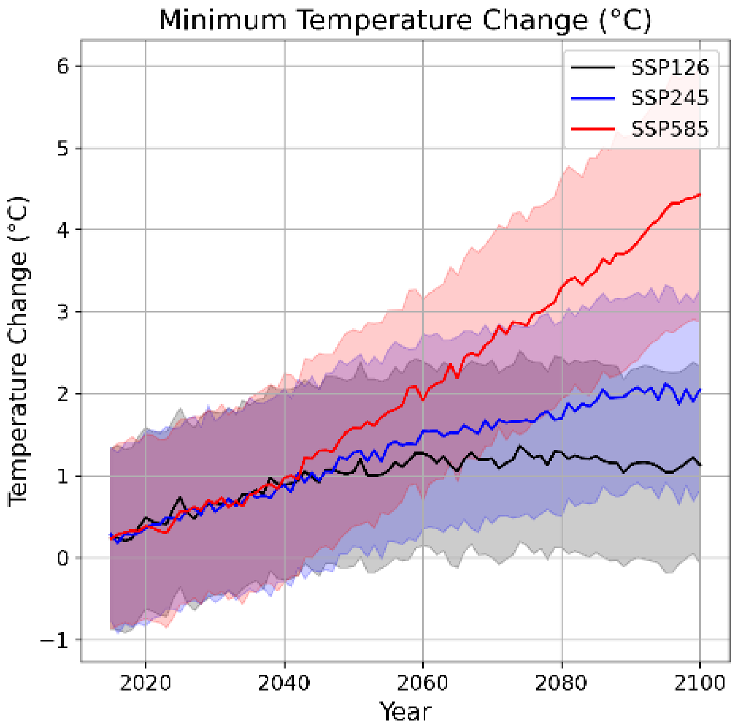

Figure 4.7: Changes in MME mean annual minimum temperature (°C) relative to 1985–2014, with uncertainty shaded (one standard deviation, 18 CMIP6 GCMs).

4.7 Projection of the Extreme Temperature and Precipitation Indices

The study calculated the Multi-Model Ensemble (MME) and analyzed the differences between projected and historical periods to assess future variations in extreme climate events (Nazrul et al., 2025). Thirteen extreme temperature indices are presented in Figures 4.8 to 4.20, while ten extreme precipitation indices are illustrated in Figures 4.21 to 4.30. In these figures, black dots indicate statistically significant changes based on the Wilcoxon rank-sum test at the 95% confidence level (Kamruzzaman et al., 2024). Furthermore, Table 4.2 summarizes the comprehensive regional statistics for all indices, highlighting the maximum and minimum values across 193 grid points and the variations across different SSP scenarios and future time periods.

Table 4.2: Comprehensive Regional Statistics of All Indices: Maximum and Minimum Values Across 193 Grid Points, Highlighting Differences Between SSP Scenarios and Time Periods

Index	Unit	Remarks	SSP1-2.6			SSP2-4.5			SSP5-8.5		
			Near future	**Mid future**	**Far Future**	**Near future**	**Mid future**	**Far Future**	**Near future**	**Mid future**	**Far Future**
TXx	°C	Maximum	1.05	2.01	2.26	0.78	1.95	3.12	0.89	2.89	5.12
		Minimum	0.47	0.94	1.01	0.13	0.92	1.42	0.22	1.51	2.99
TNx	°C	Maximum	1.09	1.92	1.96	0.86	2.07	2.80	0.94	2.89	5.08
		Minimum	0.58	1.05	1.10	0.54	1.21	1.62	0.55	1.73	3.15
TXn	°C	Maximum	0.90	1.55	1.70	0.86	1.96	2.51	0.83	2.48	4.50
		Minimum	0.39	0.72	0.75	0.25	0.89	1.12	0.16	1.21	2.10
TNn	°C	Maximum	1.05	1.61	1.71	0.96	1.95	2.72	1.03	2.85	5.49

SU	TX90p		TN90p		TX10p		TN10p		
d	%		%		%		%		
Maximum	Minimum	Maximum	Minimum	Maximum	Minimum	Maximum	Minimum	Maximum	Minimum
18.70	0.28	1.10	0.45	0.86	0.33	0.75	0.44	0.98	0.44
34.04	0.56	1.83	0.75	1.47	0.60	1.31	0.84	1.75	0.91
34.47	0.59	1.96	0.76	1.53	0.67	1.36	0.95	1.93	0.94
14.70	0.10	0.59	0.45	0.79	0.19	0.69	0.42	0.86	0.51
39.13	0.74	1.81	1.04	1.75	0.84	1.59	0.99	2.18	1.22
52.93	1.07	2.92	1.43	2.22	1.19	2.15	1.36	2.93	1.62
15.24	0.15	0.95	0.51	0.93	0.17	0.71	0.35	0.88	0.39
53.83	1.09	2.64	1.51	2.46	1.17	2.30	1.65	3.06	1.76
84.00	2.29	5.13	2.87	4.01	2.43	4.04	3.10	5.44	2.99

RX1day	CSDI		WSDI		DTR		TR		
mm	d		d		°C		d		
Maximum	Minimum	Maximum	Minimum	Maximum	Minimum	Maximum	Minimum	Maximum	Minimum
21.91	0.10	1.52	-0.15	2.60	-0.27	0.21	5.60	14.34	6.74
30.79	-0.03	2.35	-0.11	3.81	-0.34	0.18	12.97	26.39	13.85
29.48	-0.20	1.78	-0.13	4.04	-0.32	0.18	13.60	27.42	15.11
24.18	0.05	1.29	-1.01	1.12	-0.38	-0.02	6.53	13.44	3.56
31.87	0.04	2.38	-1.41	3.01	-0.55	0.01	17.64	32.16	15.36
38.56	0.66	3.34	-1.32	4.71	-0.63	0.04	22.87	42.56	19.29
22.54	0.18	2.23	-1.03	1.43	-0.41	0.17	5.81	14.32	2.80
37.29	-0.50	3.06	-1.67	3.89	-0.71	0.02	23.42	44.40	18.87
94.03	0.16	4.34	-2.22	6.72	-1.23	-0.12	28.22	76.57	24.83

R20mm	R10mm		R99p		R95p		RX5day		
d	d		mm		mm		mm		
Maximum	Minimum	Maximum	Minimum	Maximum	Minimum	Maximum	Minimum	Maximum	Minimum
3.09	-0.23	5.34	5.17	21.00	2.45	9.61	5.75	21.38	5.07
5.18	0.51	8.78	7.23	25.93	4.69	14.54	7.48	25.52	7.93
4.12	0.98	8.82	7.28	24.98	5.71	13.67	8.39	27.65	8.03
2.50	-1.54	4.86	4.54	22.64	1.86	12.10	3.94	23.88	5.61
5.23	0.28	7.88	9.97	31.70	7.67	17.29	9.64	27.16	10.71
6.67	1.42	10.52	12.98	40.63	9.78	23.05	13.33	36.77	13.72
3.32	0.03	6.80	5.59	22.02	2.04	12.43	6.00	18.61	8.15
8.96	0.51	9.34	14.68	40.37	10.07	27.08	15.85	37.68	15.51
17.15	4.55	16.32	28.98	107.20	22.44	53.78	30.36	103.04	33.14

SDII		PRCPTOT		CWD		CDD		
mm		mm		d		d		
Minimum	Maximum	Minimum	Maximum	Minimum	Maximum	Minimum	Maximum	Minimum
2.32	9.53	2.54	9.54	-5.26	4.75	-0.10	5.25	0.43
4.40	13.15	4.03	15.32	-4.80	6.11	-0.54	2.62	0.94
5.09	12.69	5.40	14.32	-6.25	8.54	-1.04	1.78	0.85
2.57	9.87	1.38	9.87	-5.83	3.71	0.18	4.82	0.20
7.25	14.57	6.52	14.96	-6.41	4.02	0.54	3.76	1.05
9.08	19.71	8.63	21.03	-6.79	4.68	-0.19	3.47	1.42
2.99	11.39	2.13	11.94	-4.57	2.56	-0.19	5.44	0.24
9.93	24.62	9.26	23.84	-8.30	2.41	0.36	5.57	1.37
20.60	45.26	22.26	50.60	-8.97	3.26	-0.33	4.51	3.18

4.7.1 Extreme Temperature Indices

4.7.1.1 Annual maxima of daily maximum temperature (TXx)

The annual maximum of daily maximum temperature (TXx) is projected to increase across all scenarios, with the highest increase occurring under SSP5-8.5 (Figure 4.8). The TXx is expected to rise by approximately 5.12°C in the far future, while lower increases of 2.26°C and 3.12°C are projected under SSP1-2.6 and SSP2-4.5, respectively. The northern-west to northern-east and southern regions are particularly vulnerable to extreme temperature increases.

4.7.1.2 Annual maxima of daily minimum temperature (TNx)

The annual TXn displays similar warming trend, with the largest predicted increase of 5.08°C in the SSP5-8.5 on timescales in the far future (Figure 4.9). Future increases are lowest in SSP1-2.6, with TNx rising by 1.96°C, whereas SSP2-4.5 projects an increase of 2.80°C. This suggests intensified night-time warming across the country.

4.7.1.3 Annual minima of daily maximum temperature (TXn)

The annual minimum of daily maximum temperature (TXn) is projected to increase substantially under SSP5-8.5, with an estimated rise of 4.50°C in the far future (Figure 4.10). Under SSP1-2.6, the increase is 1.70°C, while SSP2-4.5 projects a rise of 2.51°C. This trend indicates warmer minimum daytime temperatures, which could impact agricultural and ecological systems all across the study region.

4.7.1.4 Annual minima of daily minimum temperature (TNn)

The annual minimum of daily minimum temperature (TNn), representing the coldest nights, is projected to rise the most under SSP5-8.5, reaching 5.49°C by the far future (Figure 4.11). The corresponding increases under SSP1-2.6 and SSP2-4.5 are 1.71°C and 2.72°C, respectively. The strong warming trend suggests a reduction in cold nights, particularly in the northern and central regions.

4.7.1.5 Cold nights (TN10p)

The frequency of cold nights (TN10p) is expected to decrease significantly, with a maximum decrease of 5.44% under SSP5-8.5 in the far future (Figure 4.12). The reduction is less severe under SSP1-2.6, at 1.93%, and SSP2-4.5, at 2.93%. This decline in cold nights will contribute to increased heat stress across the study region.

4.7.1.6 Cold days (TX10p)

Similar to TN10p, a sharp downturn in the number of cold days (TX10p) is anticipated. (Figure 4.13). The highest reduction is 4.04% under SSP5-8.5, meanwhile, reductions of 1.36% and 2.15% are projected under SSP1-2.6 and SSP2-4.5, respectively, are expected. The sharp decline in cold days will further exacerbate warming trends. This phenomenon will affect all regions of the country in all future periods, specially in the far future of SSP5-8.5 scenarios.

4.7.1.7 Warm nights (TN90p)

The proportion of warm nights (TN90p) is projected to increase significantly, particularly under SSP5-8.5, where it will rise by 4.01% in the far future (Figure 4.14). The projected increase under SSP1-2.6 is 1.53%, while SSP2-4.5 shows an increase of 2.22%. These increases indicate intensified night-time heat stress. This climatic shift will influence all parts of the country in the coming decades.

4.7.1.8 Warm days (TX90p)

The frequency of warm days (TX90p) is expected to increase, with the highest rise of 5.13% under SSP5-8.5 (Figure 4.15). The increases between SSP1-2.6 and SSP2-4.5 are 1.96% and 2.92%, respectively. This indicates an overall shift toward more frequent hot days. The entire country is expected to experience this change across all future timeframes, especially under the SSP5-8.5 scenario in the far future.

4.7.1.9 Summer days (SU)

Summer days (SU), identified as days with the highest temperatures exceeding 25°C, are counted annually, will rise dramatically across SSP5-8.5, with an increase of 84 days in the far future (Figure 4.16). In comparison, SSP1-2.6 and SSP2-4.5 project increases of 34.47 days and 52.93 days, respectively. This trend suggests prolonged summer conditions. This climatic shift will influence all parts of the country in the coming decades. Regions stretching from the northwest to the northeast, along with parts of the south, are likely to experience greater impacts.

4.7.1.10 Tropical nights (TR)

The frequency of tropical nights (TR), where minimum temperature remains above 20°C, is projected to rise sharply, particularly during SSP5-8.5, with an increase of 76.57 nights in the far future (Figure 4.17). The increase is lower under SSP1-2.6

(27.42 nights) and SSP2-4.5 (42.56 nights). This will have significant implications for human comfort and energy demands. All regions of the country will be impacted in every future period, with the most significant effects projected in the far future under the SSP5-8.5 scenario.

4.7.1.11 Diurnal temperature range (DTR)

The diurnal temperature range (DTR) is defined as the difference between the highest and lowest temperatures recorded each day, is expected to decrease significantly across SSP5-8.5, with a reduction of 1.23°C in the far future (Figure 4.18). The decline under SSP1-2.6 is 0.32°C, while SSP2-4.5 projects a decrease of 0.63°C. Under SSP1-2.6 it is found that in upper part of the study region the change it not statistically significant (missing black dots). The narrowing of DTR suggests increased night-time warming relative to daytime temperatures. Extensive areas in both the northern and southern parts of the study region will be significantly affected in future.

4.7.1.12 Warm spell duration index (WSDI)

The warm spell duration index (WSDI) is projected to increase substantially, particularly during SSP5-8.5, where it will rise by 6.72 days in the far future (Figure 4.19). The corresponding growth across SSP1-2.6 and SSP2-4.5 are 4.04 days and 4.71 days, respectively. Under SSPs it is found that the south-western and south-eastern parts of the of the study region the change it not statistically significant in the future (missing black dots). This trend underscores the rising occurrence and severity of warm spells, with significant impacts anticipated in the northern and southern parts of the country, particularly in the far future under SSP5-8.5.

4.7.1.13 Cold spell duration index (CSDI)

The cold spell duration index (CSDI) is projected to decline under all emission scenarios. The sharpest reduction is within SSP5-8.5, where it decreases by 4.34 days in the far future (Figure 4.20). Under SSP1-2.6 and SSP2-4.5, reductions of 1.78 days and 3.34 days are projected, respectively. Under SSP1-2.6, changes across most of the study region are not statistically significant, as indicated by the absence of black dots. In contrast, under SSP2-4.5 and SSP5-8.5, the northern part of the region also exhibits statistically insignificant changes. The reduction in cold spells reinforces the prevailing warming trend observed in the southeastern region in the far future.

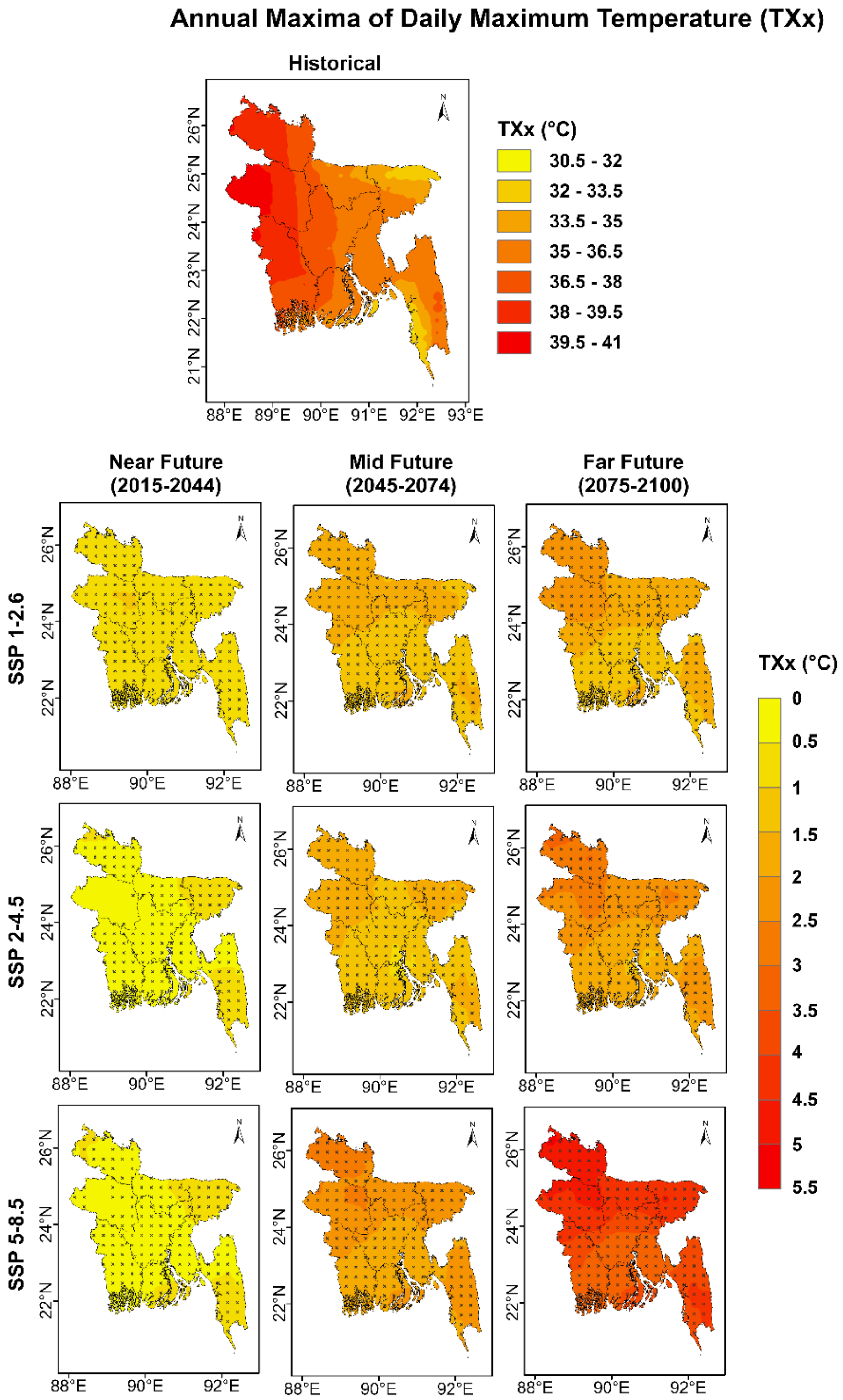

Figure 4.8: Projected changes in the Annual Maxima of Daily Maximum Temperature (TXx) across different SSP scenarios for future periods.

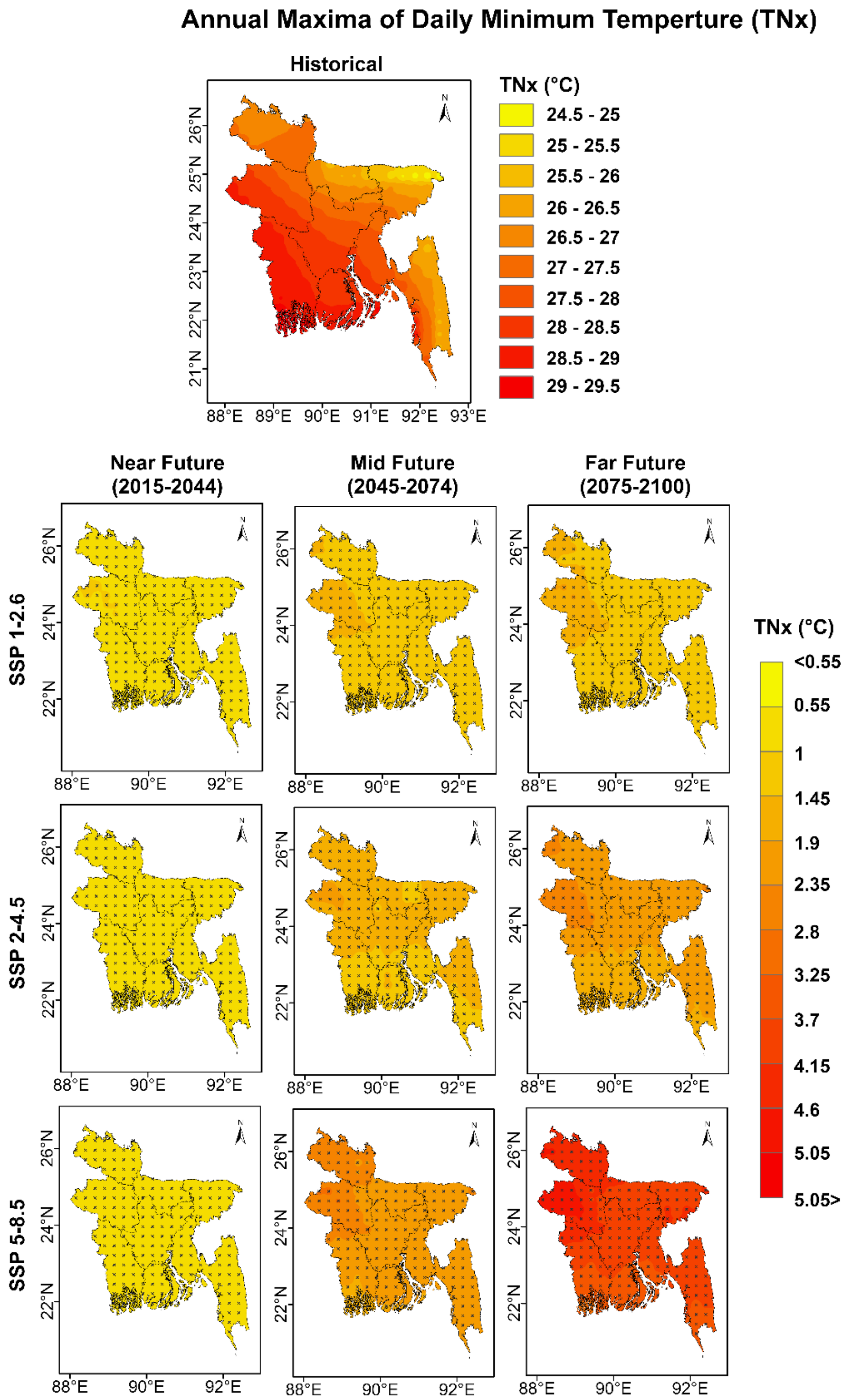

Figure 4.9: Projected changes in the Annual Maxima of Daily Minimum Temperature (TNx) across different SSP scenarios for future periods.

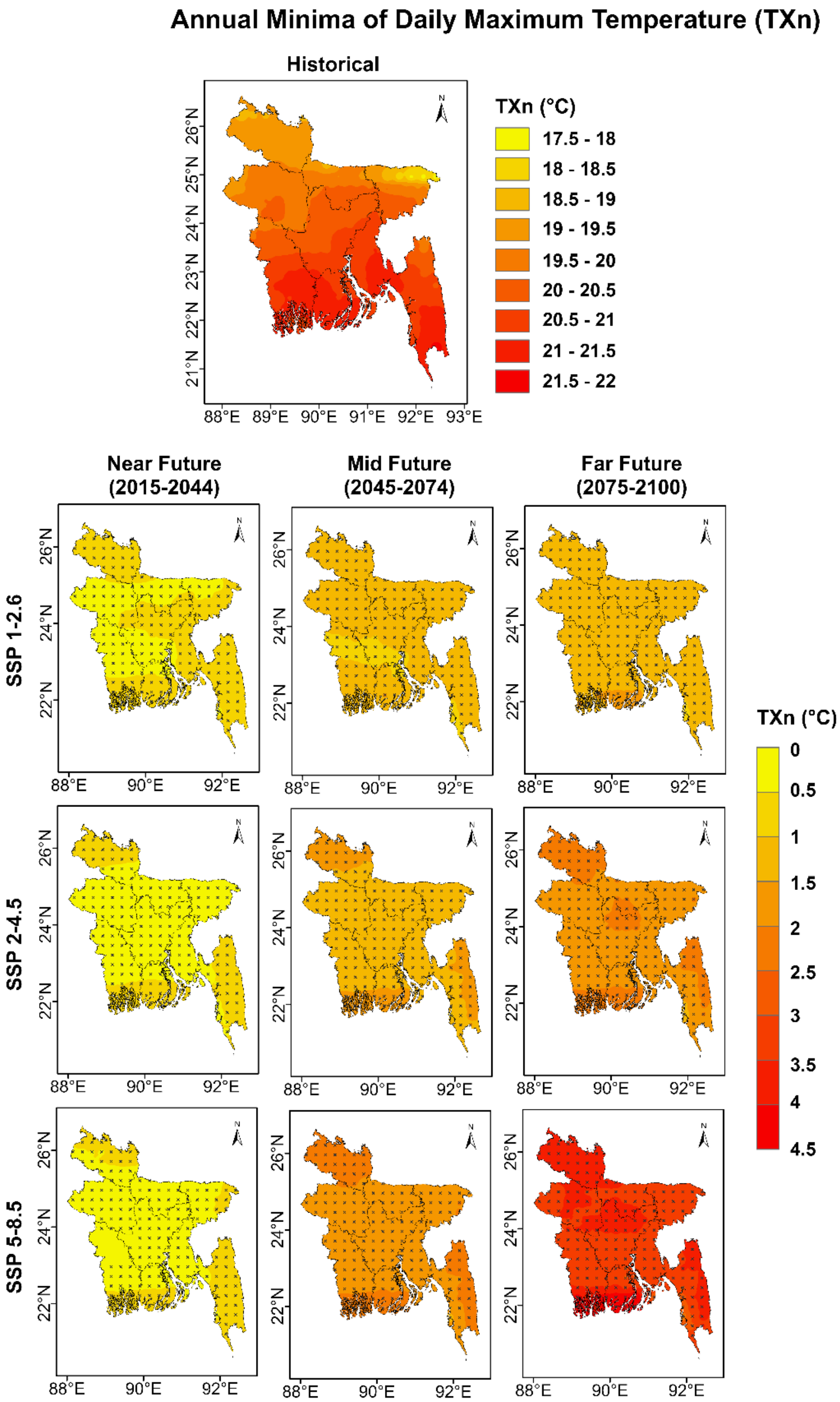

Figure 4.10: Projected changes in the Annual Minima of Daily Maximum Temperature (TXn) across different SSP scenarios for future periods.

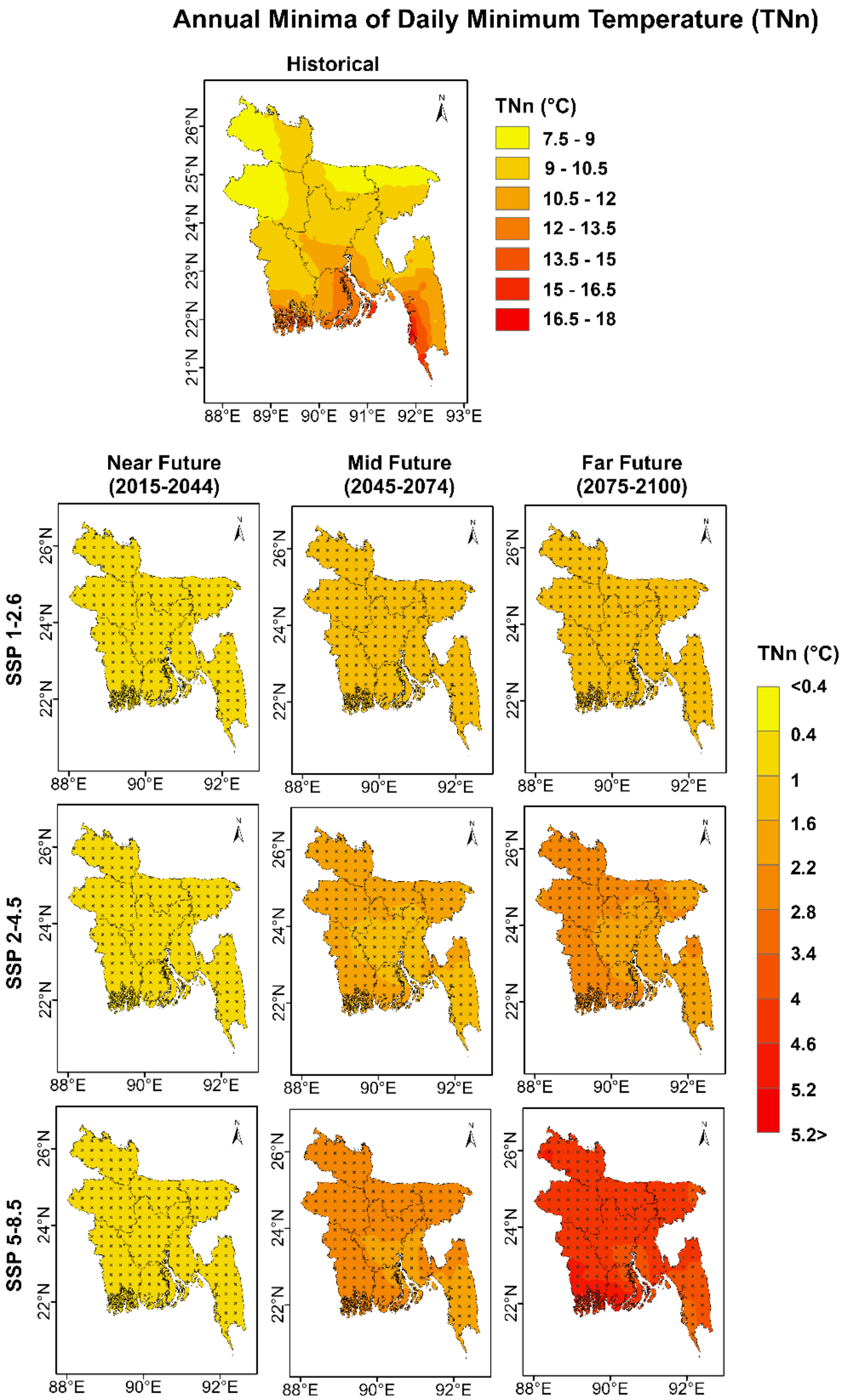

Figure 4.11: Projected changes in the Annual Minima of Daily Minimum Temperature (TNn) across different SSP scenarios for future periods.

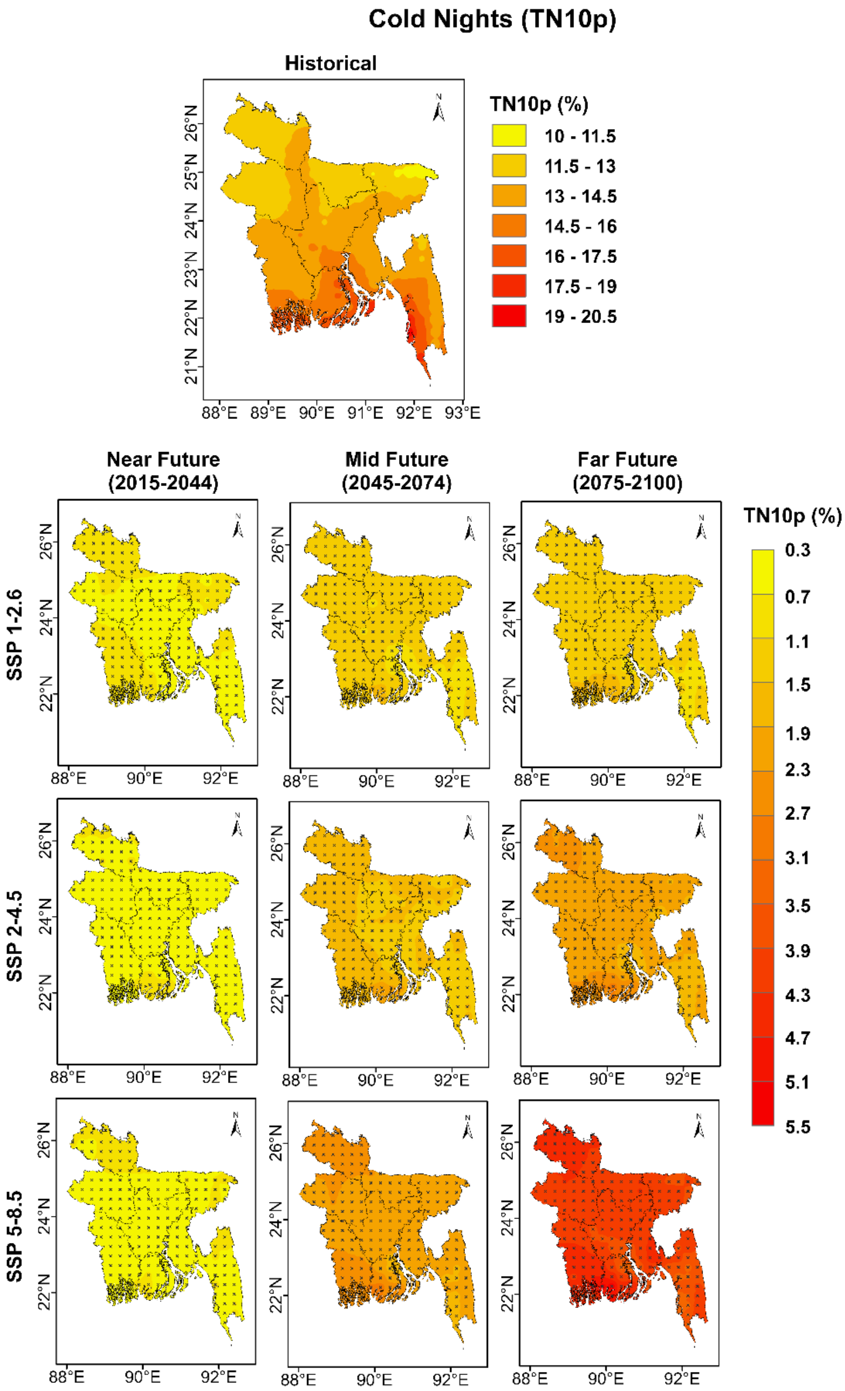

Figure 4.12: Projected changes in the Cold Nights (TN10p) across different SSP scenarios for future periods.

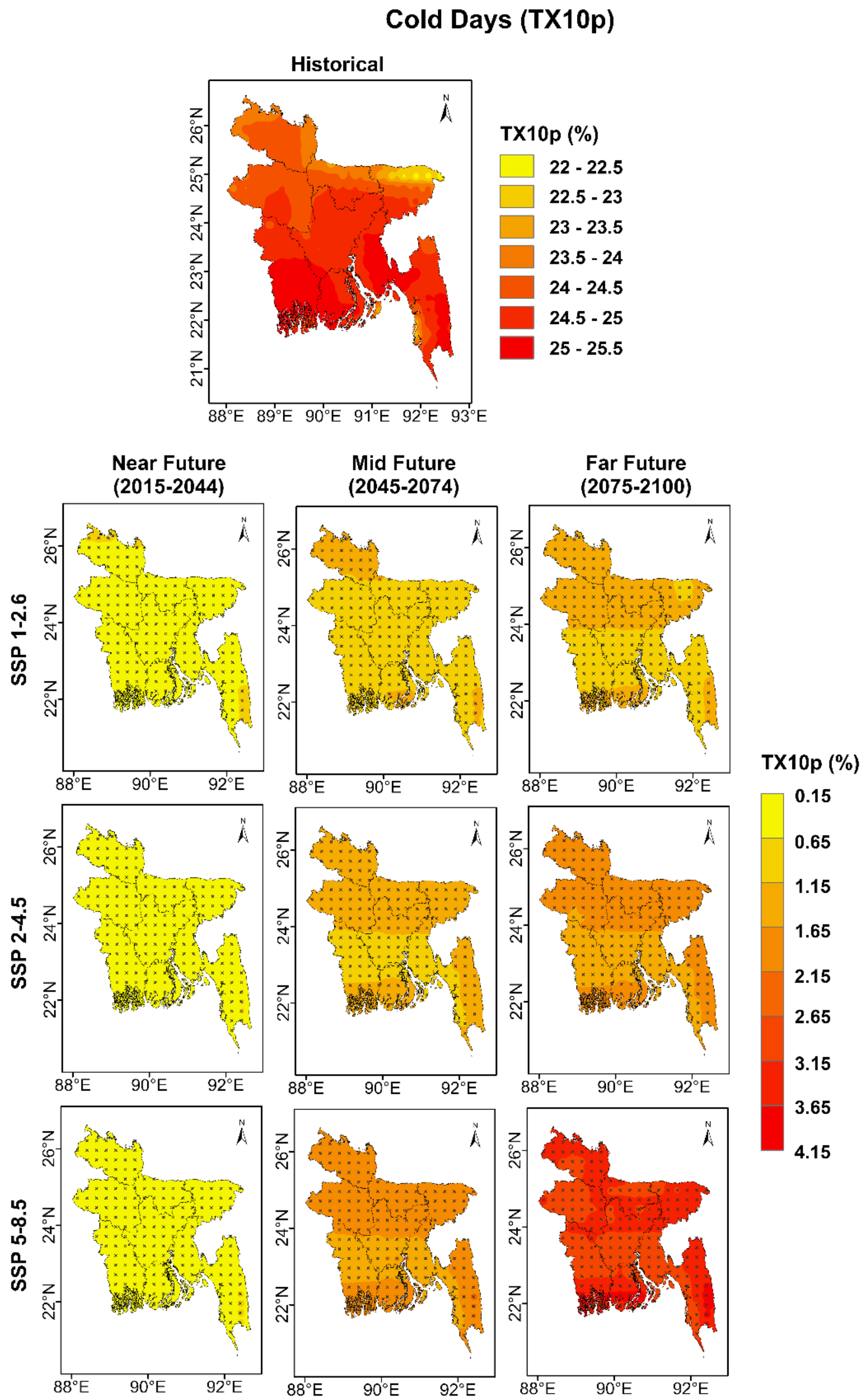

Figure 4.13: Projected changes in the Cold Days (TX10p) across different SSP scenarios for future periods.

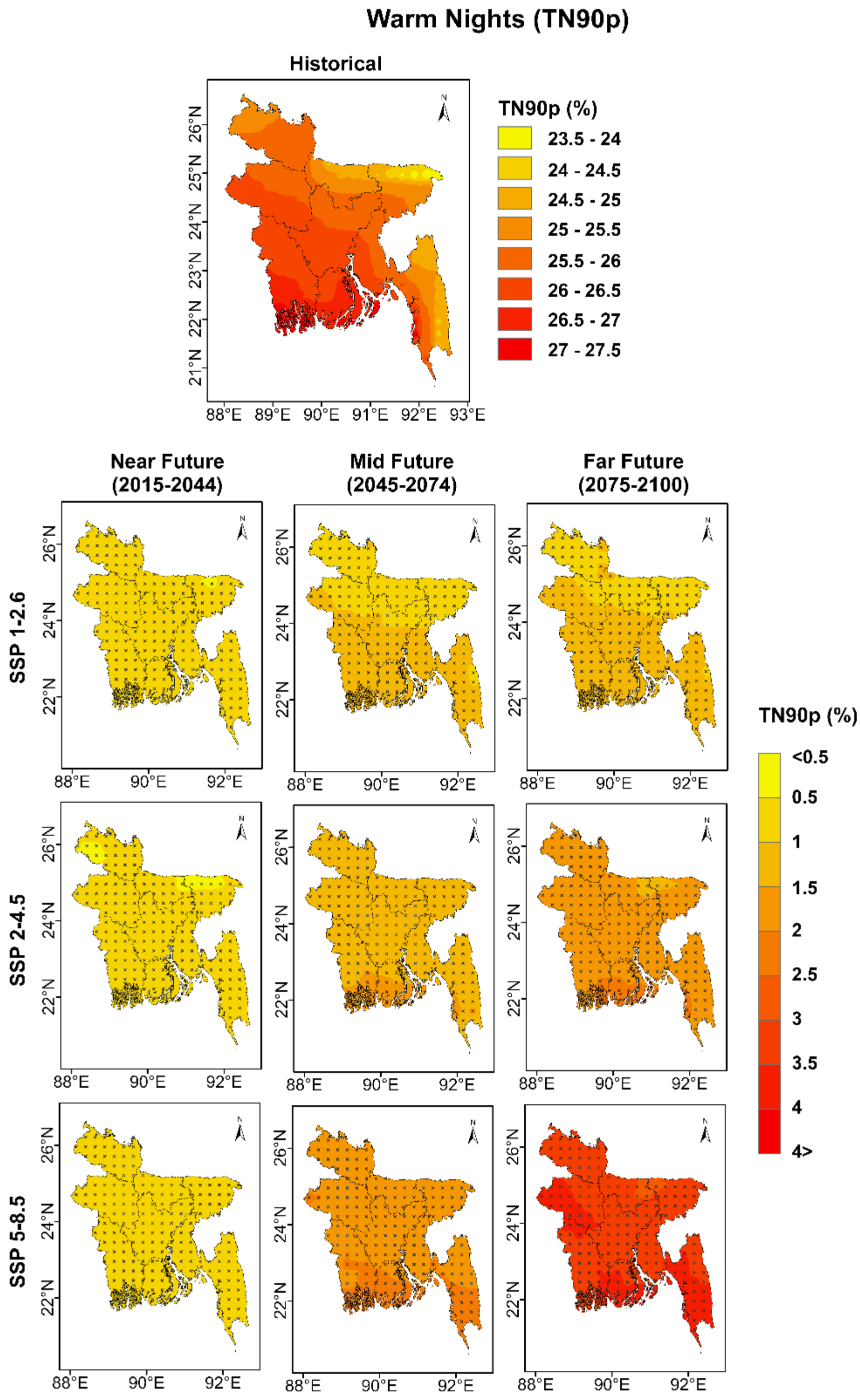

Figure 4.14: Projected changes in the Warm Nights (TN90p) across different SSP scenarios for future periods.

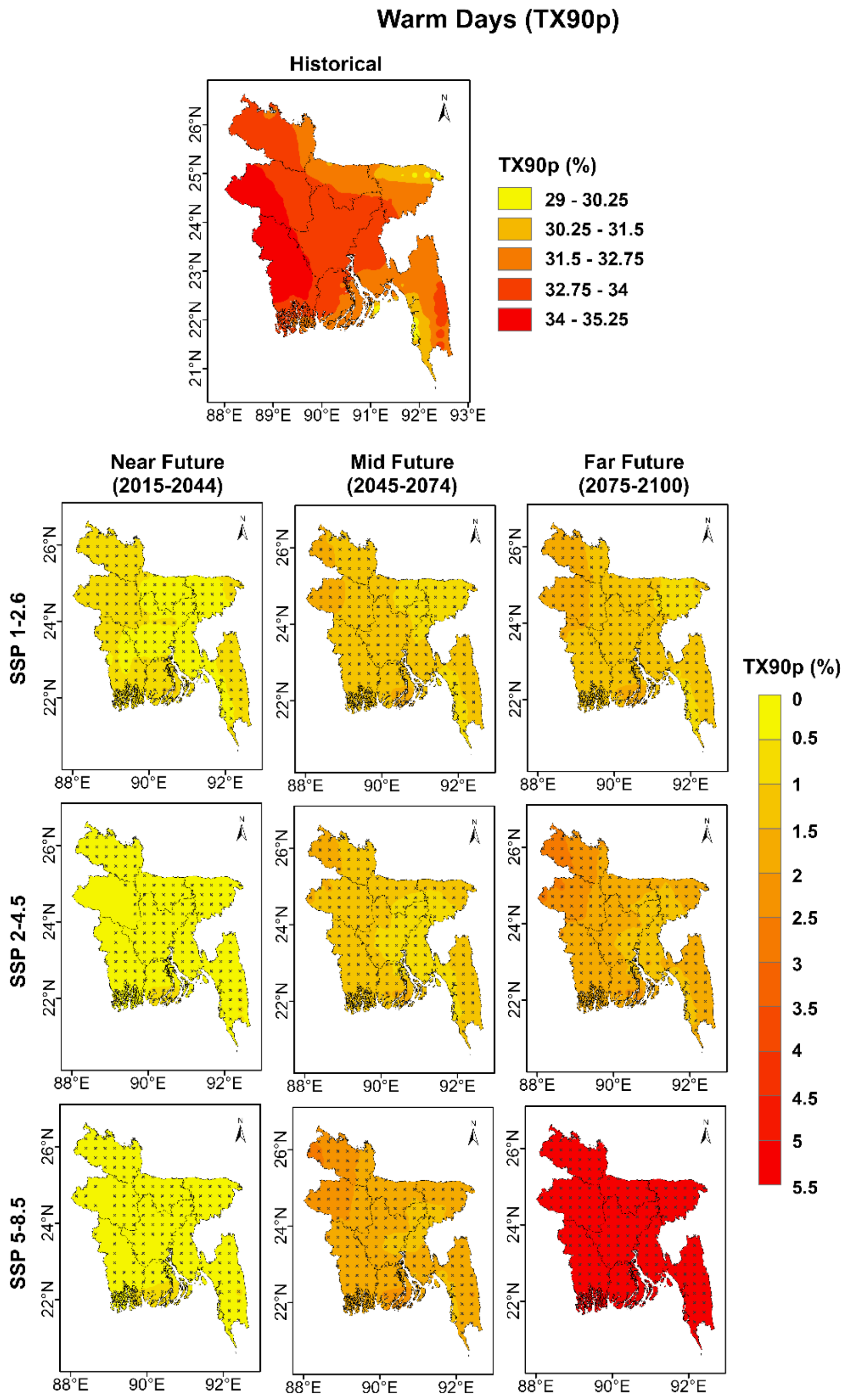

Figure 4.15: Projected changes in the Warm Days (TX90p) across different SSP scenarios for future periods.

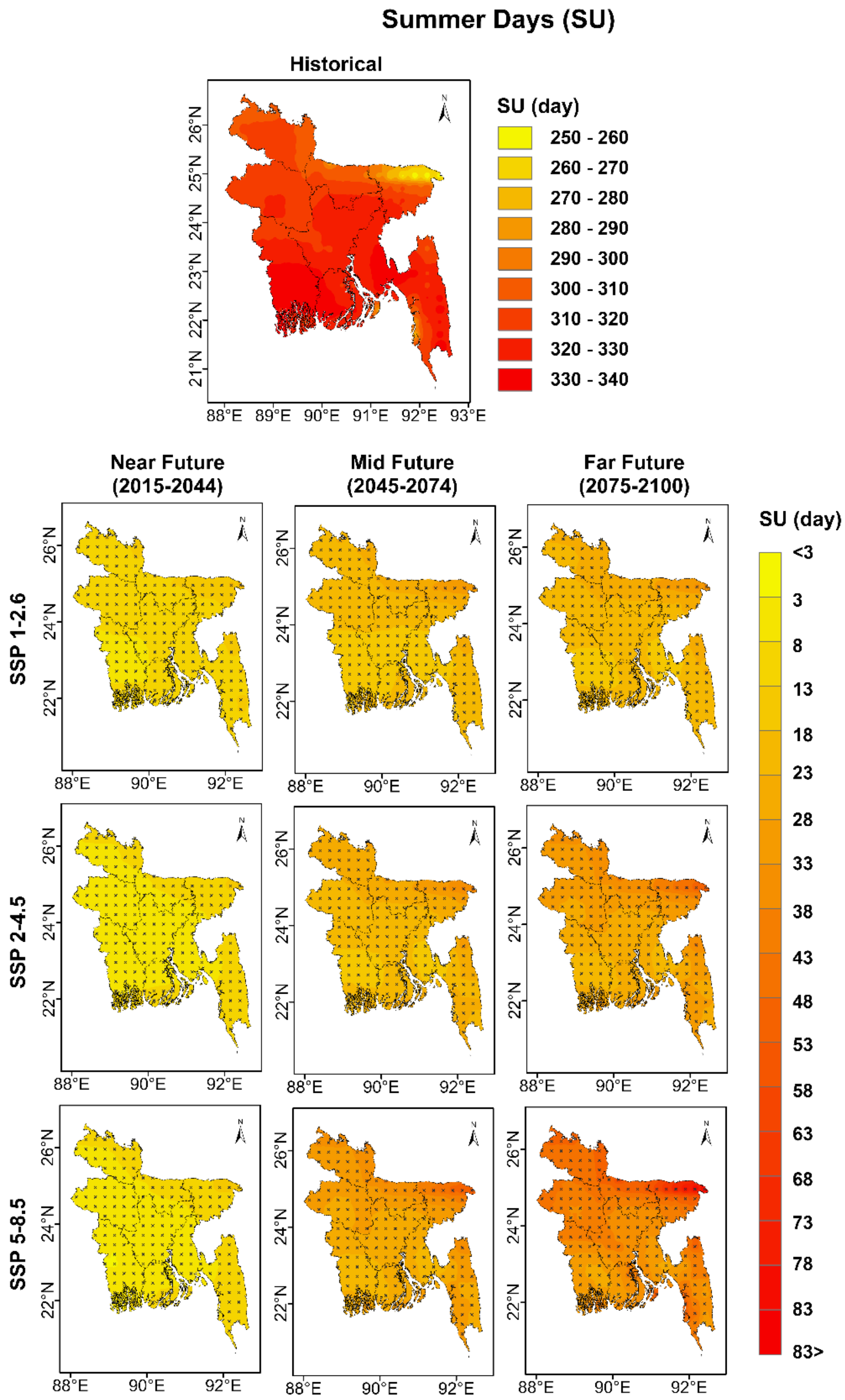

Figure 4.16: Projected changes in the Summer Days (SU) across different SSP scenarios for future periods.

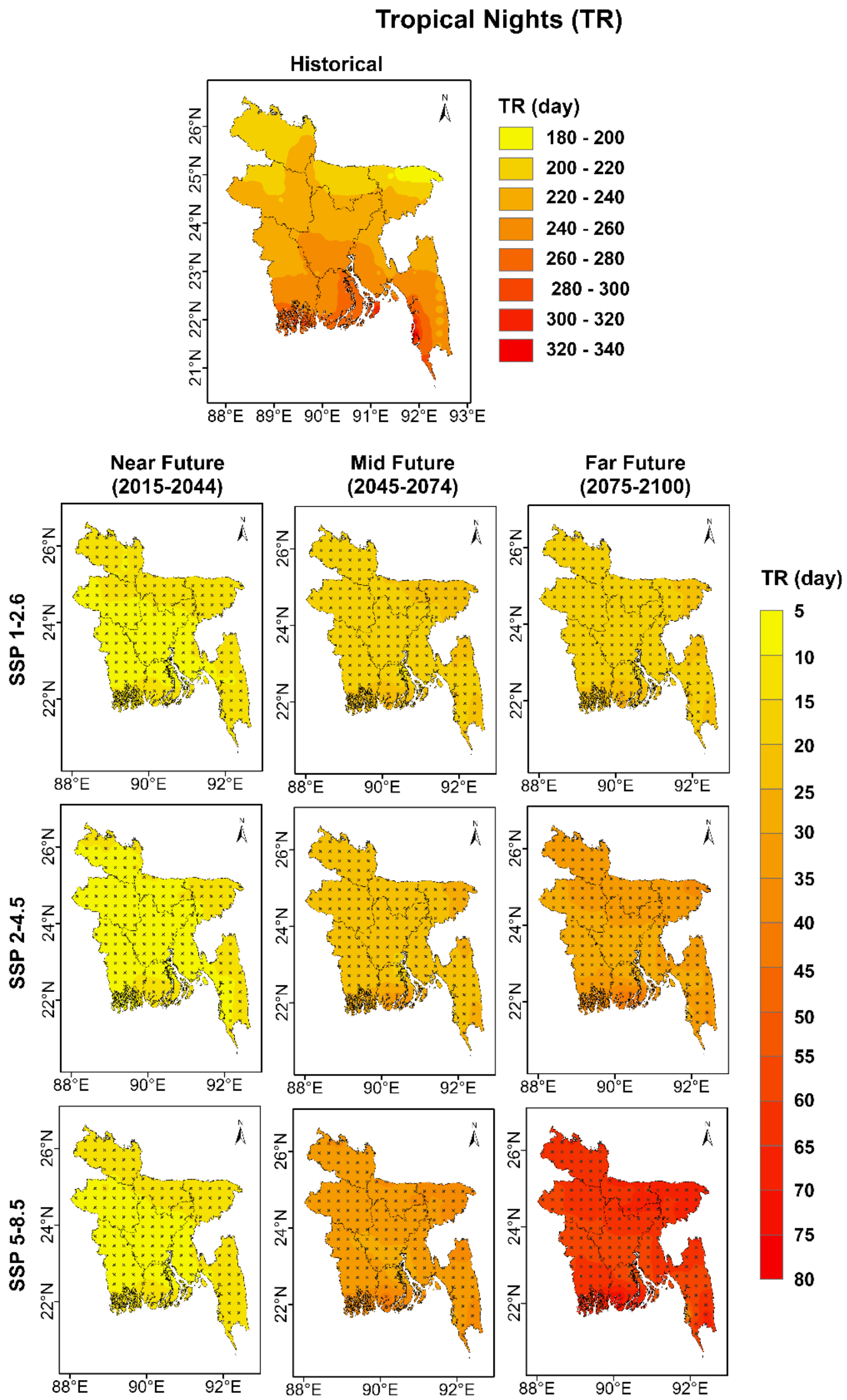

Figure 4.17: Projected changes in the Tropical Nights (TR) across different SSP scenarios for future periods.

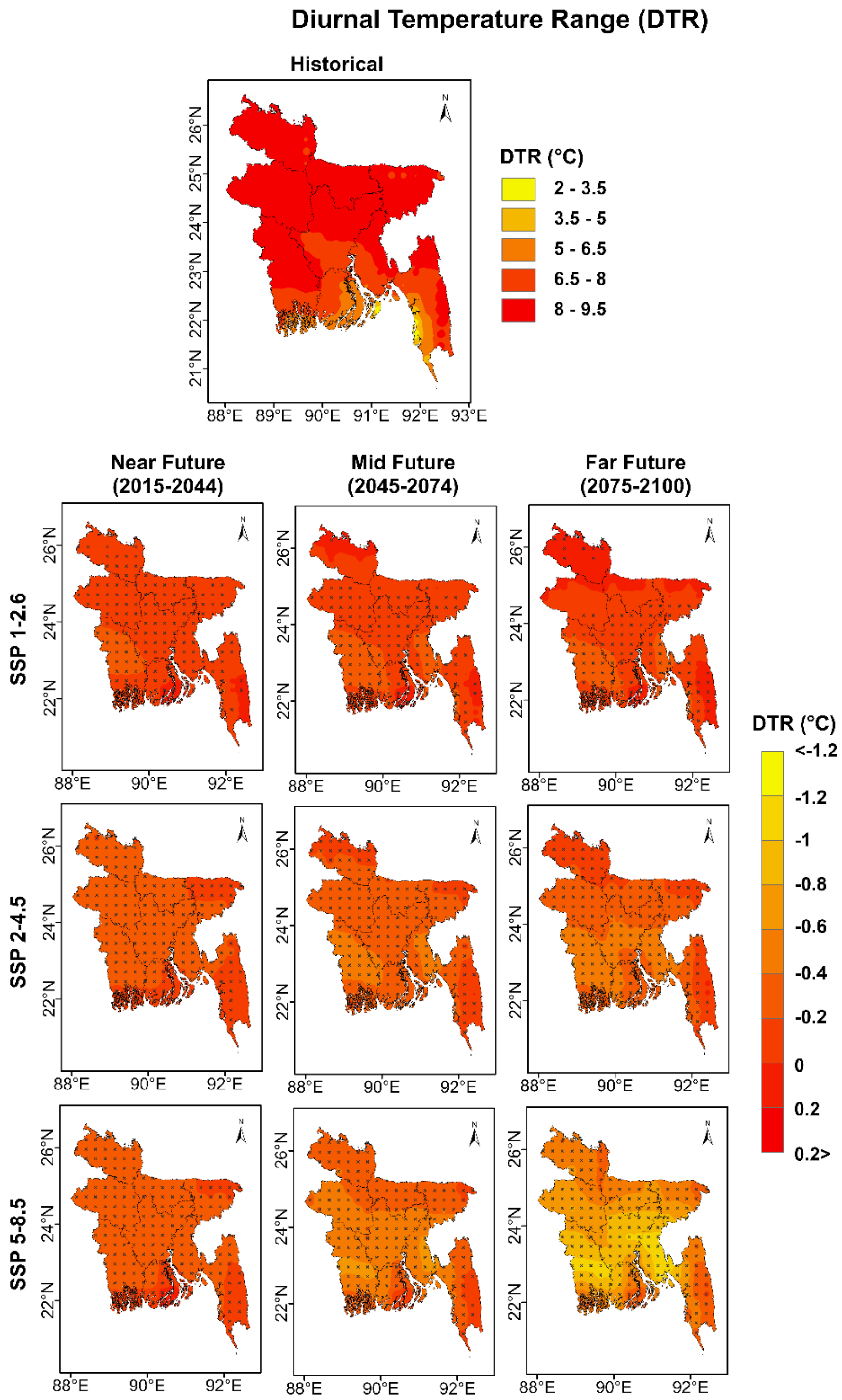

Figure 4.18: Projected changes in the Diurnal Temperature Range (DTR) across different SSP scenarios for future periods.

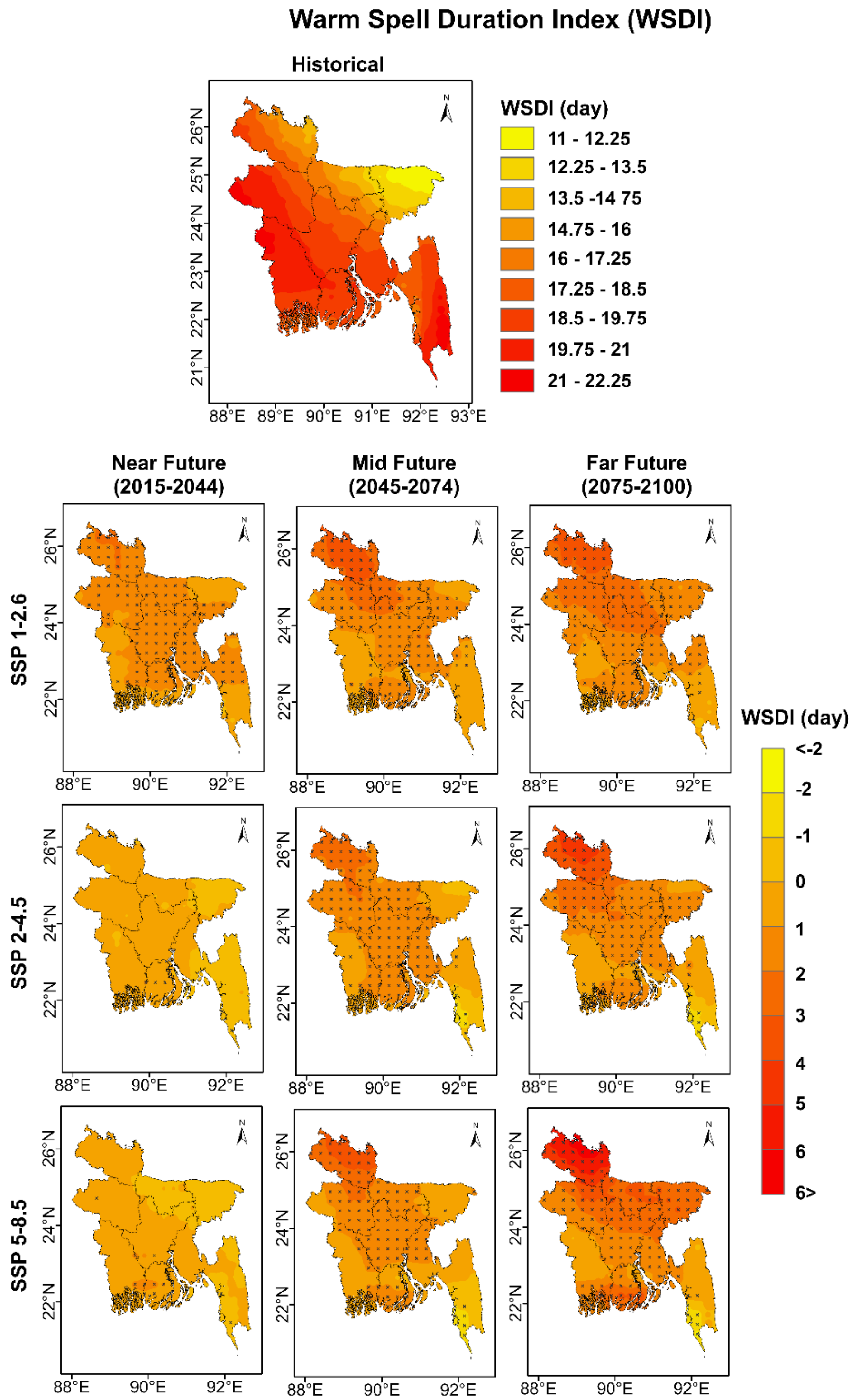

Figure 4.19: Projected changes in the Warm Spell Duration Index (WSDI) across different SSP scenarios for future periods.

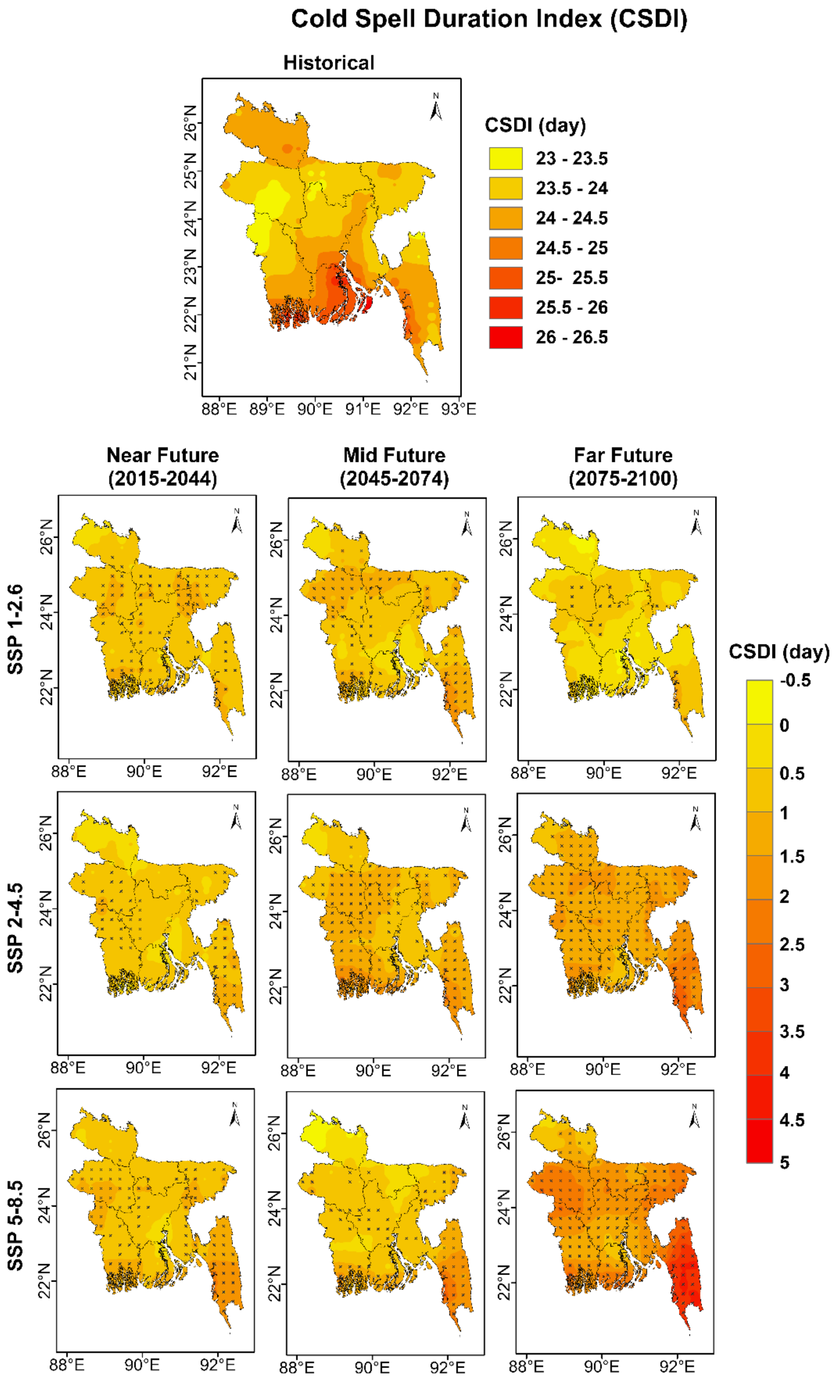

Figure 4.20: Projected changes in the Cold Spell Duration Index (CSDI) across different SSP scenarios for future periods.

4.7.2 Extreme Precipitation Indices

4.7.2.1 Max 1-day precipitation amount (RX1day)

The annual maximum 1-day precipitation (RX1day) is projected to increase substantially across all emission scenarios, pointing to a greater likelihood of extreme rainfall incidents. The highest increase is projected across SSP5-8.5, with RX1day increasing by 94.03 mm in the far future (Figure 4.21). In contrast, the projected amplification in SSP1-2.6 and SSP2-4.5 are 29.48 mm and 38.56 mm, respectively. A rising likelihood of flash floods, especially in the western and coastal regions of Bangladesh, is indicated by these trends.

4.7.2.2 Max 5-day precipitation amount (RX5day)

The maximum 5-day precipitation (RX5day), which reflects the cumulative intensity of prolonged rainfall events, is expected to rise significantly. The highest increase is projected within SSP5-8.5, reaching 103.04 mm in the far future (Figure 4.22). The corresponding climbs within SSP1-2.6 and SSP2-4.5 are 27.65 mm and 36.77 mm, respectively. These trends indicate an increased risk of severe flooding caused by prolonged heavy rainfall, especially in the western and coastal areas of the country.

4.7.2.3 Very wet days (R95p)

The very wet days (R95p) index, which measures the total precipitation from days exceeding the 95th percentile, is projected to increase markedly. The highest increase is during SSP5-8.5, with an additional 53.78 mm of rainfall in the far future (Figure 4.23). The projected upturn among SSP1-2.6 and SSP2-4.5 are 13.67 mm and 23.05 mm, respectively. The intensification of very wet days indicates an elevated risk of waterlogging and soil saturation, particularly in low-lying flood-prone areas. The effects will be most pronounced in the north to southwestern parts of the country, excluding the central to southern regions.

4.7.2.4 Extremely wet days (R99p)

The extremely wet days (R99p) index, representing total precipitation from the most extreme wet days (>99th percentile), exhibits the most significant increase during SSP5-8.5, with an additional 107.20 mm in the far future. The corresponding increases under SSP1-2.6 and SSP2-4.5 are 24.98 mm and 40.63 mm, respectively

(Figure 4.24). This pronounced increase in extreme wet days points to elevated risks of flash floods and infrastructure pressure, particularly in the western region of the country where the impacts will be most severe.

4.7.2.5 Heavy precipitation days (R10mm)

The number of heavy precipitation days (R10mm), where daily rainfall exceeds 10 mm, is estimated to growth under all SSPs. The highest increase is expected across SSP5-8.5, with an additional 16.32 days in the far future (Figure 4.25). The growth within SSP1-2.6 and SSP2-4.5 are 8.82 days and 10.52 days, respectively. In the context of SSP1-2.6 and SSP2-4.5, changes in a small portion of the northern and northeastern parts of the region are not statistically significant, while SSP5-8.5 indicates statistically significant changes throughout the region. The increasing frequency of heavy rainfall events is evident, affecting agriculture and water management throughout the country, with the exception of certain eastern areas.

4.7.2.6 Very heavy precipitation days (R20mm)

The very heavy precipitation days (R20mm) index, which tracks days with rainfall exceeding 20 mm, is expected to rise across all scenarios. The highest rise is found during SSP5-8.5, reaching 17.15 additional days in the far future (Figure 4.26). The corresponding escalations within SSP1-2.6 and SSP2-4.5 are 4.12 days and 6.67 days, respectively. The rising frequency of very heavy rainfall events signals increasing challenges for flood management and stormwater drainage systems. The effects of the phenomenon in the far future under SSP5-8.5 will be prominent in the northern to northeastern parts of the study region.

4.7.2.7 Consecutive dry days (CDD)

The consecutive dry days (CDD) index, which indicates the length of dry spells, exhibits mixed trends across emission scenarios. Across SSP1-2.6, CDD decreases slightly by 1.78 days, suggesting improved moisture availability (Figure 4.27). However, under SSP5-8.5, CDD decreases by 4.51 days in the far future, indicating the potential for more severe drought conditions, especially in the southeastern regions. The northern, eastern, and southeastern parts of the region exhibit significant changes under both SSP2-4.5 and SSP5-8.5 scenarios in the far future. This suggests increased variability between wet and dry periods, requiring adaptive water resource management.

4.7.2.8 Consecutive wet days (CWD)

The consecutive wet days (CWD) index, representing extended periods of rainfall, shows an increasing trend under lower emission scenarios but remains relatively stable within SSP5-8.5. The highest increase is observed under SSP1-2.6, with 8.54 additional wet days in the far future (Figure 4.28). In contrast, the increases under SSP2-4.5 and SSP5-8.5 are 4.68 days and 3.26 days, respectively. Across all SSP scenarios, the eastern region and parts of the coastline exhibit significant changes. The trend indicates increased seasonal fluctuations in rainfall, especially in the eastern and central regions of the country.

4.7.2.9 Total precipitation in wet days (PRCPTOT)

The total precipitation in wet days (PRCPTOT), which measures cumulative rainfall on days with at least 1 mm of precipitation, is anticipated to increase markedly under all scenarios. The highest increase occurs during SSP5-8.5, with an additional 50.60 mm in the far future (Figure 4.29). The corresponding rises during SSP1-2.6 and SSP2-4.5 are 14.32 mm and 21.03 mm, respectively. The increase in PRCPTOT suggests a growing need for enhanced flood control and water management systems. Under the SSP5-8.5 scenario, significant impacts are anticipated in the western part of the study area during the far future.

4.7.2.10 Simple daily intensity index (SDII)

The simple daily intensity index (SDII), reflecting the mean rainfall on wet days, demonstrates a significant amplification under all scenarios. The greatest rise is expected under SSP5-8.5, attaining 45.26% in the late 21st century (Figure 4.30). The projected escalations across SSP1-2.6 and SSP2-4.5 are 12.69% and 19.71%, respectively. This rise in SDII indicates more intense rainfall events, further amplifying flood risks and soil erosion concerns. In the far future under SSP5-8.5, the western region of the study area is expected to be significantly affected, with some eastern and southeastern areas facing even more severe impacts.

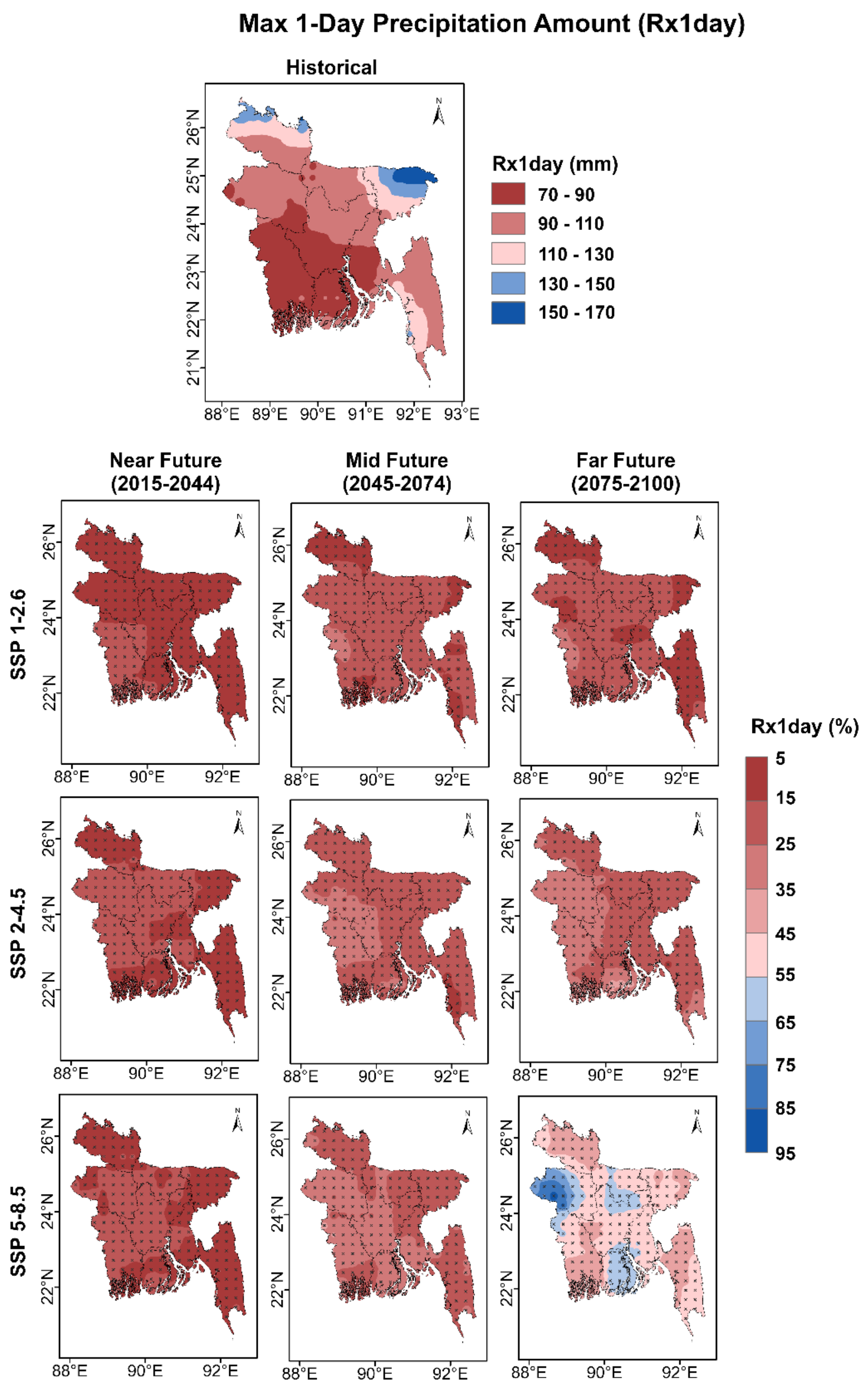

Figure 4.21: Projected changes in the Maximum 1-Day Precipitation Amount (Rx1day) across different SSP scenarios for future periods.

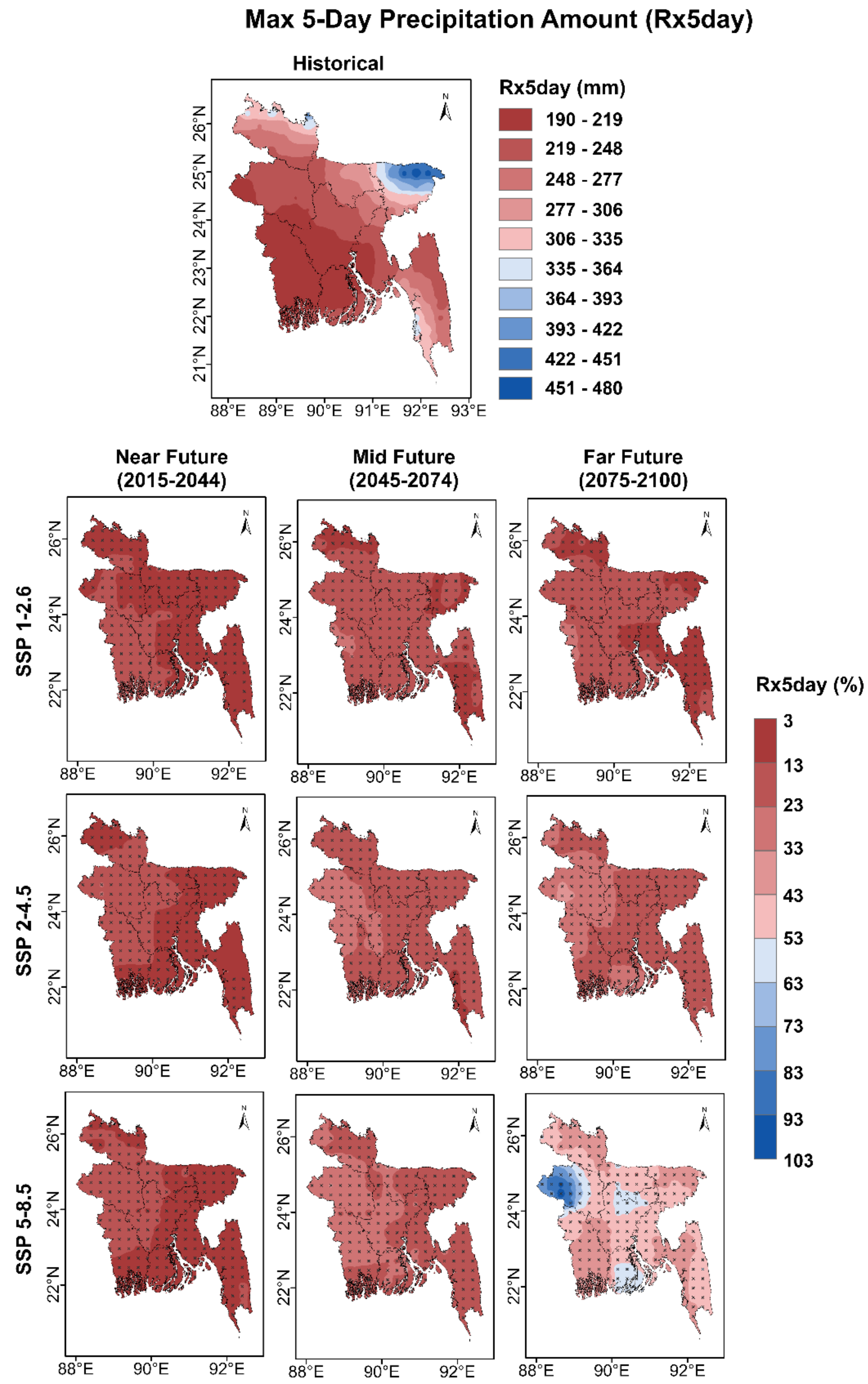

Figure 4.22: Projected changes in the Maximum 5-Day Precipitation Amount (Rx5day) across different SSP scenarios for future periods.

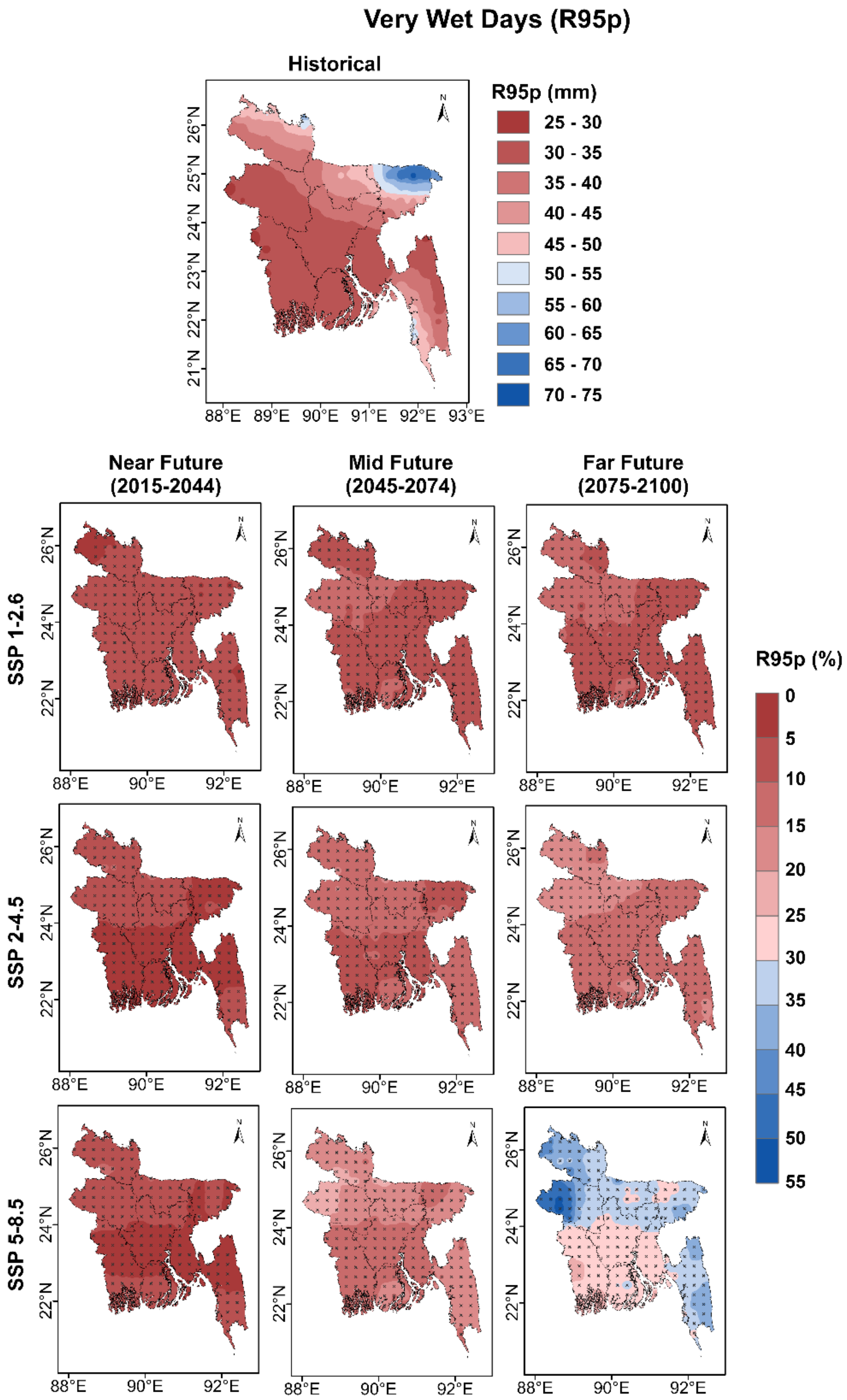

Figure 4.23: Projected changes in the Very Wet Days (R95p) across different SSP scenarios for future periods.

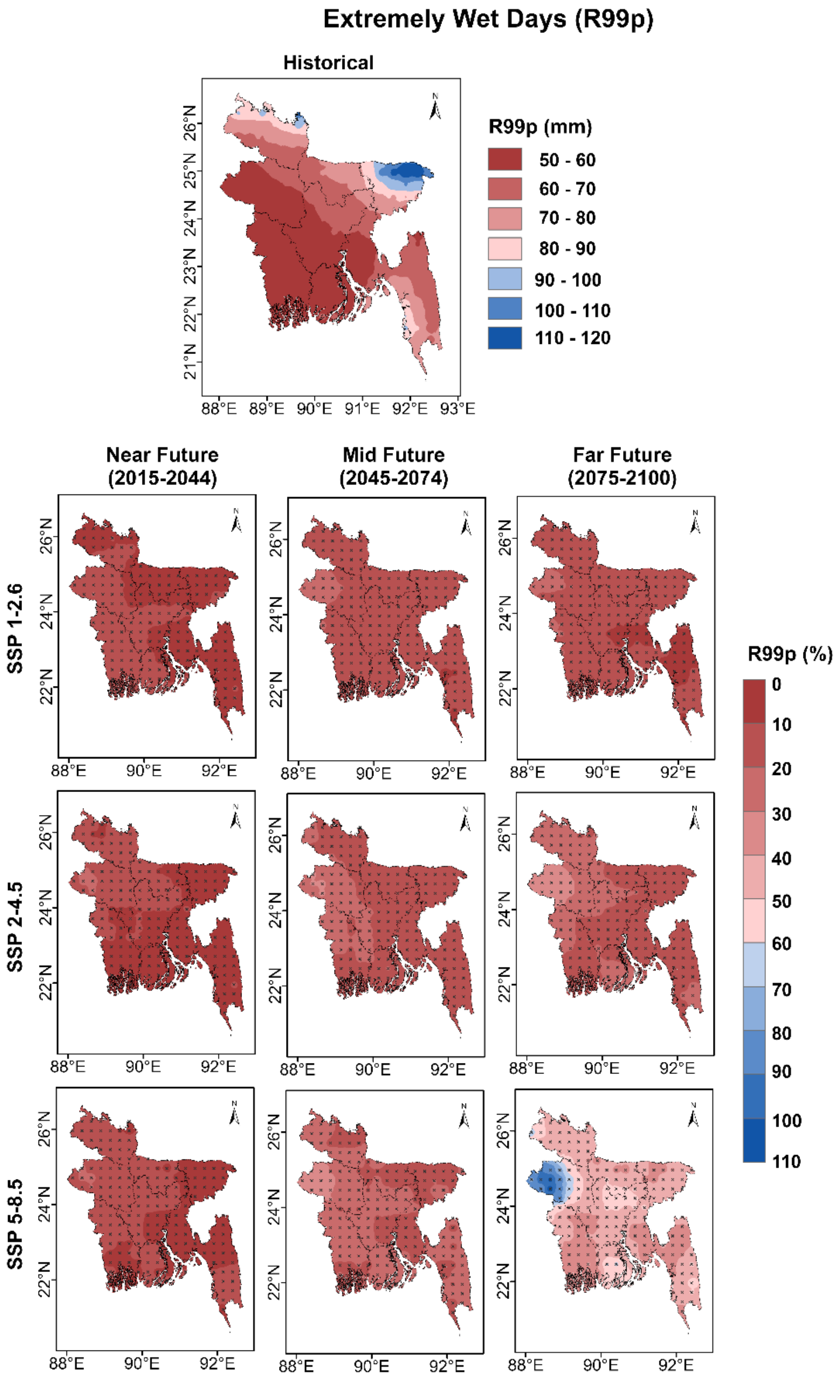

Figure 4.24: Projected changes in the Extremely Wet Days (R99p) across different SSP scenarios for future periods.

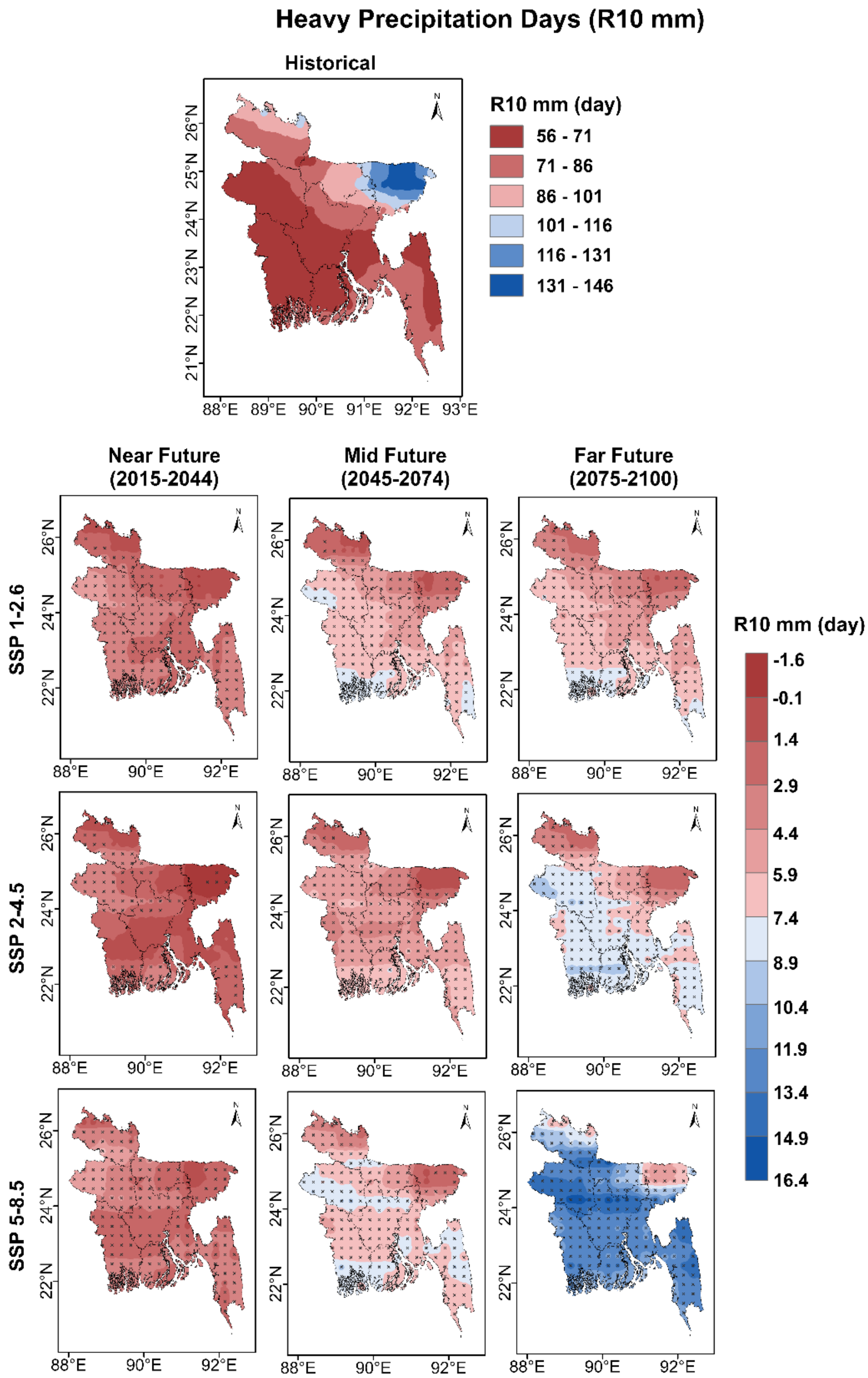

Figure 4.25: Projected changes in the Heavy Precipitation Days (R10mm) across different SSP scenarios for future periods.

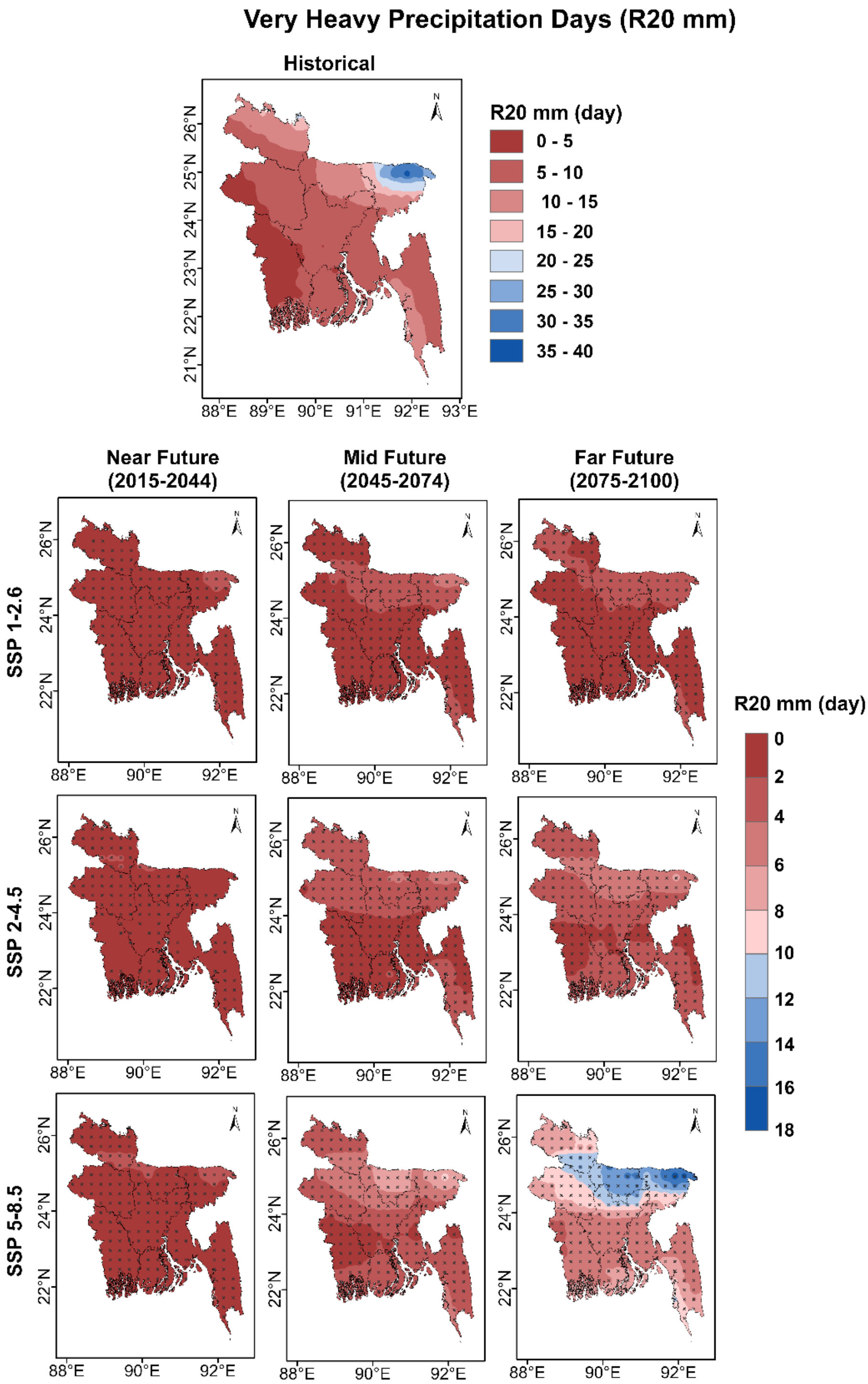

Figure 4.26: Projected changes in the Very Heavy Precipitation Days (R20mm) across different SSP scenarios for future periods.

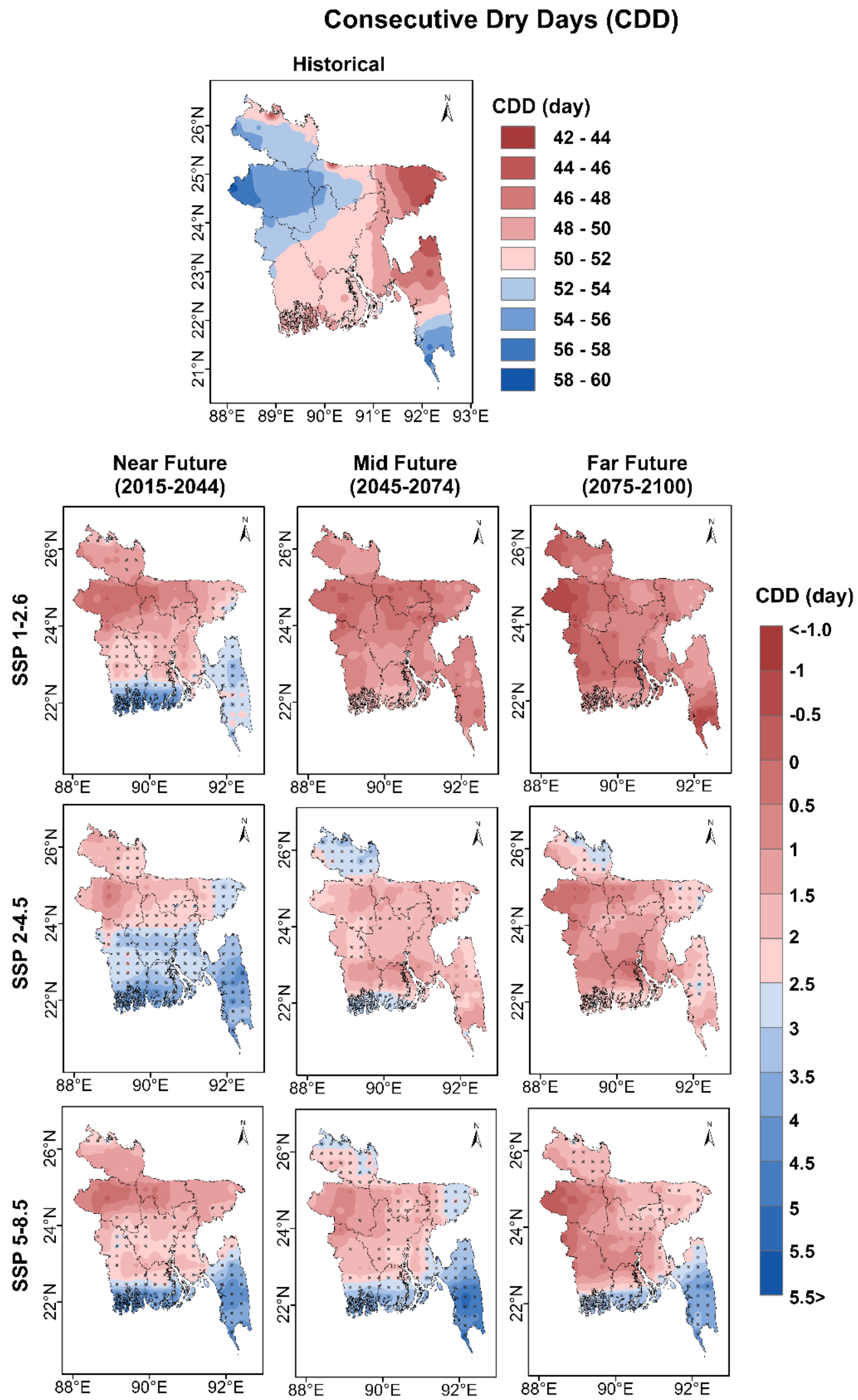

Figure 4.27: Projected changes in the Consecutive Dry Days (CDD) across different SSP scenarios for future periods.

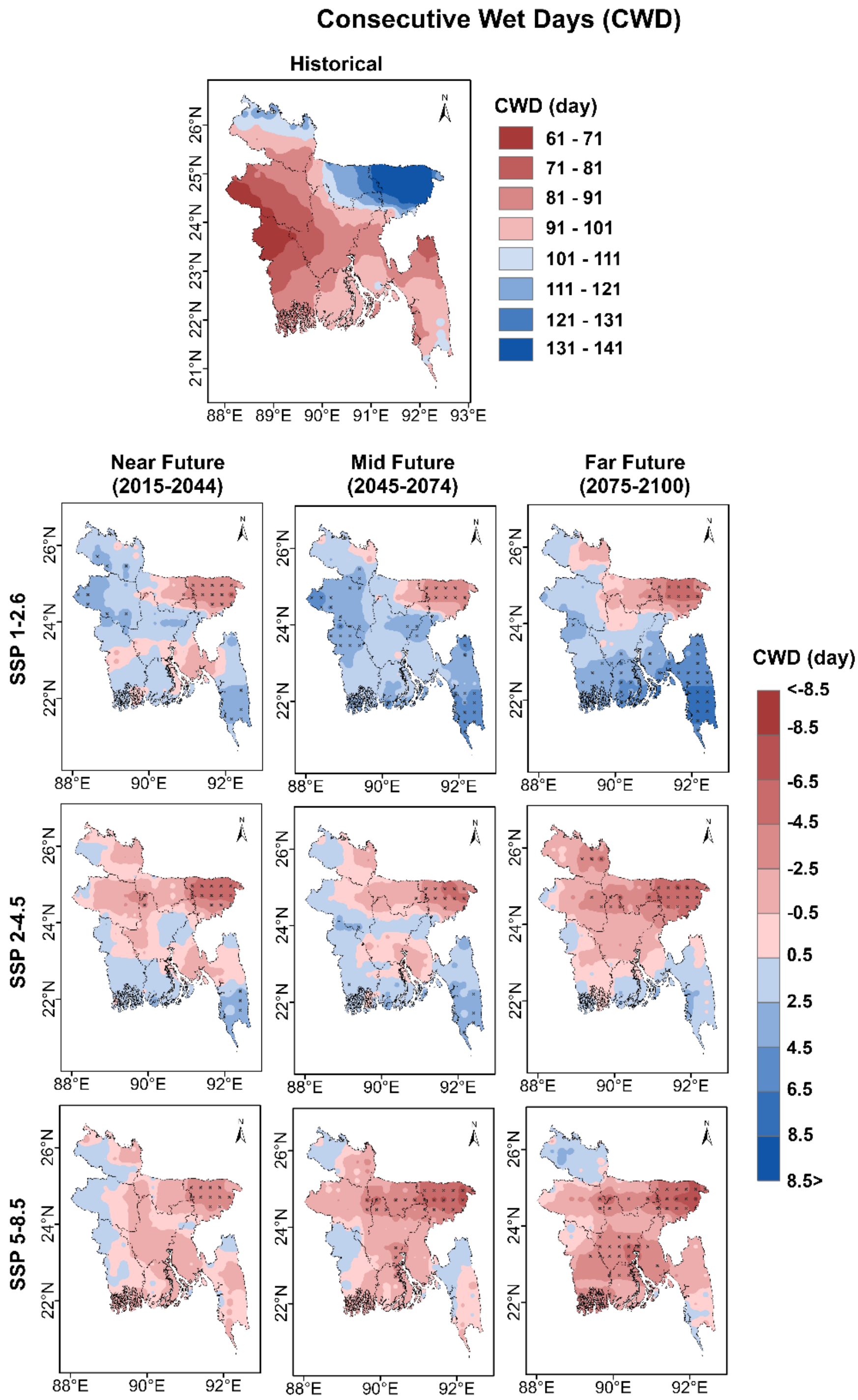

Figure 4.28: Projected changes in the Consecutive Wet Days (CWD) across different SSP scenarios for future periods.

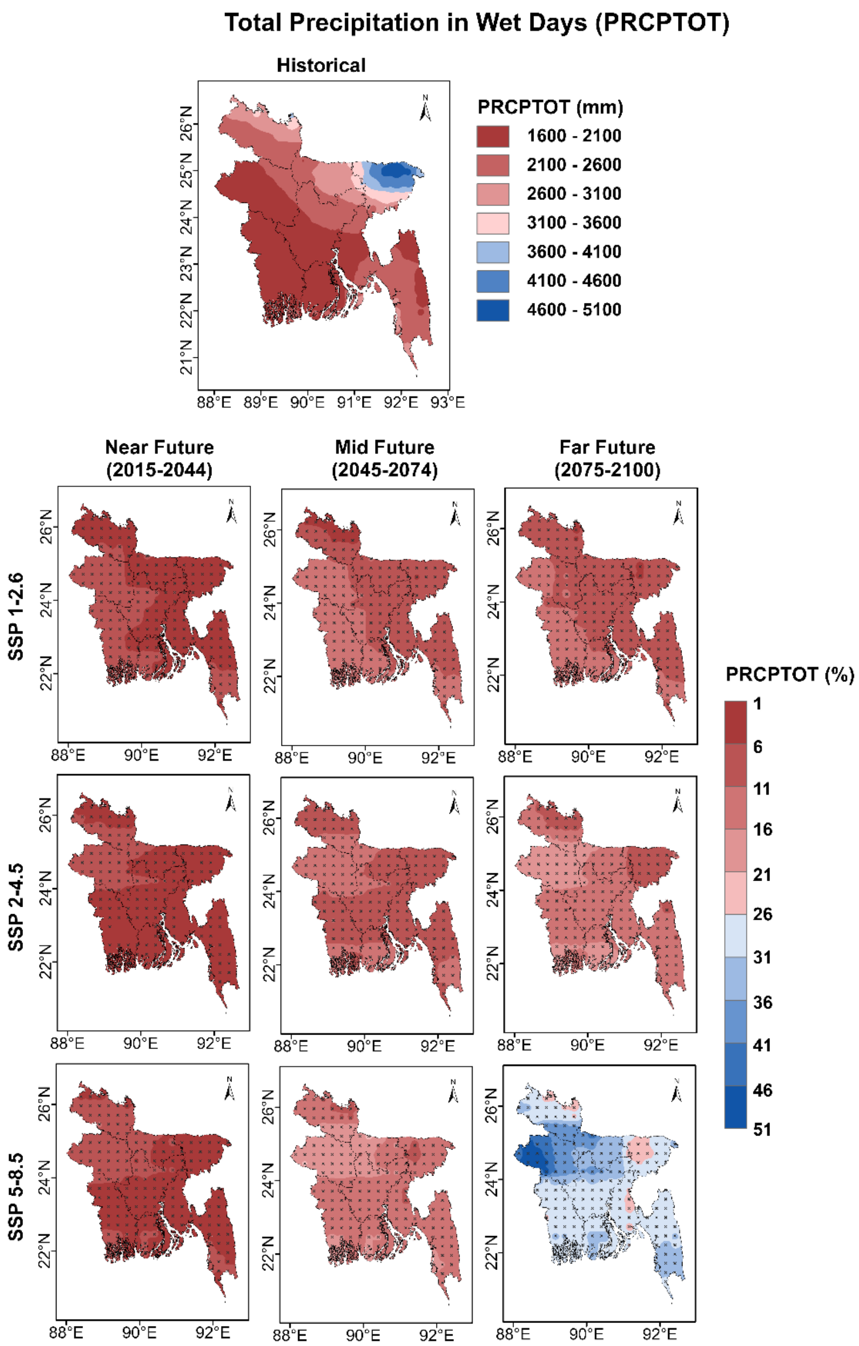

Figure 4.29: Projected changes in the Total Precipitation in Wet Days (PRCPTOT) across different SSP scenarios for future periods.

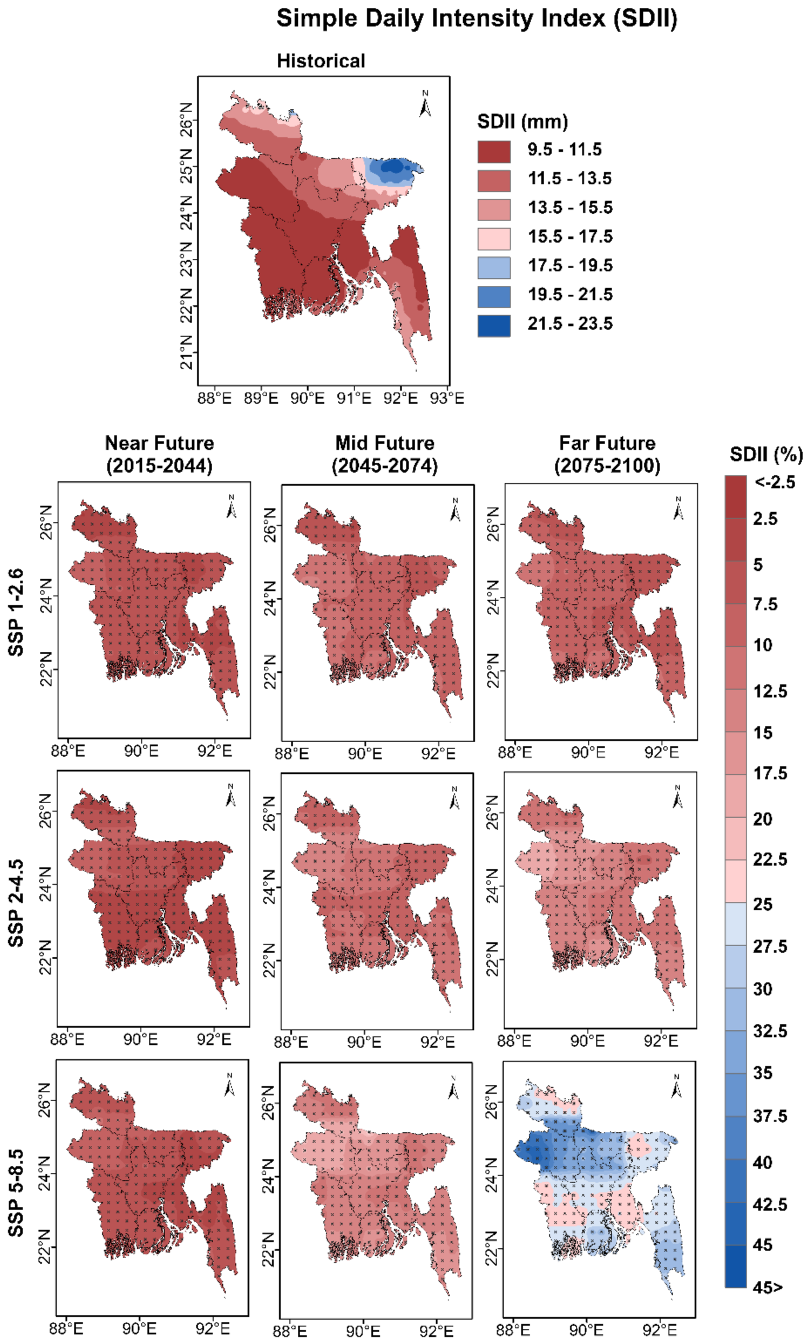

Figure 4.30: Projected changes in the Simple Daily Intensity Index (SDII) across different SSP scenarios for future periods.

4.8 Discussion

The projected changes in temperature and precipitation indices across Bangladesh indicate a future climate characterized by significant warming and increased precipitation extremes. These changes could have profound implications for environmental sustainability, water resource management, and agricultural productivity. The analysis of temperature and precipitation patterns across different Shared Socioeconomic Pathway (SSP) scenarios reveals distinct regional and temporal trends, providing a clear picture of how climate change may impact Bangladesh in the near (2015–2044), mid (2045–2074), and far future (2075–2100). The increase in temperature indices, particularly under SSP5-8.5, highlights an accelerated warming trend across Bangladesh. The maximum daily maximum temperature (TXx) and maximum daily minimum temperature (TNx) exhibit substantial increases, particularly in the far future. Under SSP5-8.5, TXx is projected to rise by 5.12°C, while TNx is expected to increase by 4.50°C, suggesting that extreme heat events will become more frequent and intense. These findings align with other regional studies forecasting significant temperature increases under high-emission scenarios, leading to heightened heat stress on human and natural systems (Alamgir et al., 2019; Das et al., 2023).

A notable finding from this work is the decreasing trend in the DTR, which indicates that there is a decreasing spread between daytime and night-time temperatures. It is projected that the greatest decrease in DTR will occur under SSP5-8. 5) in the distant future (-1.23°C) indicates elevated nighttime temperatures which have the potential to exacerbate heat stress, especially in urban areas where cooling at night is crucial for public health and energy use (Kamruzzaman, 2024a). The narrowing of DTR could disrupt critical agricultural processes since many crops rely on large temperature variations between day and night for optimal growth and development (Adekanmbi & Sizmur, 2022). The projected increase in warm indices, such as TX90p (percentage of warm days) and TN90p (percentage of warm nights), indicates that heatwaves and prolonged warm spells will become more frequent (Nazrul et al. 2025). The Warm Spell Duration Index (WSDI) is expected to increase by 6.72 days under SSP5-8.5, intensifying heat-related risks (Paul & Maity, 2023). The northern and northeastern regions are expected to experience the most significant increases in warm days (SU) and warm spell durations (WSDI), highlighting the need for adaptation measures, such as heat-resistant crop varieties, modified irrigation schedules, and improved cooling infrastructure (Akter et al., 2024).

The analysis of precipitation indices indicates that the future will be characterized by more extreme and intense rainfall events. Under SSP5-8. 5, one-day maximum precipitation (Rx1day) increases by 94.03 mm, and five-day maximum precipitation (Rx5day) will be increased by 103.04 mm. This increase implies a higher likelihood of flash floods, landslides, and other hydrological hazards, consistent with other studies predicting increased precipitation intensity as global temperatures rise (Ezaz et al., 2022; Khan et al., 2020, Nowreen et al., 2015). The spatial patterns of CDD and CWD suggest a notable shift toward wetter conditions across all scenarios. CDD is expected to decline, particularly under SSP1-2.6, where a decrease of 1.78 days is projected in the far future (Kamruzzaman et al., 2024b). Conversely, CWD is expected to increase, particularly in southern Bangladesh, where prolonged wet periods could pose challenges to existing flood management systems (Abdullah et al., 2022c; Costa et al., n.d.; Kamruzzaman et al., 2019).

The spatial distribution of extreme temperature and precipitation reveals regional hotspots of extreme in Bangladesh. The northern and northeastern areas are expected to record the largest increments in warm days and warm spells, thus demanding adaptation measures in agriculture such as heat-tolerant crops and adjusting irrigation regimes are suitable (Nazrul et al., 2025; Bastola et al., 2024; Cardell et al., 2020; Dunn et al., 2020). For the southwestern coastal area, where TNn is projected to increase at a higher rate, aggregate climate impacts, including freshwater availability and salinity intrusion, may exacerbate with negative feedback between salinity intrusion and the availability of freshwater increasing two-fold, further endangering crop production and drinking water supply. The expected rise in the frequency of extreme rainfall (expressed as R95p: very wet days, and R99p: extremely wet days) might intensify the risk of flooding in western Bangladesh, where the current drainage capacity may be insufficient. Under SSP5-8.5, these intensified precipitation events necessitate improvements in urban drainage systems, flood-resistant infrastructure, and integrated water resource management (Cea et al., 2022).

The projected increase in temperature extremes calls for proactive heat adaptation measures, especially in urban areas where high population densities make residents more susceptible to heat-related illnesses (Uddin et al., 2022). Standard strategies for preventing the consequences of long warm spells and extreme heat events include increasing urban green space, implementing heat action plans, and enhancing cooling facilities. The altered precipitation regime characterised by more heavy rainfall events and less dry days highlights the importance for nature-based solutions for water management. Policy measures should focus on improving urban drainage systems, enhancing flood defenses, and adopting sustainable land use practices that minimize runoff and improve groundwater recharge (Paul & Maity, 2023). Additionally, climate-resilient agriculture, including drought-resistant crops and optimized planting schedules, will be essential for managing shifting precipitation trends and rising temperatures.

Although this study offers a thorough assessment of Bangladesh's potential climate extremes, some limitations must be acknowledged. The use of Simple Quantile Mapping (SQM) for bias correction, though effective, introduces uncertainties, especially for rare and extreme events (Nazrul et al., 2025). Future studies should explore alternative bias correction methods, such as quantile delta mapping or Bayesian approaches, to enhance projection accuracy (Nazrul et al. 2025). Additionally, this analysis relies on 18 CMIP6 GCMs with a single realization (r1i1p1f1) for each model, which may not fully capture internal climate variability (Nazrul et al., 2025). Using multiple realizations or ensemble weighting techniques could further improve climate projections. Future research should also evaluate the socioeconomic implications of climate extremes, including impacts on agriculture, public health, and infrastructure, to support evidence-based policymaking (Nazrul et al., 2025; Bhattacharjee et al., 2023; Kamruzzaman et al., 2025).

This study offers complete insights of future climate extremes in Bangladesh by using CMIP6 multi-model ensemble (MME) data and ETCCDI indices. The results show large changes in temperature and precipitation extremes, in particular for the SSP5-8. 5, underscoring the immediate need for strategies of adaptation. Through overcoming these research gaps and the application of high-level methodologies, this study contributes to the growing literature on climate resilience that offer policy relevant findings for climate adaptation planning contextually both in Bangladesh and beyond.

Chapter 5
Conclusion and Recommendations

5.1 Conclusion

This study explores the projected future changes in climate extremes over Bangladesh considering high-resolution CMIP6 model projections and ETCCDI indices, aiming at the complete assessment of temperature and precipitation extremes under various emissions pathways. The findings indicate that temperature-based indices, such the warm spell duration index (WSDI) and maximum daily temperature (TXx), have significantly increased, whereas extreme precipitation-based indices, like the one-day maximum rainfall (RX1day), have significantly intensified. Under the SSP5-8. 5 is characterized by very marked variations in mean annual temperature reflecting strong warming. Both max and min temperatures are expected to rise, decreasing the DTR.

The consistent rise in warm-related indices and fall in cold-related indices across the country highlights a clear trajectory of rising temperature extremes. While some interannual and spatial variability exists, most temperature indices show a steady upward trend from the near- to far-future across all SSP scenarios. Precipitation indices similarly exhibit positive trends, particularly under SSP5-8.5, signaling an intensification of extreme rainfall events. Notably, the average value of the Consecutive Dry Days (CDD) index declines under all scenarios relative to the baseline period, suggesting a future characterized by shorter dry spells and more frequent, intense rainfall.

Spatial comparisons show marked disparities among regions in climate forecasts. The severity of the temperature extremes (e.g., TXx and TNx) are predicted to be highest over the north and the northeast of Bangladesh, while moderate over the southern and southwestern parts. The extremes of precipitation such as RX1day and number of heavy rainfall days (R20mm) are anticipated to be most severe in the northeastern and few coastal areas. These trends reflect increased risks of heat stress, flooding, and water resources problems in many areas including the north, north-east, and the coastline.

The findings underscore the need for region-specific adaptation strategies, including the development of climate-smart agricultural practices, sustainable water management and heat-resilient infrastructure. This study is constrained in a number of ways, including the exclusion of socioeconomic elements that influence regional risk and uncertainty regarding model bias correction techniques. Future study must fill these gaps by investigating compound extremes, utilizing high-resolution regional climate models that are rescaled to Bangladesh's diverse topography, and looking at the socioeconomic effects of climate change. In conclusion, this study emphasizes the importance of immediate proactive mitigation measures and adaptation techniques in the face of the escalating climatic extremes in Bangladesh. In the face of increasing climate change, protecting vulnerable populations and ecosystems will require combining evidence-based, locally focused adaption strategies with strong climate projections.

5.2 Implications of the Findings

The study reveals that significant changes in temperature and precipitation indices are projected across Bangladesh, particularly under the SSP5-8.5 scenario in the far future, underscoring the intensifying impacts of climate change. Temperature extremes, including increases in both maximum and minimum temperatures, indicate a narrowing Diurnal Temperature Range (DTR) and a consistent upward trajectory in warm indices, alongside a reduction in cold indices. These trends suggest a growing frequency and intensity of heat stress events, especially in northern and northeastern regions. At the same time, the CDD index is declining, indicating fewer dry spells and increased threats of intense rainfall and flash flooding, especially in the northeastern and coastal regions, while precipitation indices like RX1day and R20mm are showing increasing trends.

In the upcoming decades, Bangladesh will face significant challenges due to the predicted changes in temperature and precipitation extremes across all SSP scenarios. Increased heat stress on plants and livestock, altered crop growth cycles, and decreased agricultural yields are all consequences of intensified warming, especially under SSP5-8.5. Nighttime cooling will be restricted by the dramatic increase in tropical and warm nights, which will cause discomfort, disturb sleep, and raise daily energy needs. Reductions in cold nights and cold spells may also upset pest dynamics and ecological balance, even though they lower the risk of frost. Furthermore, the likelihood of flash floods, waterlogging, and infrastructure damage will increase due to the anticipated rise in extreme and intense rainfall events, particularly in coastal and low-lying areas. Due to alternating periods of heavy rainfall and protracted dry spells, these precipitation shifts will cause crop damage, erode fertile topsoil, interfere with sowing and harvesting schedules, and make managing water resources more difficult. Stormwater drainage systems in urban areas will be under more strain, which will lead to frequent flooding and sanitary problems. When combined, these climate extremes pose a threat to the nation's overall socioeconomic stability, human health, food security, and water availability.

These climatic changes are already posing substantial threats to key sectors in Bangladesh, including agriculture, health, infrastructure, and livelihoods. The country ranks among the most climate-vulnerable globally, having faced 185 extreme weather events between 2000 and 2019, and continues to experience sea level rise at a rate exceeding the global average, endangering coastal populations. Increased heat stress diminishes labor productivity and exacerbates health risks, especially for communities reliant on agriculture and fisheries. Although Bangladesh has made commendable strides in climate adaptation such as the Cyclone Preparedness Programme and the adoption of climate-resilient agriculture the accelerating pace and magnitude of climate change are likely to surpass current adaptation capacities. It is thus important to adopt demand-driven approaches involving the promotion of scaling up of adaptive agricultural practices, sustainable water management, climate resilient infrastructure and upgrading early warning systems. Future resilience must also be underpinned by increased investments, equitable access to climate finance, support for locally led adaptation, and a transition toward a low-carbon development pathway.

5.3 Limitations and Future Scopes

A comparative analysis with different observed datasets such as ERA5, CRU, NCEP, and other reanalysis products could provide deeper insights into the severity and variability of climate extreme events.

This study utilized 18 GMCs although there is no universally recommended method for General Circulation Model (GCM) selection. In the future, more efforts are needed to study different patterns of GCMs selection to enhance the reliability of CMIP6-derived climate projection, especially in regional climate change. In this study, the arithmetic mean of the median was employed for MME calculations, but alternative methods such as Weighted Ensemble Methods, Bayesian Model Averaging (BMA), and machine-learning-based ensemble techniques could be explored to improve projection accuracy. A comparative analysis between different MME computation techniques could enhance the reliability of future climate projections. A detailed analysis could be conducted in the future to examine how many individual GCMs agree on the statistically significant changes, rather than relying solely on the multi-model ensemble (MME) approach.

This study utilized statistical downscaling, which is computationally inexpensive and requires less processing time. However, literature suggests that dynamic downscaling through Regional Climate Models (RCMs) may provide higher spatial resolution and improved representation of local-scale climatic features. Future research could integrate dynamical downscaling approaches with CMIP6 models to improve climate projections, particularly for extreme events such as heatwaves, intense precipitation, and prolonged dry spells.

Further research could also explore bias correction techniques, as different statistical methodologies can lead to varying results. Incorporating quantile delta mapping or machine-learning-based bias correction could refine model accuracy, particularly in regions with complex topography and diverse climate regimes.

By addressing these limitations and exploring advanced methodologies, future studies can contribute to more accurate, reliable, and policy-relevant climate projections, supporting climate adaptation strategies in vulnerable regions such as Bangladesh.

References

Abbaszadeh, P., Muñoz, D. F., Moftakhari, H., Jafarzadegan, K., & Moradkhani, H. (2022). Perspective on uncertainty quantification and reduction in compound flood modeling and forecasting. IScience, 25(10). https://doi.org/10.1016/J.ISCI.2022.105201

Abdullah, A. Y. M., Bhuian, M. H., Kiselev, G., Dewan, A., Hassan, Q. K., & Rafiuddin, M. (2022). Extreme temperature and rainfall events in Bangladesh: A comparison between coastal and inland areas. International Journal of Climatology, 42(6), 3253–3273. https://doi.org/10.1002/JOC.6911

Acharya, N., Shrivastava, N. A., Panigrahi, B. K., & Mohanty, U. C. (2014). Development of an artificial neural network based multi-model ensemble to estimate the northeast monsoon rainfall over south peninsular India: An application of extreme learning machine. Climate Dynamics, 43(5–6), 1303–1310. https://doi.org/10.1007/s00382-013-1942-2

Adekanmbi, A. A., & Sizmur, T. (2022). Importance of Diurnal Temperature Range (DTR) for predicting the temperature sensitivity of soil respiration. Frontiers in Soil Science, 2. https://doi.org/10.3389/fsoil.2022.969077

Adil, L., Eckstein, D., Künzel, V., & Schäfer, L. (2025). Climate Risk Index 2025: Summary. Germanwatch e.V. https://www.germanwatch.org/en/93013

Aghakouchak, A., Chiang, F., Huning, L. S., Love, C. A., Mallakpour, I., Mazdiyasni, O., Moftakhari, H., Papalexiou, S. M., Ragno, E., & Sadegh, M. (2020). Climate extremes and compound hazards in a warming world. Annual Review of Earth and Planetary Sciences, 48(1), 519-548. https://doi.org/10.1146/annurev-earth-071719-055228

Ahmad, Q. K. (2018). Third National Communication of Bangladesh to the United Nations Framework Convention on Climate Change. Ministry of Environment, Forest and Climate Change, Government of the People's Republic of Bangladesh.

Airey, M., & Hulme, M. (1995). Evaluating climate model simulations of precipitation: methods, problems and performance. Progress in Physical Geography, 19(4), 427–448. https://doi.org/10.1177/030913339501900401

Akter, M. Y., Islam, A. R. M. T., Mallick, J., Alam, M. M., Alam, E., Shahid, S., Biswas, J. C., Alam, G. M. M., Pal, S. C., & Oliver, M. M. H. (2024). Temperature extremes Projections over Bangladesh from CMIP6 Multi-model Ensemble. Theoretical and Applied Climatology, 155(9), 8843–8869. https://doi.org/10.1007/s00704-024-05173-5

Alam, A. K. M., & Khan, M. S. H. (2022). Geomorphology of Bangladesh and potential land use. In Bangladesh Geosciences and Resources Potential (pp. 355-398). CRC Press. https://doi.org/10.1201/9781003080817-10

Alam, M. M. (2011). Statistical Downscaling of Extremes of Precipitation in Mesoscale Catchments from Different RCMs and Their Effects on Local Hydrology.

Alamgir, M., Ahmed, K., Homsi, R., Dewan, A., Wang, J.-J., & Shahid, S. (2019). Downscaling and Projection of Spatiotemporal Changes in Temperature of Bangladesh. Earth Systems and Environment, 3(3), 381–398. https://doi.org/10.1007/s41748-019-00121-0

Albergel, C., Dutra, E., Munier, S., Calvet, J. C., Munoz-Sabater, J., De Rosnay, P., & Balsamo, G. (2018). ERA-5 and ERA-Interim driven ISBA land surface model simulations: Which one performs better? Hydrology and Earth System Sciences, 22(6), 3515–3532. https://doi.org/10.5194/HESS-22-3515-2018

Alexander, L. V., Zhang, X., Peterson, T. C., Caesar, J., Gleason, B., Tank, A. M. G. K., Haylock, M., Collins, D., Trewin, B., Rahimzadeh, F., Tagipour, A., Kumar, K. R., Revadekar, J., Griffiths, G., Vincent, L., Stephenson, D. B., Burn, J., Aguilar, E., Brunet, M., Taylor, M., New, M., Zhai, P., Rusticucci, M., & Vazquez-Aguirre, J. L. (2006). Global observed changes in daily climate extremes of temperature and precipitation. Journal of Geophysical Research: Atmospheres, 111(D5), D05109. https://doi.org/10.1029/2005JD006290

Ali, M. A., & Kamraju, M. (2025). Global Climate Governance. https://doi.org/10.1007/978-981-96-2727-1

Ali, S., Bhutta, Z. A., Reboita, M. S., Goheer, M. A., Ebrahimi, S., Rozante, J. R., Kiani, R. S., Muhammad, S., Khan, F., Rahman, M. M., Shreshta, M. L., & Dan, L. (2024). A 5-km gridded product development of daily temperature and precipitation for Bangladesh, Nepal, and Pakistan from 1981 to 2016. Geoscience Data Journal, 11(3), 292–302. https://doi.org/10.1002/GDJ3.217

Ali, S., Eum, H. I., Cho, J., Dan, L., Khan, F., Dairaku, K., ... & Fahad, S. (2019). Assessment of climate extremes in future projections downscaled by multiple statistical downscaling methods over Pakistan. Atmospheric Research, 222, 114-133. https://doi.org/10.1016/j.atmosres.2019.02.009

Almazroui, M., Saeed, S., Saeed, F., Islam, M. N., & Ismail, M. (2020). Projections of Precipitation and Temperature over the South Asian Countries in CMIP6. Earth Systems and Environment, 4(2), 297–320. https://doi.org/10.1007/S41748-020-00157-7

Amini, A. (Ed.). (2019). Climate Change and Global Warming. IntechOpen. https://doi.org/10.5772/intechopen.74882

Aram, F., García, E. H., Solgi, E., & Mansournia, S. (2019). Urban green space cooling effect in cities. Heliyon, 5(4). http://doi.org/10.1016/j.heliyon.2019.e01339

Ashrafuzzaman, M., Santos, F. D., Dias, J. M., & Cerdà, A. (2022). Dynamics and Causes of Sea Level Rise in the Coastal Region of Southwest Bangladesh at Global, Regional, and Local Levels. Journal of Marine Science and Engineering, 10(6), 779. https://doi.org/10.3390/JMSE10060779

Australian Bureau of Meteorology. (n.d.). Extreme climate indices – PCCSP Pacific climate change science program. Retrieved May 4, 2025, from http://www.bom.gov.au/climate/pccsp/about-pi-extreme-indices.shtml

Babaousmail, H., Ayugi, B. O., Lim Kam Sian, K. T. C., Randriatsara, H. H. R. H., & Mumo, R. (2024). How Do CMIP6 HighResMIP Models Perform in

Simulating Precipitation Extremes over East Africa? Hydrology, 11(7). https://doi.org/10.3390/hydrology11070106

Babcock, R. C., Bustamante, R. H., Fulton, E. A., Fulton, D. J., Haywood, M. D. E., Hobday, A. J., Kenyon, R., Matear, R. J., Plagányi, E. E., Richardson, A. J., & Vanderklift, M. A. (2019). Severe continental-scale impacts of climate change are happening now: Extreme climate events impact marine habitat forming communities along 45% of Australia's coast. Frontiers in Marine Science, 6, 411. https://doi.org/10.3389/fmars.2019.00411

Balaji, V., Couvreux, F., Deshayes, J., Gautrais, J., Hourdin, F., & Rio, C. (2022). Are general circulation models obsolete? Proceedings of the National Academy of Sciences of the United States of America, 119(47). https://doi.org/10.1073/PNAS.2202075119

Bangladesh Meteorological Department. (n.d.). Bangladesh Meteorological Department. Retrieved May 4, 2025, from http://live6.bmd.gov.bd/

Barry, A. A., Caesar, J., Klein Tank, A. M. G., Aguilar, E., McSweeney, C., Cyrille, A. M., Nikiema, M. P., Narcisse, K. B., Sagna, Y., Sarr, B., Salack, S., Sanogo, S., Sarr, A., & Laogbessi, E. T. (2018). West Africa climate extremes and climate change indices. International Journal of Climatology, 38(S1), e921–e938. https://doi.org/10.1002/joc.5420

Basher, Md. A., Stiller-Reeve, M. A., Saiful Islam, A. K. M., & Bremer, S. (2018). Assessing climatic trends of extreme rainfall indices over northeast Bangladesh. Theoretical and Applied Climatology, 134(1), 441–452. https://doi.org/10.1007/s00704-017-2285-4

Bastola, S., Cho, J., Kam, J., & Jung, Y. (2024). Assessing the influence of climate change on multiple climate indices in Nepal using CMIP6 global climate models. Atmospheric Research, 311, 107720. https://doi.org/10.1016/j.atmosres.2024.107720

Behnke, R., Vavrus, S., Allstadt, A., Albright, T., Thogmartin, W. E., & Radeloff, V. C. (2016). Evaluation of downscaled, gridded climate data for the conterminous United States. Ecological Applications, 26(5), 1338–1351. https://doi.org/10.1002/15-1061

Bell, B., Hersbach, H., Simmons, A., Berrisford, P., Dahlgren, P., Horányi, A., Muñoz-Sabater, J., Nicolas, J., Radu, R., Schepers, D., Soci, C., Villaume, S., Bidlot, J. R., Haimberger, L., Woollen, J., Buontempo, C., & Thépaut, J. N. (2021). The ERA5 global reanalysis: Preliminary extension to 1950. Quarterly Journal of the Royal Meteorological Society, 147(741), 4186–4227. https://doi.org/10.1002/QJ.4174

Bell, J. E., Brown, C. L., Conlon, K., Herring, S., Kunkel, K. E., Lawrimore, J., Luber, G., Schreck, C., Smith, A., & Uejio, C. (2018). Changes in extreme events and the potential impacts on human health. Journal of the Air & Waste Management Association, 68(4), 265–287. https://doi.org/10.1080/10962247.2017.1401017

Bengtsson, L., & Shukla, J. (1988). Integration of Space and In Situ Observations to Study Global Climate Change. Bulletin of the American Meteorological Society, 69(10), 1130–1143. https://doi.org/10.1175/1520-0477(1988)069<1130:IOSAIS>2.0.CO;2

Bhattacharjee, A., Hassan, S. M. Q., Hazra, P., Kormoker, T., Islam, S., Alam, E., Islam, K., Reza, A., & Islam, M. T. (2023). Future changes of summer monsoon rainfall and temperature over Bangladesh using 27 CMIP6 models. Taylor & FrancisA Bhattacharjee, SMQ Hassan, P Hazra, T Kormoker, S Islam, E Alam, MK IslamGeocarto International, 2023•Taylor & Francis, 38(1). https://doi.org/10.1080/10106049.2023.2285342

Bhattarai, T. N., Ghimire, S., Aryal, S., Baaniya, Y., Bhattarai, S., Sharma, S., ... & Pandey, V. P. (2023). Projected changes in hydro-climatic extremes with CMIP6 climate model outputs: a case of rain-fed river systems in Western Nepal. Stochastic Environmental Research and Risk Assessment, 37(3), 965-987. https://doi.org/10.1007/s00477-022-02312-0

Brammer, H. (2014). Bangladesh's dynamic coastal regions and sea-level rise. Climate Risk Management, 1, 51–62. https://doi.org/10.1016/J.CRM.2013.10.001

Branković, Č., & Molteni, F. (2004). Seasonal climate and variability of the ECMWF ERA-40 model. Climate Dynamics, 22(2–3), 139–156. https://doi.org/10.1007/S00382-003-0370-0/FIGURES/17

Brönnimannid, S. (2022). From climate to weather reconstructions. PLOS Climate, 1(6), e0000034. https://doi.org/10.1371/JOURNAL.PCLM.0000034

Brown, P. J., Bradley, R. S., & Keimig, F. T. (2010). Changes in Extreme Climate Indices for the Northeastern United States, 1870–2005. Journal of Climate, 23(24), 6555–6572. https://doi.org/10.1175/2010JCLI3363.1

Bryan, K. (2006). Modeling Ocean Circulation. Physical Oceanography: Developments Since 1950, 29–44. https://doi.org/10.1007/0-387-33152-2_3

Carbon Brief. (2019, December 2). CMIP6: The next generation of climate models explained. https://www.carbonbrief.org/cmip6-the-next-generation-of-climate-models-explained/

Cardell, M. F., Amengual, A., Romero, R., & Ramis, C. (2020). Future extremes of temperature and precipitation in Europe derived from a combination of dynamical and statistical approaches. International Journal of Climatology, 40(11), 4800-4827. http://doi.org/10.1002/joc.6490

Cavazos, T., & Hewitson, B. C. (2005). Performance of NCEP–NCAR reanalysis variables in statistical downscaling of daily precipitation. Climate Research, 28(2), 95–107. https://doi.org/10.3354/CR028095

Cea, L., & Costabile, P. (2022). Flood risk in urban areas: Modelling, management and adaptation to climate change. A review. Hydrology, 9(3), 50. https://doi.org/10.3390/hydrology9030050

Changnon, D., Sandstrom, M., & Schaffer, C. (2003). Relating changes in agricultural practices to increasing dew points in extreme Chicago heat waves. Climate Research, 24(3), 243–254. https://doi.org/10.3354/CR024243

Chen, A., Zhang, S., & Li, Z. (2021). Impact of Automated Statistical Downscaling and Delta Downscaling methods on projecting future climate change in the northeast Tibetan Plateau. Climate Research, 83, 91–110. https://doi.org/10.3354/CR01634

Chen, G., & Ji, Z. (2024). A Review of Solar and Wind Energy Resource Projection Based on the Earth System Model. Sustainability 2024, Vol. 16, Page 3339, 16(8), 3339. https://doi.org/10.3390/SU16083339

Chen, S., Long, G., Jiang, J., Liu, D., & Zhang, C. (2023). Foundation Models for Weather and Climate Data Understanding: A Comprehensive Survey. https://arxiv.org/pdf/2312.03014

Chen, W., Xiao, A., Braconnot, P., Ciais, P., Viovy, N., & Zhang, R. (2022). Mid-Holocene high-resolution temperature and precipitation gridded reconstructions over China: Implications for elevation-dependent temperature changes. Earth and Planetary Science Letters, 593, 117656. https://doi.org/10.1016/j.epsl.2022.117656

Cho, J., Ko, G., Kim, K., & Oh, C. (2016). Climate change impacts on agricultural drought with consideration of uncertainty in CMIP5 scenarios. Irrigation and Drainage, 65(Specialissue2), 7–15. https://doi.org/10.1002/IRD.2035

Chokkavarapu, N., & Mandla, V. R. (2019). Comparative study of GCMs, RCMs, downscaling and hydrological models: a review toward future climate change impact estimation. SN Applied Sciences, 1(12), 1–15. https://doi.org/10.1007/s42452-019-1764-x

Clarke, B., Otto, F., Stuart-Smith, R., & Harrington, L. (2022). Extreme weather impacts of climate change: an attribution perspective. Environmental Research: Climate, 1(1), 012001. https://doi.org/10.1088/2752-5295/AC6E7D

Costa, R. L., Baptista, G. M. M., Gomes, H. B., Silva, F. D. S., da Rocha Júnior, R. L., Salvador, M. A., & Herdies, D. L. (2020). Analysis of climate extremes indices over northeast Brazil from 1961 to 2014. Weather Clim Extremes 28: 100254. https://doi.org/10.1016/j.wace.2020.100254

Dai, A., Wigley, T. M. L., Boville, B. A., Kiehl, J. T., & Buja, L. E. (2001). Climates of the Twentieth and Twenty-First Centuries Simulated by the NCAR Climate System Model. Journal of Climate, 14(4), 485–519. https://doi.org/10.1175/1520-0442(2001)014

Das, S., Islam, A. R. M. T., & Kamruzzaman, M. (2023). Assessment of climate change impact on temperature extremes in a tropical region with the climate projections from CMIP6 model. Climate Dynamics, 60(1–2), 603–622. https://doi.org/10.1007/S00382-022-06416-9

Dastagir, M. R. (2015). Modeling recent climate change induced extreme events in Bangladesh: A review. Weather and Climate Extremes, 7, 49–60. https://doi.org/10.1016/J.WACE.2014.10.003

Dee, D. P., Uppala, S. M., Simmons, A. J., Berrisford, P., Poli, P., Kobayashi, S., Andrae, U., Balmaseda, M. A., Balsamo, G., Bauer, P., Bechtold, P., Beljaars, A. C. M., van de Berg, L., Bidlot, J., Bormann, N., Delsol, C., Dragani, R., Fuentes, M., Geer, A. J., … Vitart, F. (2011). The ERA-Interim reanalysis: configuration and performance of the data assimilation system. Quarterly Journal of the Royal Meteorological Society, 137(656), 553–597. https://doi.org/10.1002/QJ.828

Deegala, D., Song, Y. H., Chung, E. S., Ayugi, B. O., & Shahid, S. (2023). Future extreme precipitation changes in the South Asian Summer Monsoon Dominance Region. Atmospheric Research, 295, 107029. https://doi.org/10.1016/J.ATMOSRES.2023.107029

Deng, H., Yin, Y., Zong, X., & Yin, M. (2023). Future drought risks in the Yellow River Basin and suggestions for targeted response. International Journal of Disaster Risk Reduction, 93, 103764. https://doi.org/10.1016/J.IJDRR.2023.103764

Dey, A., Sahoo, D. P., Kumar, R., & Remesan, R. (2022). A multimodel ensemble machine learning approach for CMIP6 climate model projections in an Indian River basin. International Journal of Climatology, 42(16), 9215–9236. https://doi.org/10.1002/JOC.7813

Di Virgilio, G., Ji, F., Tam, E., Nishant, N., Evans, J. P., Thomas, C., Riley, M. L., Beyer, K., Grose, M. R., Narsey, S., & Delage, F. (2022). Selecting CMIP6 GCMs for CORDEX Dynamical Downscaling: Model Performance, Independence, and Climate Change Signals. Earth's Future, 10(4), e2021EF002625. https://doi.org/10.1029/2021EF002625

Donat, M. G., Alexander, L. V., Yang, H., Durre, I., Vose, R., Dunn, R. J. H., Willett, K. M., Aguilar, E., Brunet, M., Caesar, J., Hewitson, B., Jack, C., Klein Tank, A. M. G., Kruger, A. C., Marengo, J., Peterson, T. C., Renom, M., Oria Rojas, C., Rusticucci, M., … Kitching, S. (2013). Updated analyses of temperature and precipitation extreme indices since the beginning of the twentieth century: The HadEX2 dataset. Journal of Geophysical Research: Atmospheres, 118(5), 2098–2118. https://doi.org/10.1002/JGRD.50150

Donat, M. G., Sillmann, J., & Fischer, E. M. (2020). Changes in climate extremes in observations and climate model simulations. From the past to the future. Climate Extremes and Their Implications for Impact and Risk Assessment, 31–57. https://doi.org/10.1016/B978-0-12-814895-2.00003-3

Duncan, E. W., White, N. M., & Mengersen, K. (2017). Spatial smoothing in Bayesian models: A comparison of weights matrix specifications and their impact on inference. International Journal of Health Geographics, 16(1), 1–16. https://doi.org/10.1186/S12942-017-0120-X

Dunn, R. J. H., Alexander, L. V., Donat, M. G., Zhang, X., Bador, M., Herold, N., Lippmann, T., Allan, R., Aguilar, E., Barry, A. A., Brunet, M., Caesar, J., Chagnaud, G., Cheng, V., Cinco, T., Durre, I., de Guzman, R., Htay, T. M., Wan Ibadullah, W. M., … Bin Hj Yussof, M. N. A. (2020). Development of an Updated Global Land In Situ-Based Data Set of Temperature and Precipitation Extremes: HadEX3. Journal of Geophysical Research: Atmospheres, 125(16). https://doi.org/10.1029/2019JD032263

Earth System Grid Federation. (n.d.). CMIP6 data search portal. Lawrence Livermore National Laboratory. Retrieved May 4, 2025, from https://aims2.llnl.gov/search/cmip6/

Easterling, D. R. (2013). Global Data Sets for Analysis of Climate Extremes. 347–361. https://doi.org/10.1007/978-94-007-4479-0_12

Easterling, D. R., Horton, B., Jones, P. D., Peterson, T. C., Karl, T. R., Parker, D. E., Salinger, M. J., Razuvayev, V., Plummer, N., Jamason, P., & Folland, C. K. (1997). Maximum and Minimum Temperature Trends for the Globe. Science, 277(5324), 364–367. https://doi.org/10.1126/SCIENCE.277.5324.364

Easterling, D. R., Kunkel, K. E., Wehner, M. F., & Sun, L. (2016). Detection and attribution of climate extremes in the observed record. Weather and Climate Extremes, 11, 17–27. https://doi.org/10.1016/J.WACE.2016.01.001

Easterling, D. R., Meehl, G. A., Parmesan, C., Changnon, S. A., Karl, T. R., & Mearns, L. O. (2000). Climate Extremes: Observations, Modeling, and Impacts. Science, 289(5487), 2068–2074. https://doi.org/10.1126/SCIENCE.289.5487.2068

Ebita, A., Kobayashi, S., Ota, Y., Moriya, M., Kumabe, R., Onogi, K., Harada, Y., Yasui, S., Miyaoka, K., Takahashi, K., Kamahori, H., Kobayashi, C., Endo, H., Soma, M., Oikawa, Y., & Ishimizu, T. (2011). The Japanese 55-year Reanalysis "JRA-55": An Interim Report. SOLA, 7(1), 149–152. https://doi.org/10.2151/SOLA.2011-038

Eckstein, D., Künzel, V., & Schäfer, L. (2021). The global climate risk index 2021. https://bvearmb.do/handle/123456789/1306

Eden, J. M., Widmann, M., Grawe, D., & Rast, S. (2012). Skill, Correction, and Downscaling of GCM-Simulated Precipitation. Journal of Climate, 25(11), 3970–3984. https://doi.org/10.1175/JCLI-D-11-00254.1

Edwards, P. N. (2011). History of climate modeling. Wiley Interdisciplinary Reviews: Climate Change, 2(1), 128–139. https://doi.org/10.1002/wcc.95

Enayati, M., Bozorg-Haddad, O., Bazrafshan, J., Hejabi, S., & Chu, X. (2021). Bias correction capabilities of quantile mapping methods for rainfall and temperature variables. Journal of Water and Climate Change, 12(2), 401–419. https://doi.org/10.2166/WCC.2020.261

Environment and Climate Change Canada. (n.d.). CMIP6 and Shared Socio-economic Pathways overview. Canadian Climate Data and Scenarios. Retrieved May 4, 2025, from https://climate-scenarios.canada.ca/?page=cmip6-overview-notes

Enyew, F. B., Sahlu, D., Tarekegn, G. B., Hama, S., & Debele, S. E. (2024). Performance Evaluation of CMIP6 Climate Model Projections for Precipitation and Temperature in the Upper Blue Nile Basin, Ethiopia. Climate, 12(11), 169. https://doi.org/10.3390/CLI12110169/S1

Expert Team on Climate Change Detection and Indices (ETCCDI). (n.d.). List of the 27 core climate indices and their definitions. Pacific Climate Impacts Consortium. Retrieved May 4, 2025, from https://etccdi.pacificclimate.org/list_27_indices.shtml

Eyring, V., Bony, S., Meehl, G. A., Senior, C. A., Stevens, B., Stouffer, R. J., & Taylor, K. E. (2016). Overview of the Coupled Model Intercomparison Project Phase 6 (CMIP6) experimental design and organization. Geoscientific Model Development, 9(5), 1937–1958. https://doi.org/10.5194/GMD-9-1937-2016

Ezaz, G. T., Zhang, K., Li, X., Shalehy, M. H., Hossain, M. A., & Liu, L. (2022). Spatiotemporal changes of precipitation extremes in Bangladesh during 1987–2017 and their connections with climate changes, climate oscillations, and monsoon dynamics. Global and Planetary Change, 208, 103712. https://doi.org/10.1016/j.gloplacha.2021.103712

Fahad, M. G. R., Saiful Islam, A. K. M., Nazari, R., Alfi Hasan, M., Tarekul Islam, G. M., & Bala, S. K. (2018). Regional changes of precipitation and temperature over Bangladesh using bias-corrected multi-model ensemble projections considering high-emission pathways. International Journal of Climatology, 38(4), 1634–1648. https://doi.org/10.1002/JOC.5284

Filho, W. L. (2015). Handbook of Climate Change Adaptation. Handbook of Climate Change Adaptation, 1–2198. https://doi.org/10.1007/978-3-642-38670-1

Flood Forecasting and Warning Centre. (n.d.). Flood Forecasting and Warning Centre, BWDB, Bangladesh. Bangladesh Water Development Board. Retrieved May 4, 2025, from https://www.ffwc.gov.bd

Flato, G., Marotzke, J., Abiodun, B., Braconnot, P., Chou, S. C., Collins, W., Cox, P., Driouech, F., Emori, S., Eyring, V., Forest, C., Gleckler, P., Guilyardi, E., Jakob, C., Kattsov, V., Reason, C., Rummukainen, M., & more. (2014). Evaluation of climate models. Climate Change 2013 the Physical Science Basis: Working Group I Contribution to the Fifth Assessment Report of the Intergovernmental Panel on Climate Change, 9781107057999, 741–866. https://doi.org/10.1017/CBO9781107415324.020

Foley, A. M. (2010). Uncertainty in regional climate modelling: A review. Progress in Physical Geography, 34(5), 647–670. https://doi.org/10.1177/0309133310375654

Folland, C. K., Karl, T. R., Christy, J. R., Clarke, R. A., Gruza, G. V., et al. (2001). Observed climate variability and change. In J. T. Houghton, Y. Ding, D. J. Griggs, M. Noguer, P. J. van der Linden, X. Dai, K. Maskell, & C. A. Johnson (Eds.), Climate change 2001: The scientific basis. Contribution of Working Group I to the Third Assessment Report of the Intergovernmental Panel on Climate Change (pp. 99–181). Cambridge University Press. https://hal.science/hal-03333964/

Frich, P., Alexander, L. V., Della-Marta, P., Gleason, B., Haylock, M., Tank Klein, A. M. G., & Peterson, T. (2002). Observed coherent changes in climatic extremes during the second half of the twentieth century. Climate Research, 19(3), 193–212. https://doi.org/10.3354/CR019193

Fyfe, J., Fox-Kemper, B., Kopp, R., & Garner, G. (2021). Summary for policymakers of the Working Group I contribution to the IPCC Sixth Assessment Report – Data for Figure SPM.8 (v20210809) [Data set]. NERC EDS Centre for Environmental Data Analysis. https://doi.org/10.5285/98af2184e13e4b91893ab72f301790db

Gao, L., Wei, J., Wang, L., Bernhardt, M., Schulz, K., & Chen, X. (2018). A high-resolution air temperature data set for the Chinese Tian Shan in 1979-2016. Earth System Science Data, 10(4), 2097–2114. https://doi.org/10.5194/ESSD-10-2097-2018

Gao, X., Zhu, Q., Yang, Z., & Wang, H. (2018). Evaluation and Hydrological Application of CMADS against TRMM 3B42V7, PERSIANN-CDR, NCEP-CFSR, and Gauge-Based Datasets in Xiang River Basin of China. Water 2018, Vol. 10, Page 1225, 10(9), 1225. https://doi.org/10.3390/W10091225

Gariano, S. L., & Guzzetti, F. (2016). Landslides in a changing climate. Earth-Science Reviews, 162, 227–252. https://doi.org/10.1016/J.EARSCIREV.2016.08.011

Gautam, R., Borgohain, A., Pathak, B., Kundu, S. S., & Aggarwal, S. P. (2024). Investigation of meteorological variables and associated extreme events over North-East India and its adjoining areas using high-resolution IMDAA reanalysis. Natural Hazards, 1-36. https://doi.org/10.1007/s11069-024-06979-2

General Economics Division (GED), Bangladesh Planning Commission. (2018). Bangladesh Delta Plan 2100: Bangladesh in the 21st century, Volume 1: Strategy. Ministry of Planning, Government of the People's Republic of Bangladesh

General Economics Division, Bangladesh Planning Commission. (2020). Eighth five year plan: July 2020–June 2025—Promoting prosperity and fostering inclusiveness. Government of the People's Republic of Bangladesh.

Gent, P. R. (2013). Coupled Models and Climate Projections. International Geophysics, 103, 609–623. https://doi.org/10.1016/B978-0-12-391851-2.00023-4

Gharbia, S. S., Gill, L., Johnston, P., & Pilla, F. (2016). Multi-GCM ensembles performance for climate projection on a GIS platform. Modeling Earth Systems and Environment, 2(2), 1–21. https://doi.org/10.1007/S40808-016-0154-2/FIGURES/13

Gramcianinov, C. B., Campos, R. M., de Camargo, R., Hodges, K. I., Guedes Soares, C., & da Silva Dias, P. L. (2020). Analysis of Atlantic extratropical storm tracks characteristics in 41 years of ERA5 and CFSR/CFSv2 databases. Ocean Engineering, 216, 108111. https://doi.org/10.1016/J.OCEANENG.2020.108111

Gudmundsson, L., Bremnes, J. B., Haugen, J. E., & Engen-Skaugen, T. (2012). Technical Note: Downscaling RCM precipitation to the station scale using statistical transformations – a comparison of methods. Hydrology and Earth System Sciences, 16(9), 3383–3390. https://doi.org/10.5194/hess-16-3383-2012

Haider, S., Karim, M. R., Islam, M. S., Megumi, T. A., & Rahnama, Q. S. (2024). Extreme weather events and Spatio-temporal characterization of climate change variables in Bangladesh during 1975–2019. https://doi.org/10.1016/j.heliyon.2024.e27118

Haile, G. G., Tang, Q., Li, W., Liu, X., & Zhang, X. (2020). Drought: Progress in broadening its understanding. Wiley Interdisciplinary Reviews: Water, 7(2), e1407. https://doi.org/10.1002/WAT2.1407

Hajat, S., Vardoulakis, S., Heaviside, C., & Eggen, B. (2014). Climate change effects on human health: projections of temperature-related mortality for the UK during the 2020s, 2050s and 2080s. J Epidemiol Community Health, 68(7), 641–648. https://doi.org/10.1136/JECH-2013-202449

Harada, Y., Kamahori, H., Kobayashi, C., Endo, H., Kobayashi, S., Ota, Y., Onoda, H., Onogi, K., Miyaoka, K., & Takahashi, K. (2016). The JRA-55 Reanalysis: Representation of Atmospheric Circulation and Climate Variability. Journal of the Meteorological Society of Japan. Ser. II, 94(3), 269–302. https://doi.org/10.2151/JMSJ.2016-015

Hasan, M. A., Islam, A. K. M. S., & Akanda, A. S. (2018). Climate projections and extremes in dynamically downscaled CMIP5 model outputs over the Bengal delta: a quartile based bias-correction approach with new gridded data. Climate Dynamics, 51(5–6), 2169–2190. https://doi.org/10.1007/s00382-017-4006-1

Heo, J. H., Ahn, H., Shin, J. Y., Kjeldsen, T. R., & Jeong, C. (2019). Probability Distributions for a Quantile Mapping Technique for a Bias Correction of Precipitation Data: A Case Study to Precipitation Data Under Climate Change. Water 2019, Vol. 11, Page 1475, 11(7), 1475. https://doi.org/10.3390/W11071475

Her, Y., Yoo, S. H., Cho, J., Hwang, S., Jeong, J., & Seong, C. (2019). Uncertainty in hydrological analysis of climate change: multi-parameter vs. multi-GCM ensemble predictions. Scientific Reports 2019 9:1, 9(1), 1–22. https://doi.org/10.1038/s41598-019-41334-7

Hersbach, H., Bell, B., Berrisford, P., Hirahara, S., Horányi, A., Muñoz-Sabater, J., Nicolas, J., Peubey, C., Radu, R., Schepers, D., Simmons, A., Soci, C., Abdalla, S., Abellan, X., Balsamo, G., Bechtold, P., Biavati, G., Bidlot, J., Bonavita, M., … Thépaut, J. N. (2020). The ERA5 global reanalysis.

Quarterly Journal of the Royal Meteorological Society, 146(730), 1999–2049. https://doi.org/10.1002/QJ.3803

Houghton, J. T. . (2001). Climate change 2001 : the scientific basis. Contribution of Working Group I. Edited by J.T. Houghton and others. Cambridge University Press.

Hourdin, F., Grandpeix, J. Y., Rio, C., Bony, S., Jam, A., Cheruy, F., Rochetin, N., Fairhead, L., Idelkadi, A., Musat, I., Dufresne, J. L., Lahellec, A., Lefebvre, M. P., & Roehrig, R. (2013). LMDZ5B: The atmospheric component of the IPSL climate model with revisited parameterizations for clouds and convection. Climate Dynamics, 40(9–10), 2193–2222. https://doi.org/10.1007/S00382-012-1343-Y/FIGURES/23

Hunziker, S., Gubler, S., Calle, J., Moreno, I., Andrade, M., Velarde, F., Ticona, L., Carrasco, G., Castellón, Y., Oria, C., Croci-Maspoli, M., Konzelmann, T., Rohrer, M., & Brönnimann, S. (2017). Identifying, attributing, and overcoming common data quality issues of manned station observations. International Journal of Climatology, 37(11), 4131–4145. https://doi.org/10.1002/JOC.5037

Huo, W., Li, Z., Wang, J., Yao, C., Zhang, K., & Huang, Y. (2019). Multiple hydrological models comparison and an improved Bayesian model averaging approach for ensemble prediction over semi-humid regions. Stochastic Environmental Research and Risk Assessment, 33(1), 217–238. https://doi.org/10.1007/S00477-018-1600-7

Imran, H. M., Kala, J., Uddin, S., Islam, A. S., & Acharya, N. (2023). Spatiotemporal analysis of temperature and precipitation extremes over Bangladesh using a novel gridded observational dataset. Weather and climate extremes, 39, 100544. https://doi.org/10.1016/j.wace.2022.100544

Intergovernmental Panel on Climate Change (IPCC). (2007). Climate change 2007: Synthesis report. Contribution of Working Groups I, II and III to the Fourth Assessment Report of the Intergovernmental Panel on Climate Change (Core Writing Team, R. K. Pachauri & A. Reisinger, Eds.). IPCC. https://www.ipcc.ch/report/ar4/syr/

Intergovernmental Panel on Climate Change (IPCC). (2013). Climate change 2013: The physical science basis. Contribution of Working Group I to the Fifth Assessment Report of the Intergovernmental Panel on Climate Change (T. F. Stocker, D. Qin, G.-K. Plattner, M. Tignor, S. K. Allen, J. Boschung, ... P. M. Midgley, Eds.). Cambridge University Press. https://www.ipcc.ch/report/ar5/wg1/

Intergovernmental Panel on Climate Change (IPCC). (2021). Climate change 2021: The physical science basis. Contribution of Working Group I to the Sixth Assessment Report of the Intergovernmental Panel on Climate Change (V. Masson-Delmotte, P. Zhai, A. Pirani, S. L. Connors, C. Péan, S. Berger, ... B. Zhou, Eds.). Cambridge University Press. https://doi.org/10.1017/9781009157896

Intergovernmental Panel on Climate Change. (n.d.). Data Distribution Centre. Retrieved May 4, 2025, from https://www.ipcc-data.org/

International Centre for Climate Change and Development (ICCCAD). (2024). Climate change impacts in Bangladesh: What climate change means for a country and its people. ICCCAD. https://icccad.net/publications/climate_change_impacts_in_bangladesh_report_2024/

Islam, A. R. M. T., Akter, M. Y., Fattah, M. A., Mallick, J., Parvin, I., Islam, H. M. T., Shahid, S., Kabir, Z., & Kamruzzaman, M. (2024). Modulation of coupling climatic extremes and their climate signals in a subtropical monsoon country. Theoretical and Applied Climatology, 155(6), 4827–4849. https://doi.org/10.1007/S00704-024-04892-Z

Islam, H. M. T., Islam, A. R. M. T., Abdullah-Al-Mahbub, M., Shahid, S., Tasnuva, A., Kamruzzaman, M., Hu, Z., Elbeltagi, A., Kabir, M. M., Salam, M. A., & Ibrahim, S. M. (2021). Spatiotemporal changes and modulations of extreme climatic indices in monsoon-dominated climate region linkage with large-scale atmospheric oscillation. Atmospheric Research, 264, 105840. https://doi.org/10.1016/J.ATMOSRES.2021.105840

Islam, M. A., & Cartwright, N. (2020). Evaluation of climate reanalysis and space-borne precipitation products over Bangladesh. Hydrological Sciences

Journal, 65(7), 1112–1128. https://doi.org/10.1080/02626667.2020.1730845

Islam, M. T. (2023). Role of Bangladesh Government in Disaster Management. 235–279. https://doi.org/10.1007/978-981-99-1631-3_5

Jahan, F., Sinha, N. C., Rahman, M. M., Rahman, M. M., Mondal, M. S. H., & Islam, M. A. (2019). Comparison of missing value estimation techniques in rainfall data of Bangladesh. Theoretical and Applied Climatology, 136(3–4), 1115–1131. https://doi.org/10.1007/S00704-018-2537-Y

Jayasankar, C. B., Rajendran, K., & Surendran, S. (2018). Monsoon Climate Change Projection for the Orographic West Coast of India Using High-Resolution Nested Dynamical Downscaling Model. Journal of Geophysical Research: Atmospheres, 123(15), 7821–7838. https://doi.org/10.1029/2018JD028677

Jerin, J. N., Islam, H. M. T., Islam, A. R. M. T., Shahid, S., Hu, Z., Badhan, M. A., Chu, R., & Elbeltagi, A. (2021). Spatiotemporal trends in reference evapotranspiration and its driving factors in Bangladesh. Theoretical and Applied Climatology, 144(1–2), 793–808. https://doi.org/10.1007/S00704-021-03566-4

Jihan, M. A. T., Popy, S., Kayes, S., Rasul, G., Maowa, A. S., & Rahman, M. M. (2025). Climate change scenario in Bangladesh: historical data analysis and future projection based on CMIP6 model. Scientific Reports, 15(1), 1–22. https://doi.org/10.1038/S41598-024-81250-Z

Jones, J. A. A. (1999). Climate change and sustainable water resources: placing the threat of global warming in perspective. Hydrological Sciences Journal, 44(4), 541–557. https://doi.org/10.1080/02626669909492251

Jose, D. M., Vincent, A. M., & Dwarakish, G. S. (2022). Improving multiple model ensemble predictions of daily precipitation and temperature through machine learning techniques. Scientific Reports, 12(1), 1–25. https://doi.org/10.1038/S41598-022-08786-W

Kalnay, E., Kanaimitsu, M., Kistler, R., Collins, W., Deaven, D., Gandin, L., Iredell, M., Saha, S., White, G., Woollen, J., Zhu, Y., Chelliah, M., Ebisuzaki, W., Higgins, W., Janowiak, J., Mo, K. C., Ropelewski, C., Wang, J., Leetiaa, A., … Joseph, D. (2018). The NCEP/NCAR 40-year reanalysis project. Renewable Energy: Four Volume Set, 1–4, 146–194. https://doi.org/10.4324/9781315793245-16

Kamruzzaman, M., Biswas, J. C., Islam, H. M. T., & Hossain, A. M. K. Z. (2024a). Interannual Climate Variability and Its Impacts on Major Crop Productivity. Climate Change and Soil-Water-Plant Nexus, 297–329. https://doi.org/10.1007/978-981-97-6635-2_10

Kamruzzaman, M., Islam, H. M. T., Ahmed, S., Bhattacharjya, D. K., Khan, M. S. K., Mahmud, G. I., Almazroui, M., & Shahid, S. (2023a). Evaluating the Effects of Climate Change on Thermal Bioclimatic Indices in a Tropical Region Using Climate Projections from the Bias-Corrected CMIP6 Model. Earth Systems and Environment, 7(4), 699–722. https://doi.org/10.1007/S41748-023-00360-2

Kamruzzaman, M., Islam, H. M. T., Ahmed, S., Bhattacharjya, D. K., Khan, Md. S. K., Mahmud, G. I., & Shahid, S. (2023b). Assessment of climate change impact on thermal bioclimatic indicators in a tropical region with the climate projections from CMIP6 modele Dynamics. https://doi.org/10.21203/RS.3.RS-2895116/V1

Kamruzzaman, M., Islam, H. M. T., Rahman, M. S., Ahmed, S., Lipi, L. F., Khan, M. A. R., Tran, L. S. P., & Hossain, A. M. K. Z. (2025). Assessing the impacts of future climate extremes on boro rice cultivation in the northeastern Haor region of Bangladesh: insights from CMIP6 multi-model ensemble projections. Theoretical and Applied Climatology, 156(1). https://doi.org/10.1007/S00704-024-05270-5

Kamruzzaman, M., Jang, M. W., Cho, J., & Hwang, S. (2019). Future Changes in Precipitation and Drought Characteristics over Bangladesh under CMIP5 Climatological Projections. Water 2019, Vol. 11, Page 2219, 11(11), 2219. https://doi.org/10.3390/W11112219

Kamruzzaman, M., Shahid, S., Roy, D., Islam, A., Hwang, S., Cho, J., Zaman, M., Sultana, T., Rashid, T., & Akter, F. (2021). Assessment of CMIP6 global climate models in reconstructing rainfall climatology of Bangladesh. International Journal of Climatology, 42. https://doi.org/10.1002/joc.7452

Kamruzzaman, M., Shariot-Ullah, M., Islam, R., Amin, M. G. M., Islam, H. M. T., Ahmed, S., Yildiz, S., Muktadir, A., & Shahid, S. (2024b). Projections of future bioclimatic indicators using bias-corrected CMIP6 models: a case study in a tropical monsoon region. Environmental Science and Pollution Research. https://doi.org/10.1007/S11356-024-35487-W

Kamruzzaman, M., Wahid, S., Shahid, S., Alam, E., Mainuddin, M., Islam, H. M. T., Cho, J., Rahman, M. M., Chandra Biswas, J., & Thorp, K. R. (2023c). Predicted changes in future precipitation and air temperature across Bangladesh using CMIP6 GCMs. Heliyon, 9(5). https://doi.org/10.1016/j.heliyon.2023.e16274

Karim, R., Waaje, A., & Roshid, M. M. (2024, October 8). Adaptation strategies for climate change impacts in Bangladesh. The Daily Star. https://www.thedailystar.net/opinion/views/news/adaptation-strategies-climate-change-impacts-bangladesh-3722791

Khadgarai, S., Kumar, V., & Pradhan, P. K. (2021). The connection between extreme precipitation variability over monsoon Asia and large-scale circulation patterns. Atmosphere, 12(11), 1492. https://doi.org/10.3390/atmos12111492

Khan, J. U., Islam, A. K. M. S., Das, M. K., Mohammed, K., Bala, S. K., & Islam, G. M. T. (2020). Future changes in meteorological drought characteristics over Bangladesh projected by the CMIP5 multi-model ensemble. Climatic Change, 162(2), 667–685. https://doi.org/10.1007/S10584-020-02832-0

Khan, M. J. U., Islam, A. S., Bala, S. K., & Islam, G. T. (2020). Changes in climate extremes over Bangladesh at 1.5° C, 2° C, and 4° C of global warming with high-resolution regional climate modeling. Theoretical and Applied Climatology, 140, 1451-1466. https://doi.org/10.1007/s00704-020-03164-w

Khan, M. J. U., Islam, A. K. M. S., Das, M. K., Mohammed, K., Bala, S. K., & Tarekul Islam, G. M. (2019). Observed trends in climate extremes over

Bangladesh from 1981 to 2010. Climate Research, 77(1), 45–61. https://doi.org/10.3354/cr01539

Kim, Y. T., Yu, J. U., Kim, T. W., & Kwon, H. H. (2024). A novel approach to a multi-model ensemble for climate change models: Perspectives on the representation of natural variability and historical and future climate. Weather and Climate Extremes, 44, 100688. https://doi.org/10.1016/J.WACE.2024.100688

Kistler, R., Kalnay, E., Collins, W., Saha, S., White, G., Woollen, J., Chelliah, M., Ebisuzaki, W., Kanamitsu, M., Kousky, V., van den Dool, H., Jenne, R., & Fiorino, M. (2001). The NCEP–NCAR 50-Year Reanalysis: Monthly Means CD-ROM and Documentation. Bulletin of the American Meteorological Society, 82(2), 247–268. http://www.jstor.org/stable/26215517

Klein Tank, A. M. G., Zwiers, F. W., & Zhang, X. (2009). Guidelines on analysis of extremes in a changing climate in support of informed decisions for adaptation (WCDMP-No. 72, WMO-TD No. 1500, p. 56). World Meteorological Organization.

Knutti, R. (2008). Why are climate models reproducing the observed global surface warming so well? Geophysical Research Letters, 35(18). https://doi.org/10.1029/2008GL034932

Kobayashi, C., Endo, H., Ota, Y., Kobayashi, S., Onoda, H., Harada, Y., Onogi, K., & Kamahori, H. (2014). Preliminary Results of the JRA-55C, an Atmospheric Reanalysis Assimilating Conventional Observations Only. SOLA, 10(1), 78–82. https://doi.org/10.2151/SOLA.2014-016

Kobayashi, S., Ota, Y., Harada, Y., Ebita, A., Moriya, M., Onoda, H., Onogi, K., Kamahori, H., Kobayashi, C., Endo, H., Miyaoka, K., & Kiyotoshi, T. (2015). The JRA-55 Reanalysis: General Specifications and Basic Characteristics. Journal of the Meteorological Society of Japan. Ser. II, 93(1), 5–48. https://doi.org/10.2151/JMSJ.2015-001

Koutavarapu, R., Umakanth, N., Satyanarayana, T., Kumar, M. S., Rao, M. C., Lee, D. Y., & Shim, J. (2021). Study of statistical estimated parameters using ERA5 reanalysis data over Khulna region during monsoon season. Acta

Geophysica, 69(5), 1963–1978. https://doi.org/10.1007/S11600-021-00662-X/METRICS

Kuglitsch, F. G., Toreti, A., Xoplaki, E., Della-Marta, P. M., Luterbacher, J., & Wanner, H. (2009). Homogenization of daily maximum temperature series in the Mediterranean. Journal of Geophysical Research: Atmospheres, 114(D15), 15108. https://doi.org/10.1029/2008JD011606

Kumar, P., Wiltshire, A., Mathison, C., Asharaf, S., Ahrens, B., Lucas-Picher, P., Christensen, J. H., Gobiet, A., Saeed, F., Hagemann, S., & Jacob, D. (2013). Downscaled climate change projections with uncertainty assessment over India using a high resolution multi-model approach. Science of The Total Environment, 468–469, S18–S30. https://doi.org/10.1016/J.SCITOTENV.2013.01.051

Latonin, M. M., Bashmachnikov, I. L., Bobylev, L. P., & Davy, R. (2021). Multi-model ensemble mean of global climate models fails to reproduce early twentieth century Arctic warming. Polar Science, 30, 100677. https://doi.org/10.1016/J.POLAR.2021.100677

Lavers, D. A., Simmons, A., Vamborg, F., & Rodwell, M. J. (2022). An evaluation of ERA5 precipitation for climate monitoring. Quarterly Journal of the Royal Meteorological Society, 148(748), 3152–3165. https://doi.org/10.1002/QJ.4351

Lee, M.-U., Park, J.-Y., Kim, H.-K., Byun, Y.-H., Sung, H.-M., Park, J.-S., Jeon, W.-J., Lee, M.-U., Park, J.-Y., Kim, H.-K., Byun, Y.-H., Sung, H.-M., Park, J.-S., & Jeon, W.-J. (2024). Irreversibility of Extreme Precipitation in East Asia under Multi-Scenario to Carbon Neutrality. EGUGA, 3741. https://doi.org/10.5194/EGUSPHERE-EGU24-3741

Lin, L., Gao, T., Luo, M., Ge, E., Yang, Y., Liu, Z., Zhao, Y., & Ning, G. (2020). Contribution of urbanization to the changes in extreme climate events in urban agglomerations across China. Science of The Total Environment, 744, 140264. https://doi.org/10.1016/J.SCITOTENV.2020.140264

Liu, J., Shanguan, D., Liu, S., & Ding, Y. (2018). Evaluation and Hydrological Simulation of CMADS and CFSR Reanalysis Datasets in the Qinghai-Tibet

Plateau. Water 2018, Vol. 10, Page 513, 10(4), 513. https://doi.org/10.3390/W10040513

Hossain, M. L., & Hossain, M. K. (2012). Climate change, sea level rise and coastal vulnerabilities of Bangladesh with adaptation options. University of Chittagong, Bangladesh.

Lorenz, R., Argüeso, D., Donat, M. G., Pitman, A. J., Hurk, B. Van Den, Berg, A., Lawrence, D. M., Chéruy, F., Ducharne, A., Hagemann, S., Meier, A., Milly, P. C. D., & Seneviratne, S. I. (2016). Influence of land-atmosphere feedbacks on temperature and precipitation extremes in the GLACE-CMIP5 ensemble. Journal of Geophysical Research: Atmospheres, 121(2), 607–623. https://doi.org/10.1002/2015JD024053

Madadgar, S., & Moradkhani, H. (2014). Improved Bayesian multimodeling: Integration of copulas and Bayesian model averaging. Water Resources Research, 50(12), 9586–9603. https://doi.org/10.1002/2014WR015965

Maher, N., Milinski, S., & Ludwig, R. (2021). Large ensemble climate model simulations: Introduction, overview, and future prospects for utilising multiple types of large ensemble. Earth System Dynamics, 12(2), 401–418. https://doi.org/10.5194/ESD-12-401-2021

Mallick, J., Islam, A. R. Md. T., Ghose, B., Islam, H. M. T., Rana, Y., Hu, Z., Bhat, S. A., Pal, S. C., & Ismail, Z. Bin. (2022a). Spatiotemporal trends of temperature extremes in Bangladesh under changing climate using multi-statistical techniques. Theoretical and Applied Climatology, 147(1), 307–324. https://doi.org/10.1007/s00704-021-03828-1

Mallick, J., Salam, R., Islam, H. T., Shahid, S., Kamruzzaman, M., Pal, S. C., ... & Islam, A. R. M. T. (2022b). Recent changes in temperature extremes in subtropical climate region and the role of large-scale atmospheric oscillation patterns. Theoretical and Applied Climatology, 148(1), 329-347. https://doi.org/10.1007/s00704-021-03914-4

Manabe, S., & Stouffer, R. J. (1988). Two Stable Equilibria of a Coupled Ocean-Atmosphere Model. Journal of Climate, 1(9), 841–866. https://doi.org/10.1175/1520-0442(1988)001

Maraun, D., Wetterhall, F., Ireson, A. M., Chandler, R. E., Kendon, E. J., Widmann, M., Brienen, S., Rust, H. W., Sauter, T., Themel, M., Venema, V. K. C., Chun, K. P., Goodess, C. M., Jones, R. G., Onof, C., Vrac, M., & Thiele-Eich, I. (2010). Precipitation downscaling under climate change: Recent developments to bridge the gap between dynamical models and the end user. Reviews of Geophysics, 48(3). https://doi.org/10.1029/2009RG000314

Masson-Delmotte, V., Zhai, P., Pirani, A., Connors, S. L., Péan, C., Berger, S., ... Zhou, B. (Eds.). (2021). Climate change 2021: The physical science basis. Contribution of Working Group I to the Sixth Assessment Report of the Intergovernmental Panel on Climate Change. Cambridge University Press. https://doi.org/10.1017/9781009157896

Materia, S., García, L. P., van Straaten, C., Sungmin, O., Mamalakis, A., Cavicchia, L., Coumou, D., de Luca, P., Kretschmer, M., & Donat, M. (2024). Artificial intelligence for climate prediction of extremes: State of the art, challenges, and future perspectives. Wiley Interdisciplinary Reviews: Climate Change, 15(6), e914. https://doi.org/10.1002/WCC.914

McNicholl, B., Lee, Y. H., Campbell, A. G., & Dev, S. (2022). Evaluating the Reliability of Air Temperature from ERA5 Reanalysis Data. IEEE Geoscience and Remote Sensing Letters, 19. https://doi.org/10.1109/LGRS.2021.3137643

Meehl, G. A., Zwiers, F., Evans, J., Knutson, T., Mearns, L., & Whetton, P. (2000). Trends in Extreme Weather and Climate Events: Issues Related to Modeling Extremes in Projections of Future Climate Change. Bulletin of the American Meteorological Society, 81(3), 427–436. https://doi.org/10.1175/1520-0477(2000)081

Merrifield, A. L., Brunner, L., Lorenz, R., Medhaug, I., & Knutti, R. (2020). An investigation of weighting schemes suitable for incorporating large ensembles into multi-model ensembles. Earth System Dynamics, 11(3), 807–834. https://doi.org/10.5194/ESD-11-807-2020

Mesgari, E., Hosseini, S. A., Partoo, L. G., Hemmesy, M. S., & Houshyar, M. (2022). Assessment of CMIP6 models' performances and projection of precipitation based on SSP scenarios over the MENAP region. Journal of

Water and Climate Change, 13(10), 3607–3619. https://doi.org/10.2166/WCC.2022.195

Mishu, R. A., Mallick, J., Akter, M. Y., Fattah, M. A., Kamruzzaman, M., Salam, M. A., ... & Islam, A. R. M. T. (2025). Spatial and temporal variability of future extreme precipitation in Bangladesh using CMIP6 models. Journal of Water and Climate Change, 16(4), 1281-1309. https://doi.org/10.2166/wcc.2025.415

Mondal, S. K., Huang, J., Wang, Y., Su, B., Kundzewicz, Z. W., Jiang, S., Zhai, J., Chen, Z., Jing, C., & Jiang, T. (2022). Changes in extreme precipitation across South Asia for each 0.5 °C of warming from 1.5 °C to 3.0°C above pre-industrial levels. Atmospheric Research, 266, 105961. https://doi.org/10.1016/J.ATMOSRES.2021.105961

Nasreen, M., Hossain, K. M., & Khan, M. M. (2023). Coastal Disaster Risk Management in Bangladesh. London: Routledge. https://doi.org/10.4324/9781003253495

Ministry of Environment, Forest and Climate Change. (2023). Climate change initiatives of Bangladesh towards climate resilience. Government of the People's Republic of Bangladesh.

Ministry of Environment, Forest and Climate Change. (2022). National adaptation plan of Bangladesh (2023–2050). Government of the People's Republic of Bangladesh. https://moef.portal.gov.bd/sites/default/files/files/moef.portal.gov.bd/npfblock/903c6d55_3fa3_4d24_a4e1_0611eaa3cb69/National%20Adaptation%20Plan%20of%20Bangladesh%20%282023-2050%29%20%281%29.pdf

Nazrul, F. B., Karim, M. R., Pavan, W., & Kamruzzaman, M. (2025). Future Climate Extremes in Bangladesh: Insights from a Multi-Model Ensemble of CMIP6 Simulations. Earth Systems and Environment, 1-20. https://doi.org/10.1007/s41748-025-00681-4

Nicholls, N., & Alexander, L. (2007). Has the climate become more variable or extreme? Progress 1992-2006. Progress in Physical Geography, 31(1), 77–87. https://doi.org/10.1177/0309133307073885

Nicholls, N., Gruza, G. V., Jouzel, J., Karl, T. R., Ogallo, L. A., et al. (1996). Observed climate variability and change. In J. T. Houghton, L. G. Meira Filho, B. A. Callander, N. Harris, A. Kattenberg, & K. Maskell (Eds.), Climate change 1995: The science of climate change. Contribution of Working Group I to the Second Assessment Report of the Intergovernmental Panel on Climate Change (pp. 137–192). Cambridge University Press. https://hal.science/hal-03344530/

Noguer, M., Jones, R., & Murphy, J. (1998). Sources of systematic errors in the climatology of a regional climate model over Europe. Climate Dynamics, 14(10), 691–712. https://doi.org/10.1007/S003820050249

Northrop, P. J., & Chandler, R. E. (2014). Quantifying Sources of Uncertainty in Projections of Future Climate. Journal of Climate, 27(23), 8793–8808. https://doi.org/10.1175/JCLI-D-14-00265.1

Nowreen, S., Murshed, S. B., Islam, A. K. M. S., & Bhaskaran, B. (2013, March). Change of future climate extremes for the Haor basin area of Bangladesh. In 4th International Conference on Water and Flood Management. Institute of Water and Flood Management, Bangladesh University of Engineering and Technology, Dhaka, Bangladesh.

Nowreen, S., Murshed, S. B., Islam, A. S., Bhaskaran, B., & Hasan, M. A. (2015). Changes of rainfall extremes around the haor basin areas of Bangladesh using multi-member ensemble RCM. Theoretical and Applied Climatology, 119, 363-377. https://doi.org/10.1007/s00704-014-1101-7

Olauson, J. (2018). ERA5: The new champion of wind power modelling? Renewable Energy, 126, 322–331. https://doi.org/10.1016/J.RENENE.2018.03.056

O'Neill, B. C., Tebaldi, C., Van Vuuren, D. P., Eyring, V., Friedlingstein, P., Hurtt, G., Knutti, R., Kriegler, E., Lamarque, J. F., Lowe, J., Meehl, G. A., Moss, R., Riahi, K., & Sanderson, B. M. (2016). The Scenario Model Intercomparison Project (ScenarioMIP) for CMIP6. Geoscientific Model Development, 9(9), 3461–3482. https://doi.org/10.5194/GMD-9-3461-2016

Otto, F. E., Zhang, X., & Seneviratne, S. (2021). Summary for policymakers of the Working Group I contribution to the IPCC Sixth Assessment Report—Data for Figure SPM.3 [Data set]. NERC EDS Centre for Environmental Data Analysis.

Palme, M. (2021). Urban Heat Island Studies in Hot and Humid Climates: A Review of the State of Art in Latin-America. Advances in 21st Century Human Settlements, 123–141. https://doi.org/10.1007/978-981-33-4050-3_6

Palmer, T. N., Doblas-Reyes, F. J., Hagedorn, R., & Weisheimer, A. (2005). Probabilistic prediction of climate using multi-model ensembles: from basics to applications. Philosophical Transactions of the Royal Society B: Biological Sciences, 360(1463), 1991–1998. https://doi.org/10.1098/RSTB.2005.1750

Parker, W. S. (2024). Climate Science. Elements in the Philosophy of Science. https://doi.org/10.1017/9781009619301

Paul, A. R., & Maity, R. (2023). Future projection of climate extremes across contiguous northeast India and Bangladesh. Scientific Reports, 13(1), 15616. https://doi.org/10.1038/s41598-023-42360-2

Perkins, S. E., & Alexander, L. V. (2013). On the Measurement of Heat Waves. Journal of Climate, 26(13), 4500–4517. https://doi.org/10.1175/JCLI-D-12-00383.1

Pervin, L., & Khan, M. S. M. (2022). Variability and trends of climate extremes indices from the observed and downscaled GCMs data over 1950–2020 period in Chattogram City, Bangladesh. Journal of Water and Climate Change, 13(2), 975-998. https://doi.org/10.2166/wcc.2021.331

Petersen, M. R., Jacobsen, D. W., Ringler, T. D., Hecht, M. W., & Maltrud, M. E. (2015). Evaluation of the arbitrary Lagrangian–Eulerian vertical coordinate method in the MPAS-Ocean model. Ocean Modelling, 86, 93–113. https://doi.org/10.1016/J.OCEMOD.2014.12.004

Peterson, T., Anderson, D., Cohen, S., Cortez-Vazquez, M., Murnane, R., Parmesan, C., Phillips, D., Pulwarty, R., & Stone, J. (2008). Why weather and climate extremes matter. In Weather and climate extremes in a changing climate: Regions of focus: North America, Hawaii, Caribbean, and U.S. Pacific Islands (pp. 11–34). U.S. Climate Change Science Program.

Pierce, D. W., Barnett, T. P., Santer, B. D., & Gleckler, P. J. (2009). Selecting global climate models for regional climate change studies. Proceedings of the National Academy of Sciences, 106(21), 8441-8446. https://doi.org/10.1073/pnas.0900094106

Pierce, D. W., Cayan, D. R., Maurer, E. P., Abatzoglou, J. T., & Hegewisch, K. C. (2015). Improved Bias Correction Techniques for Hydrological Simulations of Climate Change. Journal of Hydrometeorology, 16(6), 2421–2442. https://doi.org/10.1175/JHM-D-14-0236.1

Pradhan, P., Shrestha, S., Sundaram, S. M., & Virdis, S. G. (2021). Evaluation of the CMIP5 general circulation models for simulating the precipitation and temperature of the Koshi River Basin in Nepal. Journal of Water and Climate Change, 12(7), 3282-3296. https://doi.org/10.2166/wcc.2021.124

Provenzale, A. (2014). Climate models. Rendiconti Lincei, 25(1), 49–58. https://doi.org/10.1007/S12210-013-0268-7/FIGURES/3

Raäisaänen, J. (2007). How reliable are climate models?. Tellus A: Dynamic Meteorology and Oceanography, 59(1), 2-29. https://doi.org/10.1111/J.1600-0870.2006.00211.X

Raftery, A. E., Gneiting, T., Balabdaoui, F., & Polakowski, M. (2005). Using Bayesian Model Averaging to Calibrate Forecast Ensembles. Monthly Weather Review, 133(5), 1155–1174. https://doi.org/10.1175/MWR2906.1

Rahman, A. A., Alam, M., Alam, S. S., Uzzaman, M. R., Rashid, M., & Rabbani, G. (2007). Risks, vulnerability and adaptation in Bangladesh. Human Development Report, 8.

Rahman, H., Easha, A. A., Fatema, N., Islam, M. J., & Alam, M. (2024). Climate Change Adaptation Strategy of the Coastal Indigenous Community of Bangladesh. Advances in Civil Engineering, 2024(1), 5395870. https://doi.org/10.1155/2024/5395870

Rahman, M. A., & Rahman, S. (2015). Natural and traditional defense mechanisms to reduce climate risks in coastal zones of Bangladesh. Weather and Climate Extremes, 7, 84-95. https://doi.org/10.1016/j.wace.2014.12.004

Rahman, M. C., Rahaman, M. S., Biswas, J. C., Rahman, N. M. F., Islam, M. A., Sarkar, M. A. R., Islam, M. S., & Maniruzzaman, M. (2023). Climate change and risk scenario in Bangladesh. Asia-Pacific Journal of Regional Science, 7(2), 381–404. https://doi.org/10.1007/S41685-022-00252-9

Rahman, M., Tumon, M. S. H., Islam, M. M., Chen, N., Pham, Q. B., Ullah, K., ... & Dewan, A. (2023). Could climate change exacerbate droughts in Bangladesh in the future?. Journal of Hydrology, 625, 130096. https://doi.org/10.1016/j.jhydrol.2023.130096

Rahman, Md. M., Biswas, J. C., & Meena, R. S. (Eds.). (2024). Climate Change and Soil-Water-Plant Nexus. https://doi.org/10.1007/978-981-97-6635-2

Rahman, R., & Salehin, M. (2013). Flood Risks and Reduction Approaches in Bangladesh. 65–90. https://doi.org/10.1007/978-4-431-54252-0_4

Rahman, S., & Islam, A. S. (2023). Predictions of Land Use and Land Cover (LULC) and Runoff of the Teesta River Basin under Different Emission and Socioeconomic Scenarios. https://doi.org/10.21203/RS.3.RS-3277212/V1

Rahman, S. M., Rahman, S. M., Ali, Md. S., Mamun, Md. A. Al, & Uddin, Md. N. (2020). Estimation of seasonal boundaries using temperature data: a case of northwest part of Bangladesh. Mathematics of Climate and Weather Forecasting, 6(1), 50–62. https://doi.org/10.1515/MCWF-2020-0102

Raju, K. S., & Kumar, D. N. (2020). Review of approaches for selection and ensembling of GCMs. Journal of Water and Climate Change, 11(3), 577–599. https://doi.org/10.2166/WCC.2020.128

Rajulapati, C. R., Abdelmoaty, H. M., Nerantzaki, S. D., & Papalexiou, S. M. (2022). Changes in the risk of extreme temperatures in megacities worldwide. Climate Risk Management, 36, 100433. https://doi.org/10.1016/J.CRM.2022.100433

Randall, D. A., Wood, R. A., Bony, S., Colman, R., Fichefet, T., Fyfe, J., Kattsov, V., Pitman, A., Shukla, J., Srinivasan, J., Stouffer, R. J., Sumi, A., & Taylor,

K. E. (2007). Climate models and their evaluation. In S. Solomon, D. Qin, M. Manning, Z. Chen, M. Marquis, K. B. Averyt, ... & H. L. Miller (Eds.), Climate change 2007: The physical science basis. Contribution of Working Group I to the Fourth Assessment Report of the Intergovernmental Panel on Climate Change (pp. 589–662). Cambridge University Press.

Rehana, S., Yeleswarapu, P., Basha, G., & Munoz-Arriola, F. (2022). Precipitation and temperature extremes and association with large-scale climate indices: An observational evidence over India. Journal of Earth System Science, 131(3), 1–20. https://doi.org/10.1007/S12040-022-01911-3

Rhymee, H., Shams, S., Ratnayake, U., & Rahman, E. K. A. (2022). Comparing Statistical Downscaling and Arithmetic Mean in Simulating CMIP6 Multi-Model Ensemble over Brunei. Hydrology, 9(9), 161. https://doi.org/10.3390/HYDROLOGY9090161

Roundy, J. K., Ferguson, C. R., & Wood, E. F. (2014). Impact of land-atmospheric coupling in CFSv2 on drought prediction. Climate Dynamics, 43(1–2), 421–434. https://doi.org/10.1007/S00382-013-1982-7/FIGURES/8

Saha, S., Moorthi, S., Pan, H. L., Wu, X., Wang, J., Nadiga, S., Tripp, P., Kistler, R., Woollen, J., Behringer, D., Liu, H., Stokes, D., Grumbine, R., Gayno, G., Wang, J., Hou, Y. T., Chuang, H. Y., Juang, H. M. H., Sela, J., … Goldberg, M. (2010). The NCEP Climate Forecast System Reanalysis. Bulletin of the American Meteorological Society, 91(8), 1015–1058. https://doi.org/10.1175/2010BAMS3001.1

Saha, S., Moorthi, S., Wu, X., Wang, J., Nadiga, S., Tripp, P., Behringer, D., Hou, Y. T., Chuang, H. Y., Iredell, M., Ek, M., Meng, J., Yang, R., Mendez, M. P., Van Den Dool, H., Zhang, Q., Wang, W., Chen, M., & Becker, E. (2014). The NCEP Climate Forecast System Version 2. Journal of Climate, 27(6), 2185–2208. https://doi.org/10.1175/JCLI-D-12-00823.1

Sahabi-Abed, S., & Selmane, A. N. E. I. (2023). Spatiotemporal projections of extreme temperature indices over Algeria using CMIP6-global climate models. International Journal of Big Data Mining for Global Warming, 5(2), 1–18. https://doi.org/10.1142/S2630534823300026

Sanderson, B. M., Wehner, M., & Knutti, R. (2017). Skill and independence weighting for multi-model assessments. Geoscientific Model Development, 10(6), 2379–2395. https://doi.org/10.5194/GMD-10-2379-2017

Sándor, R., Ehrhardt, F., Grace, P., Recous, S., Smith, P., Snow, V., Soussana, J. F., Basso, B., Bhatia, A., Brilli, L., Doltra, J., Dorich, C. D., Doro, L., Fitton, N., Grant, B., Harrison, M. T., Skiba, U., Kirschbaum, M. U. F., Klumpp, K., … Bellocchi, G. (2023). Residual correlation and ensemble modelling to improve crop and grassland models. Environmental Modelling & Software, 161, 105625. https://doi.org/10.1016/J.ENVSOFT.2023.105625

Sansom, P. G., Stephenson, D. B., & Bracegirdle, T. J. (2021). On Constraining Projections of Future Climate Using Observations and Simulations From Multiple Climate Models. Journal of the American Statistical Association, 116(534), 546–557. https://doi.org/10.1080/01621459.2020.1851696

Sarwar, Md. G. M. (2013). Sea-Level Rise Along the Coast of Bangladesh. 217–231. https://doi.org/10.1007/978-4-431-54252-0_10

Ramamasy, S., & Baas, S. (2007). Climate variability and change: Adaptation to drought in Bangladesh—A resource book and training guide. Food and Agriculture Organization of the United Nations (FAO) and Asian Disaster Preparedness Center (ADPC). https://www.fao.org/4/a1247e/a1247e01.pdf

Seneviratne, S. I., & Hauser, M. (2020). Regional Climate Sensitivity of Climate Extremes in CMIP6 Versus CMIP5 Multimodel Ensembles. Earth's Future, 8(9), e2019EF001474. https://doi.org/10.1029/2019EF001474

Seneviratne, S. I., Nicholls, N., Easterling, D., Goodess, C. M., Kanae, S., Kossin, J., Luo, Y., Marengo, J., Mc Innes, K., Rahimi, M., Reichstein, M., Sorteberg, A., Vera, C., Zhang, X., Rusticucci, M., Semenov, V., Alexander, L. V., Allen, S., Benito, G., … Zwiers, F. W. (2012). Changes in Climate Extremes and their Impacts on the Natural Physical Environment. Managing the Risks of Extreme Events and Disasters to Advance Climate Change Adaptation: Special Report of the Intergovernmental Panel on Climate Change, 9781107025066, 109–230. https://doi.org/10.1017/CBO9781139177245.006

Shashikanth, K., Ghosh, S., Vittal, H., & Karmakar, S. (2018). Future projections of Indian summer monsoon rainfall extremes over India with statistical downscaling and its consistency with observed characteristics. Climate Dynamics, 51(1–2), 1–15. https://doi.org/10.1007/S00382-017-3604-2

Shell, K. M. (2013). Consistent Differences in Climate Feedbacks between Atmosphere–Ocean GCMs and Atmospheric GCMs with Slab-Ocean Models. Journal of Climate, 26(12), 4264–4281. https://doi.org/10.1175/JCLI-D-12-00519.1

Shiru, M. S., Kim, J. H., & Chung, E. S. (2022). Variations in Projections of Precipitations of CMIP6 Global Climate Models under SSP 2–45 and SSP 5–85. KSCE Journal of Civil Engineering, 26(12), 5404–5416. https://doi.org/10.1007/S12205-022-0149-7

Sillmann, J., Kharin, V. V., Zhang, X., Zwiers, F. W., & Bronaugh, D. (2013a). Climate extremes indices in the CMIP5 multimodel ensemble: Part 1. Model evaluation in the present climate. Journal of Geophysical Research: Atmospheres, 118(4), 1716–1733. https://doi.org/10.1002/JGRD.50203

Sillmann, J., Kharin, V. V., Zwiers, F. W., Zhang, X., & Bronaugh, D. (2013b). Climate extremes indices in the CMIP5 multimodel ensemble: Part 2. Future climate projections. Journal of Geophysical Research: Atmospheres, 118(6), 2473–2493. https://doi.org/10.1002/JGRD.50188

Singh, H., & Mohanty, M. P. (2023). Can atmospheric reanalysis datasets reproduce flood inundation at regional scales? A systematic analysis with ERA5 over Mahanadi River Basin, India. Environmental Monitoring and Assessment, 195(10), 1–22. https://doi.org/10.1007/S10661-023-11798-2

Singh, M., Ouedraogo, M., & Nain, A. S. (2025). Spatio-temporal analysis of the extremes of precipitation and temperature in the capital cities of India. https://doi.org/10.31223/X55423

Soci, C., Hersbach, H., Simmons, A., Poli, P., Bell, B., Berrisford, P., Horányi, A., Muñoz-Sabater, J., Nicolas, J., Radu, R., Schepers, D., Villaume, S., Haimberger, L., Woollen, J., Buontempo, C., & Thépaut, J. N. (2024). The ERA5 global reanalysis from 1940 to 2022. Quarterly Journal of the Royal

Meteorological Society, 150(764), 4014–4048. https://doi.org/10.1002/QJ.4803

Stocker, Thomas. (2011). Introduction to climate modelling. https://books.google.com/books/about/Introduction_to_Climate_Modelling.html?id=D4zulgFb5JwC

Stouffer, R. J., & Manabe, S. (1999). Response of a Coupled Ocean–Atmosphere Model to Increasing Atmospheric Carbon Dioxide: Sensitivity to the Rate of Increase. Journal of Climate, 12(8), 2224–2237. https://doi.org/10.1175/1520-0442(1999)012

Sun, Y., & Hu, T. (2023). Detection of the anthropogenic signal and urbanization effects in extreme temperature changes in eastern China. Atmospheric and Oceanic Science Letters, 16(2), 100332. https://doi.org/10.1016/J.AOSL.2023.100332

Tabassum, A., Park, K., Shin, J., Jin, H.-G., & Baik, J.-J. (2024). Long-term changes in temperature, specific humidity, and precipitation in Bangladesh revealed by ERA5 data. Theoretical and Applied Climatology, 155(3), 1915–1925. https://doi.org/10.1007/s00704-023-04732-6

Tao, Y., Yang, T., Faridzad, M., Jiang, L., He, X., & Zhang, X. (2018). Non-stationary bias correction of monthly CMIP5 temperature projections over China using a residual-based bagging tree model. International Journal of Climatology, 38(1), 467–482. https://doi.org/10.1002/joc.5188

Tarek, M., Brissette, F. P., & Arsenault, R. (2020). Evaluation of the ERA5 reanalysis as a potential reference dataset for hydrological modelling over North America. Hydrology and Earth System Sciences, 24(5), 2527–2544. https://doi.org/10.5194/HESS-24-2527-2020

Tebaldi, C., & Knutti, R. (2007). The use of the multi-model ensemble in probabilistic climate projections. Philosophical Transactions of the Royal Society A: Mathematical, Physical and Engineering Sciences, 365(1857), 2053–2075. https://doi.org/10.1098/RSTA.2007.2076

Henderson-Sellers, A., & McGuffie, K. (2011). The future of the world's climate (2nd ed.). Elsevier Science.

Talukder, A., Shaid, S., Hwang, S., Alam, E., Islam, K., & Kamruzzaman, M. (2025). Optimizing the multi-model ensemble of CMIP6 GCMs for climate simulation over Bangladesh. Scientific Reports, 15(1), 11343. https://doi.org/10.1038/s41598-025-96446-0

Tian, J., Zhang, Z., Ahmed, Z., Zhang, L., Su, B., Tao, H., & Jiang, T. (2021). Projections of precipitation over China based on CMIP6 models. Stochastic Environmental Research and Risk Assessment, 35(4), 831–848. https://doi.org/10.1007/S00477-020-01948-0/FIGURES/7

Trenberth, K. E. (1993). Climate system modeling. Climate System Modeling. https://doi.org/10.1201/9780429356667-8

Trenberth, K. E. (2018). Climate change caused by human activities is happening and it already has major consequences. Journal of Energy & Natural Resources Law, 36(4), 463–481. https://doi.org/10.1080/02646811.2018.1450895

Trenberth, K. E., & Olson, J. G. (1988). An Evaluation and Intercomparison of Global Analyses from the National Meteorological Center and the European Centre for Medium Range Weather Forecasts. Bulletin of the American Meteorological Society, 69(9), 1047–1057. https://doi.org/10.1175/1520-0477(1988)069<1047:AEAIOG>2.0.CO;2

Uddin, Md. J., Wahiduzzaman, M., Islam, A. R. Md. T., Eibek, K. U., & Nasrin, Z. Most. (2022). Impacts of climate modes on temperature extremes over Bangladesh using statistical methods. Meteorology and Atmospheric Physics, 134(2), 24. https://doi.org/10.1007/s00703-022-00868-8

Umma, H., Rajib, S., & Yukiko, T. (2011). Socioeconomic impact of droughts in Bangladesh. Community, Environment and Disaster Risk Management, 8, 25–48. https://doi.org/10.1108/S2040-7262(2011)0000008008

Ummenhofer, C. C., & Meehl, G. A. (2017). Extreme weather and climate events with ecological relevance: a review. Philosophical Transactions of the Royal Society B: Biological Sciences, 372(1723). https://doi.org/10.1098/RSTB.2016.0135

UN Women & Ministry of Environment, Forest and Climate Change. (2022). Bangladesh state of gender equality and climate change report. UN Women Bangladesh. https://asiapacific.unwomen.org/en/digital-library/publications/2022/09/state-of-gender-equality-and-climate-change-in-bangladesh#:~:text=The%20State%20of%20Gender%20Equality,relevant%20sectoral%20policies%20and%20actions.

UNICEF Bangladesh. (2022, June 19). Bangladesh Country Office: Humanitarian Situation Report No. 2 – North-Eastern Flash Flood. ReliefWeb. https://reliefweb.int/report/bangladesh/bangladesh-country-office-humanitarian-situation-report-no-2-north-eastern-flash-flood-19-june-2022

Urraca, R., Huld, T., Gracia-Amillo, A., Martinez-de-Pison, F. J., Kaspar, F., & Sanz-Garcia, A. (2018). Evaluation of global horizontal irradiance estimates from ERA5 and COSMO-REA6 reanalyses using ground and satellite-based data. Solar Energy, 164, 339–354. https://doi.org/10.1016/J.SOLENER.2018.02.059

van der Linden, P., Dempsey, P., Dunn, R., Caesar, J., Kurnik, B., Dankers, R., Jol, A., Kunz, M., van Lanen, H., Benestad, R., Parry, S., Hilden, M., Marx, A., Mysiak, J., & Kendon, L. (2015). Extreme weather and climate in Europe.

van Oldenborgh, G. J., Balmaseda, M. A., Ferranti, L., Stockdale, T. N., & Anderson, D. L. T. (2005). Evaluation of Atmospheric Fields from the ECMWF Seasonal Forecasts over a 15-Year Period. Journal of Climate, 18(16), 3250–3269. https://doi.org/10.1175/JCLI3421.1

Wang, B., Zheng, L., Liu, D. L., Ji, F., Clark, A., & Yu, Q. (2018). Using multi-model ensembles of CMIP5 global climate models to reproduce observed monthly rainfall and temperature with machine learning methods in Australia. International Journal of Climatology, 38(13), 4891–4902. https://doi.org/10.1002/JOC.5705

Wang, O., Liang, J., Gu, Y., Haywood, J. M., Chen, Y., Fang, C., & Wang, Q. (2024). Projected future changes in extreme precipitation over China under stratospheric aerosol intervention. https://doi.org/10.5194/EGUSPHERE-2023-2904

Wang, T., Li, Z., Ma, Z., Gao, Z., & Tang, G. (2023). Diverging identifications of extreme precipitation events from satellite observations and reanalysis products: A global perspective based on an object-tracking method. Remote Sensing of Environment, 288, 113490. https://doi.org/10.1016/J.RSE.2023.113490

Wegler, M., & Kuenzer, C. (2024). Potential of Earth Observation to Assess the Impact of Climate Change and Extreme Weather Events in Temperate Forests—A Review. Remote Sensing, 16(12), 2224. https://doi.org/10.3390/RS16122224/S1

Wilcoxon, F. (1992). Individual Comparisons by Ranking Methods. In S. Kotz & N. L. Johnson (Eds.), Breakthroughs in Statistics: Methodology and Distribution (pp. 196–202). Springer New York. https://doi.org/10.1007/978-1-4612-4380-9_16

World Bank. (2024). Climate risk country profile: Bangladesh. Climate Change Knowledge Portal. https://climateknowledgeportal.worldbank.org/sites/default/files/country-profiles/16813-WB_Bangladesh%20Country%20Profile-WEB.pdf

World Meteorological Organization. (2024, March 19). Climate change indicators reached record levels in 2023: WMO. https://wmo.int/news/media-centre/climate-change-indicators-reached-record-levels-2023-wm

Wu, H., & Levinson, D. (2021). The ensemble approach to forecasting: A review and synthesis. Transportation Research Part C: Emerging Technologies, 132, 103357. https://doi.org/10.1016/J.TRC.2021.103357

Xoplaki, E., Fleitmann, D., Luterbacher, J., Wagner, S., Haldon, J. F., Zorita, E., Telelis, I., Toreti, A., & Izdebski, A. (2016). The Medieval Climate Anomaly and Byzantium: A review of the evidence on climatic fluctuations, economic performance and societal change. Quaternary Science Reviews, 136, 229–252. https://doi.org/10.1016/J.QUASCIREV.2015.10.004

Xu, W., Lei, X., Chen, S., Yu, T., Hu, Z., Zhang, M., Jiang, L., Bao, R., Guan, X., Ma, M., Wei, J., Gao, L., & Feng, A. (2022). How Well Does the ERA5 Reanalysis Capture the Extreme Climate Events Over China? Part II:

Extreme Temperature. Frontiers in Environmental Science, 10. https://doi.org/10.3389/fenvs.2022.921659

Yang, J., & Hu, M. (2018). Filling the missing data gaps of daily MODIS AOD using spatiotemporal interpolation. Science of The Total Environment, 633, 677–683. https://doi.org/10.1016/J.SCITOTENV.2018.03.202

Yang, B., Wei, L., Tang, H., Li, Y., Wang, Y., Zhang, F., Zhou, J., Zhang, T., & Lv, T. (2024). Future changes in extremes across China based on NEX-GDDP-CMIP6 models. Climate Dynamics, 62(10), 9587–9617. https://doi.org/10.1007/s00382-024-07408-7

Yang, M., Zhao, H., Xian, X., Qi, Y., Li, Q., Guo, J., Chen, L., & Liu, W. (2023). Reconstructed Global Invasion and Spatio-Temporal Distribution Pattern Dynamics of Sorghum halepense under Climate and Land-Use Change. Plants, 12(17), 3128. https://doi.org/10.3390/PLANTS12173128/S1

Yildiz, S., Islam, H. M. T., Rashid, T., Sadeque, A., Shahid, S., & Kamruzzaman, M. (2024). Exploring Climate Change Effects on Drought Patterns in Bangladesh Using Bias-Corrected CMIP6 GCMs. Earth Systems and Environment, 8(1), 21–43. https://doi.org/10.1007/s41748-023-00362-0

Yin, H., & Sun, Y. (2018). Characteristics of extreme temperature and precipitation in China in 2017 based on ETCCDI indices. Advances in Climate Change Research, 9(4), 218–226. https://doi.org/10.1016/j.accre.2019.01.001

Ying, H., Zhang, H., Sun, Y., Zhao, J., Zhang, Z., Guo, X., ... & Deng, G. (2020). CMIP5-based spatiotemporal changes of extreme temperature events during 2021–2100 in Mainland China. Sustainability, 12(11), 4418. https://doi.org/10.3390/su12114418

Yuan, X., Wood, E. F., Luo, L., & Pan, M. (2011). A first look at Climate Forecast System version 2 (CFSv2) for hydrological seasonal prediction. Geophysical Research Letters, 38(13). https://doi.org/10.1029/2011GL047792

Zhai, J., Mondal, S. K., Fischer, T., Wang, Y., Su, B., Huang, J., Tao, H., Wang, G., Ullah, W., & Uddin, M. J. (2020). Future drought characteristics through a multi-model ensemble from CMIP6 over South Asia. Atmospheric

Research, 246, 105111. https://doi.org/10.1016/J.ATMOSRES.2020.105111

Zhang, F., Wei, L. X., & Li, Y. H. (2023). Evaluation and projection of extreme high temperature indices in southwestern China using NEX-GDDP-CMIP6. J. Meteor. Res, 37(0), 1-20. https://doi.org/10.1007/s13351-024-3059-4

Zhang, M., & Gao, Y. (2023). Time of emergence in climate extremes corresponding to Köppen-Geiger classification. Weather and Climate Extremes, 41, 100593. https://doi.org/10.1016/j.wace.2023.100593

Zhang, S., & Li, X. (2021). Future projections of offshore wind energy resources in China using CMIP6 simulations and a deep learning-based downscaling method. Energy, 217, 119321. https://doi.org/10.1016/J.ENERGY.2020.119321

Zhang, X., Alexander, L., Hegerl, G. C., Jones, P., Tank, A. K., Peterson, T. C., Trewin, B., & Zwiers, F. W. (2011). Indices for monitoring changes in extremes based on daily temperature and precipitation data. In Wiley Interdisciplinary Reviews: Climate Change (Vol. 2, Issue 6, pp. 851–870). Wiley-Blackwell. https://doi.org/10.1002/wcc.147

Zhang, X., & Yang, F. (2004). RClimDex (1.0) user manual. Climate Research Branch, Environment Canada. Retrieved from https://rcc.acmad.org/procedure/RClimDexUserManual.pdf

Zhang, Y., & Thorburn, P. J. (2022). Handling missing data in near real-time environmental monitoring: A system and a review of selected methods. Future Generation Computer Systems, 128, 63–72. https://doi.org/10.1016/J.FUTURE.2021.09.033

Zuckerman, D. M., & Chong, L. T. (2017). Weighted Ensemble Simulation: Review of Methodology, Applications, and Software. Annual Review of Biophysics, 46(Volume 46, 2017), 43–57. https://doi.org/10.1146/ANNUREV-BIOPHYS-070816-033834

Zwiers, F. W., Alexander, L. V., Hegerl, G. C., Knutson, T. R., Kossin, J. P., Naveau, P., Nicholls, N., Schär, C., Seneviratne, S. I., & Zhang, X. (2013). Climate Extremes: Challenges in Estimating and Understanding Recent

Changes in the Frequency and Intensity of Extreme Climate and Weather Events. In Climate Science for Serving Society (pp. 339–389). Springer Netherlands. https://doi.org/10.1007/978-94-007-6692-1_13

Appendix A: List of Publications from this Thesis Work

Journal Article

Nazrul, F. B., Karim, M. R., Pavan, W., & Kamruzzaman, M. (2025). Future Climate Extremes in Bangladesh: Insights from a Multi-Model Ensemble of CMIP6 Simulations. Earth Systems and Environment, 1-20. https://doi.org/10.1007/s41748-025-00681-4

Conference Paper

Nazrul, F. B., Karim, M. R., & Kamruzzaman, M. (2023, December 9–10). Assessing future extreme climate events in Bangladesh: Insights from CMIP6 multi-model ensemble projections. Paper presented at the 4th International Conference on Meteorology and Climate Science (ICMCS), Dhaka, Bangladesh.

Appendix B: Coordinates

Table B1: Coordinates of 30 meteorological stations operated by the Bangladesh Meteorological Department (BMD) across Bangladesh

Longitude	Latitude	Elevation (m)	District
88.68	25.65	37.58	DINAJPUR
89.23	25.73	32.61	RANGPUR
89.37	24.85	17.9	BOGRA
88.7	24.37	19.5	RAJSHAHI
90.43	24.72	18	MYMENSINGH
91.88	24.9	33.53	SYLHET
89.05	24.13	12.9	ISHWARDI
91.73	24.3	21.95	SRIMANGAL
90.38	23.77	8.45	DHAKA
89.85	23.6	8.1	FARIDPUR
89.17	23.18	6.1	JESSORE
90.18	23.17	7	MADARIPUR
90.7	23.27	4.88	CHANDPUR
91.18	23.43	7.5	COMILLA
89.08	22.72	3.96	SATKHIRA
89.53	22.78	3.6	KHULNA
90.37	22.75	2.1	BARISAL
90.65	22.68	4.3	BHOLA
90.33	22.33	1.5	PATUAKHALI
90.23	21.98	1.83	KHEPUPARA
91.1	22.87	4.87	MAIJDEE COURT
91.42	23.03	6.4	FENI
91.1	22.43	2.44	HATIYA
91.43	22.48	2.1	SANDWIP
91.7	22.58	7.3	SITAKUNDA
91.81	22.35	33.2	CHITTAGONG CITY
91.85	21.82	2.74	KUTUBDIA
92.2	22.53	68.89	RANGAMATI
91.97	21.45	2.1	COX'S BAZAR
92.3	20.87	5.5	TEKNAF

Table B2: Coordinates of 193 ERA5 datapoints across Bangladesh

ID	Longitude	Latitude	ID	Longitude	Latitude
ID00090	88.15311432	25.96100044	ID00323	90.15348053	23.71100044
ID00095	88.15311432	24.71100044	ID00324	90.15348053	23.46100044
ID00117	88.4031601	26.21100044	ID00325	90.15348053	23.21100044
ID00118	88.4031601	25.96100044	ID00326	90.15348053	22.96100044
ID00119	88.4031601	25.71100044	ID00327	90.15348053	22.71100044
ID00122	88.4031601	24.96100044	ID00328	90.15348053	22.46100044
ID00123	88.4031601	24.71100044	ID00329	90.15348053	22.21100044
ID00124	88.4031601	24.46100044	ID00330	90.15348053	21.96100044
ID00145	88.65320587	26.21100044	ID00346	90.40352631	24.96100044
ID00146	88.65320587	25.96100044	ID00347	90.40352631	24.71100044
ID00147	88.65320587	25.71100044	ID00348	90.40352631	24.46100044
ID00150	88.65320587	24.96100044	ID00349	90.40352631	24.21100044
ID00151	88.65320587	24.71100044	ID00350	90.40352631	23.96100044
ID00152	88.65320587	24.46100044	ID00351	90.40352631	23.71100044
ID00155	88.65320587	23.71100044	ID00352	90.40352631	23.46100044
ID00173	88.90325165	26.21100044	ID00353	90.40352631	23.21100044
ID00174	88.90325165	25.96100044	ID00354	90.40352631	22.96100044
ID00175	88.90325165	25.71100044	ID00355	90.40352631	22.71100044
ID00176	88.90325165	25.46100044	ID00356	90.40352631	22.46100044
ID00178	88.90325165	24.96100044	ID00357	90.40352631	22.21100044
ID00179	88.90325165	24.71100044	ID00358	90.40352631	21.96100044
ID00180	88.90325165	24.46100044	ID00374	90.65356445	24.96100044
ID00181	88.90325165	24.21100044	ID00375	90.65356445	24.71100044
ID00182	88.90325165	23.96100044	ID00376	90.65356445	24.46100044
ID00183	88.90325165	23.71100044	ID00377	90.65356445	24.21100044
ID00184	88.90325165	23.46100044	ID00378	90.65356445	23.96100044
ID00186	88.90325165	22.96100044	ID00379	90.65356445	23.71100044
ID00202	89.15329742	25.96100044	ID00380	90.65356445	23.46100044
ID00203	89.15329742	25.71100044	ID00381	90.65356445	23.21100044
ID00204	89.15329742	25.46100044	ID00383	90.65356445	22.71100044
ID00205	89.15329742	25.21100044	ID00385	90.65356445	22.21100044
ID00206	89.15329742	24.96100044	ID00386	90.65356445	21.96100044

ID00207	89.15329742	24.71100044	ID00402	90.90361023	24.96100044
ID00208	89.15329742	24.46100044	ID00403	90.90361023	24.71100044
ID00209	89.15329742	24.21100044	ID00404	90.90361023	24.46100044
ID00210	89.15329742	23.96100044	ID00405	90.90361023	24.21100044
ID00211	89.15329742	23.71100044	ID00406	90.90361023	23.96100044
ID00212	89.15329742	23.46100044	ID00407	90.90361023	23.71100044
ID00213	89.15329742	23.21100044	ID00408	90.90361023	23.46100044
ID00214	89.15329742	22.96100044	ID00409	90.90361023	23.21100044
ID00215	89.15329742	22.71100044	ID00410	90.90361023	22.96100044
ID00216	89.15329742	22.46100044	ID00411	90.90361023	22.71100044
ID00217	89.15329742	22.21100044	ID00430	91.15365601	24.96100044
ID00218	89.15329742	21.96100044	ID00431	91.15365601	24.71100044
ID00230	89.4033432	25.96100044	ID00432	91.15365601	24.46100044
ID00231	89.4033432	25.71100044	ID00433	91.15365601	24.21100044
ID00232	89.4033432	25.46100044	ID00434	91.15365601	23.96100044
ID00233	89.4033432	25.21100044	ID00435	91.15365601	23.71100044
ID00234	89.4033432	24.96100044	ID00436	91.15365601	23.46100044
ID00235	89.4033432	24.71100044	ID00437	91.15365601	23.21100044
ID00236	89.4033432	24.46100044	ID00438	91.15365601	22.96100044
ID00237	89.4033432	24.21100044	ID00439	91.15365601	22.71100044
ID00238	89.4033432	23.96100044	ID00441	91.15365601	22.21100044
ID00239	89.4033432	23.71100044	ID00458	91.40370178	24.96100044
ID00240	89.4033432	23.46100044	ID00459	91.40370178	24.71100044
ID00241	89.4033432	23.21100044	ID00460	91.40370178	24.46100044
ID00242	89.4033432	22.96100044	ID00461	91.40370178	24.21100044
ID00243	89.4033432	22.71100044	ID00465	91.40370178	23.21100044
ID00244	89.4033432	22.46100044	ID00466	91.40370178	22.96100044
ID00246	89.4033432	21.96100044	ID00486	91.65374756	24.96100044
ID00257	89.65338898	26.21100044	ID00487	91.65374756	24.71100044
ID00258	89.65338898	25.96100044	ID00488	91.65374756	24.46100044
ID00259	89.65338898	25.71100044	ID00494	91.65374756	22.96100044
ID00260	89.65338898	25.46100044	ID00495	91.65374756	22.71100044
ID00261	89.65338898	25.21100044	ID00514	91.90379333	24.96100044
ID00262	89.65338898	24.96100044	ID00515	91.90379333	24.71100044
ID00263	89.65338898	24.71100044	ID00516	91.90379333	24.46100044
ID00264	89.65338898	24.46100044	ID00517	91.90379333	24.21100044

ID00265	89.65338898	24.21100044	ID00521	91.90379333	23.21100044
ID00266	89.65338898	23.96100044	ID00522	91.90379333	22.96100044
ID00267	89.65338898	23.71100044	ID00523	91.90379333	22.71100044
ID00268	89.65338898	23.46100044	ID00524	91.90379333	22.46100044
ID00269	89.65338898	23.21100044	ID00525	91.90379333	22.21100044
ID00270	89.65338898	22.96100044	ID00526	91.90379333	21.96100044
ID00271	89.65338898	22.71100044	ID00527	91.90379333	21.71100044
ID00272	89.65338898	22.46100044	ID00542	92.15383911	24.96100044
ID00273	89.65338898	22.21100044	ID00543	92.15383911	24.71100044
ID00274	89.65338898	21.96100044	ID00544	92.15383911	24.46100044
ID00289	89.90343475	25.21100044	ID00547	92.15383911	23.71100044
ID00290	89.90343475	24.96100044	ID00548	92.15383911	23.46100044
ID00291	89.90343475	24.71100044	ID00549	92.15383911	23.21100044
ID00292	89.90343475	24.46100044	ID00550	92.15383911	22.96100044
ID00293	89.90343475	24.21100044	ID00551	92.15383911	22.71100044
ID00294	89.90343475	23.96100044	ID00552	92.15383911	22.46100044
ID00295	89.90343475	23.71100044	ID00553	92.15383911	22.21100044
ID00296	89.90343475	23.46100044	ID00554	92.15383911	21.96100044
ID00297	89.90343475	23.21100044	ID00555	92.15383911	21.71100044
ID00298	89.90343475	22.96100044	ID00556	92.15383911	21.46100044
ID00299	89.90343475	22.71100044	ID00557	92.15383911	21.21100044
ID00300	89.90343475	22.46100044	ID00570	92.40388489	24.96100044
ID00301	89.90343475	22.21100044	ID00579	92.40388489	22.71100044
ID00317	90.15348053	25.21100044	ID00580	92.40388489	22.46100044
ID00318	90.15348053	24.96100044	ID00581	92.40388489	22.21100044
ID00319	90.15348053	24.71100044	ID00582	92.40388489	21.96100044
ID00320	90.15348053	24.46100044	ID00583	92.40388489	21.71100044
ID00321	90.15348053	24.21100044	ID00584	92.40388489	21.46100044
ID00322	90.15348053	23.96100044			

Appendix C: Summary of the Research Gap

Table C1: Summary of Recent Studies on Temperature and Precipitation Extremes in South Asia Using CMIP Models

Author	Region	Variables	Analysis type	CMIP Model	GCMs or RCMs	ETCCDI
Akter et al., 2024	Bangladesh	Temperature	Future projection	CMIP6	13	8
Ali et al., 2019	Pakistan	Temperature and Precipitation	Future projection	CMIP5	14	6
Basher et al., 2018	Northeast Bangladesh	Precipitation	Trend analysis	-	-	8
Bhattarai et al., 2023	Western Nepal	Temperature and Precipitation	Future projection	CMIP6	5	16
Deegala et al., 2023	South Asia	Precipitation	Future projection	CMIP6	10	5
Gautam et al., 2024	North-East India	Temperature and Precipitation	Trend analysis	-	-	21
Haider et al., 2024	Bangladesh	Temperature and Precipitation	Trend analysis	-	-	21

Hasan et al., 2018	Bengal Delta	Temperature and Precipitation	Future projection	CMIP5	5	5
Imran et al., 2023	Bangladesh	Temperature and Precipitation	Trend analysis	-	-	29
Kamruzzaman et al., 2019	Bangladesh	Temperature and Precipitation	Future projection	CMIP5	29	6
Kamruzzaman et al., 2024	South Asia	Precipitation	Future projection	CMIP5, CMIP6	17	11
Khadgarai et al., 2021	Monsoon Asia	Precipitation	Trend analysis	-	-	7
Khan et al., 2020	Bangladesh	Temperature and Precipitation	Future projection	CMIP5	11	23
Lee et al., 2024	East Asia	Precipitation	Future projection	CMIP6	8	6
Mallick et al., 2022a	Bangladesh	Temperature	Trend analysis	-	-	10
Mallick et al., 2022b	Bangladesh	Temperature	Trend analysis	-	-	8
Mishu et al., 2025	Bangladesh	Precipitation	Future projection	CMIP6	13	8
Mondal et al., 2022	South Asia	Precipitation	Future projection	CMIP6	20	4

Nowreen et al., (2013)	Haor Basin, Bangladesh	Precipitation	Future projection	-	-	10
Paul et al., 2023	Northeast India and Bangladesh	Temperature and Precipitation	Future projection	CMIP6	14	20
Pervin et al., 2022	Chattogram, Bangladesh	Temperature and Precipitation	Trend analysis	CMIP5	3	22
Pradhan et al., 2021	Koshi River Basin, Nepal	Temperature and Precipitation	Performance evaluation	CMIP5	11	7
Talukder et al., 2025	South Asia	Precipitation	Future projection	CMIP6	19	4
Ying et al., 2020	China	Temperature	Future projection	CMIP5	12	7
Zhang et al., 2023	Full world	Temperature and Precipitation	Performance evaluation	CMIP6	19	27
Zhang et al., 2023	Southwestern China	Temperature	Future projection	CMIP6	26	1

Appendix D: Code

D1: Code for Simple Quantile Mapping (SQM) downscaling and ETCCDI indices calculation

```
prjdir <- "F:/2022_BGD_5km/seamless/SQM-BGD"
dbdir <- "F:/2022_BGD_5km/Database"
library(SQM)
#SQM::Install.Required.Packages()

##########################################################################
# 1. Edit user input part of SQMGrid.yaml and upload to EnvList
##########################################################################
EnvList <- SetWorkingEnvironment(envfile = file.path(prjdir, "SQM.yaml"))

##########################################################################
# 2. Preparing required data
##########################################################################
# 2.1 Boundary GIS(Shape) file should exist in [dbdir]
# 2.2 Clipped CMIP6 NetCDF files should exist in [dbdir]/cmip6_daily
# 2.3 Observed weather station files should exist in  [dbdir]/observed/User

##########################################################################
# 3. SQM Downscaling
##########################################################################
DailyExtractAll(EnvList)
Cmip6CombineHistroicalFuture(EnvList)
DailyQMapAll(EnvList)
CalStationClimateSummary (EnvList, DsNms="SQM", smon=1, emon=12)
CalStationClimateSummaryGraph (EnvList, dsnm="SQM")

##########################################################################
# 4. Calculate ETCCDI Climate Index
##########################################################################
CalClimateIndexAll (EnvList, smonth=1, emonth =12)
CalMmeClimateIndexScenarios(EnvList, smonth=1, emonth =12)
CalPchngClimateIndex(EnvList, smonth=1, emonth =12)
CalDifferenceClimateIndex(EnvList, smonth=1, emonth =12)
```

```
## Create GIS maps
CreateEtccdiIndexVectorMaps(EnvList, bondID = "ADM2_EN", smonth = 1, emonth =
12)
## Draw summary figures
PlotShapeClimateIndexReproSummary (EnvList, idxtype="ETCCDI")
PlotShapeClimateIndexFutureSummary (EnvList, scnnms=NULL, funms=NULL,
idxnms=NULL, idxtype="ETCCDI")
```

D2: Code for significance test and identify significant ID

```
library(data.table)
Sig_2015_2044 <- NULL
Sig_2044_2074 <- NULL
Sig_2075_2100 <- NULL
for(bio in 1:19) {
 ind <- sprintf("%02d", bio)
 setwd("E:/MSc_final/Paper/FBN_Paper_v1/Significance test/Individual/Individual")

 # Load historical data
 fl <- list.files(pattern = paste("_bio", ind, "_SY1985EY2014", sep = ""))
 dat <- NULL
 for(i in 1:length(fl)) {
  dt <- data.frame(fread(fl[i]))
  dat[[i]] <- dt[, 2:31]
 }
 his <- Reduce("+", dat) / length(dat)

 # Load future data (2015-2100)
 fl <- list.files(pattern = paste("_ssp126_bio", ind, "_SY2015EY2100", sep = ""))
 dat <- NULL
 for(i in 1:length(fl)) {
  dt <- data.frame(fread(fl[i]))
  dat[[i]] <- dt[, 2:87]  # Columns 2 to 87 represent future data
 }
 fut <- Reduce("+", dat) / length(dat)

 # Splitting the future data into the three periods
 fut_2015_2044 <- fut[, 1:30]  # First 30 columns represent 2015-2044
```

```r
  fut_2044_2074 <- fut[, 31:60]  # Next 30 columns represent 2044-2074
  fut_2075_2100 <- fut[, 61:86]  # Last columns represent 2075-2100

  # Perform Wilcoxon tests for each period
  options(scipen = 999)

  # p-values for 2015-2044
  pval_2015_2044 <- NULL
  for(i in 1:nrow(his)) {
    pval_2015_2044 <- c(pval_2015_2044, wilcox.test(as.numeric(his[i,]),
as.numeric(fut_2015_2044[i,]), paired = F)[3]$p.value)
  }
  Sig_2015_2044[[bio]] <- pval_2015_2044

  # p-values for 2044-2074
  pval_2044_2074 <- NULL
  for(i in 1:nrow(his)) {
    pval_2044_2074 <- c(pval_2044_2074, wilcox.test(as.numeric(his[i,]),
as.numeric(fut_2044_2074[i,]), paired = F)[3]$p.value)
  }
  Sig_2044_2074[[bio]] <- pval_2044_2074

  # p-values for 2075-2100
  pval_2075_2100 <- NULL
  for(i in 1:nrow(his)) {
    pval_2075_2100 <- c(pval_2075_2100, wilcox.test(as.numeric(his[i,]),
as.numeric(fut_2075_2100[i,]), paired = F)[3]$p.value)
  }
  Sig_2075_2100[[bio]] <- pval_2075_2100

  print(bio); flush.console()
}

# Combine p-values into matrices for each period
Pval_2015_2044 <- do.call(cbind, Sig_2015_2044)
Pval_2044_2074 <- do.call(cbind, Sig_2044_2074)
Pval_2075_2100 <- do.call(cbind, Sig_2075_2100)
```

```
cn <- paste("Bio", c(1:19), sep = "")
colnames(Pval_2015_2044) <- cn
colnames(Pval_2044_2074) <- cn
colnames(Pval_2075_2100) <- cn

# Convert matrices to data.tables
Pval_2015_2044_dt <- as.data.table(Pval_2015_2044)
Pval_2044_2074_dt <- as.data.table(Pval_2044_2074)
Pval_2075_2100_dt <- as.data.table(Pval_2075_2100)

# Define the output paths
output_path_2015_2044 <- "E:/MSc_final/FBN_Paper_v1/Significance
test/Individual/Pval_SSp126_2015_2044.csv"
output_path_2044_2074 <- "E:/MSc_final/FBN_Paper_v1/Significance
test/Individual/Pval_SSp126_2044_2074.csv"
output_path_2075_2100 <- "E:/MSc_final/FBN_Paper_v1/Significance
test/Individual/Pval_SSp126_2075_2100.csv"

# Save the outputs as CSV files
fwrite(Pval_2015_2044_dt, output_path_2015_2044)
fwrite(Pval_2044_2074_dt, output_path_2044_2074)
fwrite(Pval_2075_2100_dt, output_path_2075_2100)
##########################################################################
library(data.table)

Sig_2015_2044 <- NULL
Sig_2044_2074 <- NULL
Sig_2075_2100 <- NULL

for(bio in 1:19) {
  ind <- sprintf("%02d", bio)
  setwd("E:/MSc_final/FBN_Paper_v1/Significance test/Towhid
vai/Individual/Individual")

  # Load historical data
  fl <- list.files(pattern = paste("_bio", ind, "_SY1985EY2014", sep = ""))
  dat <- NULL
  for(i in 1:length(fl)) {
    dt <- data.frame(fread(fl[i]))
```

```
  dat[[i]] <- dt[, 2:31]
}
his <- Reduce("+", dat) / length(dat)

# Load future data (2015-2100)
fl <- list.files(pattern = paste("_ssp245_bio", ind, "_SY2015EY2100", sep = ""))
dat <- NULL
for(i in 1:length(fl)) {
  dt <- data.frame(fread(fl[i]))
  dat[[i]] <- dt[, 2:87]  # Columns 2 to 87 represent future data
}
fut <- Reduce("+", dat) / length(dat)

# Splitting the future data into the three periods
fut_2015_2044 <- fut[, 1:30]  # First 30 columns represent 2015-2044
fut_2044_2074 <- fut[, 31:60]  # Next 30 columns represent 2044-2074
fut_2075_2100 <- fut[, 61:86]  # Last columns represent 2075-2100

# Perform Wilcoxon tests for each period
options(scipen = 999)

# p-values for 2015-2044
pval_2015_2044 <- NULL
for(i in 1:nrow(his)) {
  pval_2015_2044 <- c(pval_2015_2044, wilcox.test(as.numeric(his[i,]),
as.numeric(fut_2015_2044[i,]), paired = F)[3]$p.value)
}
Sig_2015_2044[[bio]] <- pval_2015_2044

# p-values for 2044-2074
pval_2044_2074 <- NULL
for(i in 1:nrow(his)) {
  pval_2044_2074 <- c(pval_2044_2074, wilcox.test(as.numeric(his[i,]),
as.numeric(fut_2044_2074[i,]), paired = F)[3]$p.value)
}
Sig_2044_2074[[bio]] <- pval_2044_2074

# p-values for 2075-2100
```

```
  pval_2075_2100 <- NULL
  for(i in 1:nrow(his)) {
    pval_2075_2100 <- c(pval_2075_2100, wilcox.test(as.numeric(his[i,]),
as.numeric(fut_2075_2100[i,]), paired = F)[3]$p.value)
  }
  Sig_2075_2100[[bio]] <- pval_2075_2100

  print(bio); flush.console()
}

# Combine p-values into matrices for each period
Pval_2015_2044 <- do.call(cbind, Sig_2015_2044)
Pval_2044_2074 <- do.call(cbind, Sig_2044_2074)
Pval_2075_2100 <- do.call(cbind, Sig_2075_2100)

cn <- paste("Bio", c(1:19), sep = "")
colnames(Pval_2015_2044) <- cn
colnames(Pval_2044_2074) <- cn
colnames(Pval_2075_2100) <- cn

# Convert matrices to data.tables
Pval_2015_2044_dt <- as.data.table(Pval_2015_2044)
Pval_2044_2074_dt <- as.data.table(Pval_2044_2074)
Pval_2075_2100_dt <- as.data.table(Pval_2075_2100)

# Define the output paths
output_path_2015_2044 <- "E:/MSc_final/FBN_Paper_v1/Significance
test/Individual/Pval_SSp245_2015_2044.csv"
output_path_2044_2074 <- "E:/MSc_final/FBN_Paper_v1/Significance
test/Individual/Pval_SSp245_2044_2074.csv"
output_path_2075_2100 <- "E:/MSc_final/FBN_Paper_v1/Significance
test/Individual/Pval_SSp245_2075_2100.csv"

# Save the outputs as CSV files
fwrite(Pval_2015_2044_dt, output_path_2015_2044)
fwrite(Pval_2044_2074_dt, output_path_2044_2074)
fwrite(Pval_2075_2100_dt, output_path_2075_2100)
##############################################################################
library(data.table)
```

```
Sig_2015_2044 <- NULL
Sig_2044_2074 <- NULL
Sig_2075_2100 <- NULL

for(bio in 1:19) {
 ind <- sprintf("%02d", bio)
 setwd("E:/MSc_final/FBN_Paper_v1/Significance test/Individual/Individual")

 # Load historical data
 fl <- list.files(pattern = paste("_bio", ind, "_SY1985EY2014", sep = ""))
 dat <- NULL
 for(i in 1:length(fl)) {
  dt <- data.frame(fread(fl[i]))
  dat[[i]] <- dt[, 2:31]
 }
 his <- Reduce("+", dat) / length(dat)

 # Load future data (2015-2100)
 fl <- list.files(pattern = paste("_ssp370_bio", ind, "_SY2015EY2100", sep = ""))
 dat <- NULL
 for(i in 1:length(fl)) {
  dt <- data.frame(fread(fl[i]))
  dat[[i]] <- dt[, 2:87]  # Columns 2 to 87 represent future data
 }
 fut <- Reduce("+", dat) / length(dat)

 # Splitting the future data into the three periods
 fut_2015_2044 <- fut[, 1:30]  # First 30 columns represent 2015-2044
 fut_2044_2074 <- fut[, 31:60]  # Next 30 columns represent 2044-2074
 fut_2075_2100 <- fut[, 61:86]  # Last columns represent 2075-2100

 # Perform Wilcoxon tests for each period
 options(scipen = 999)

 # p-values for 2015-2044
 pval_2015_2044 <- NULL
```

```
  for(i in 1:nrow(his)) {
    pval_2015_2044 <- c(pval_2015_2044, wilcox.test(as.numeric(his[i,]),
as.numeric(fut_2015_2044[i,]), paired = F)[3]$p.value)
  }
  Sig_2015_2044[[bio]] <- pval_2015_2044

  # p-values for 2044-2074
  pval_2044_2074 <- NULL
  for(i in 1:nrow(his)) {
    pval_2044_2074 <- c(pval_2044_2074, wilcox.test(as.numeric(his[i,]),
as.numeric(fut_2044_2074[i,]), paired = F)[3]$p.value)
  }
  Sig_2044_2074[[bio]] <- pval_2044_2074

  # p-values for 2075-2100
  pval_2075_2100 <- NULL
  for(i in 1:nrow(his)) {
    pval_2075_2100 <- c(pval_2075_2100, wilcox.test(as.numeric(his[i,]),
as.numeric(fut_2075_2100[i,]), paired = F)[3]$p.value)
  }
  Sig_2075_2100[[bio]] <- pval_2075_2100

  print(bio); flush.console()
}

# Combine p-values into matrices for each period
Pval_2015_2044 <- do.call(cbind, Sig_2015_2044)
Pval_2044_2074 <- do.call(cbind, Sig_2044_2074)
Pval_2075_2100 <- do.call(cbind, Sig_2075_2100)

cn <- paste("Bio", c(1:19), sep = "")
colnames(Pval_2015_2044) <- cn
colnames(Pval_2044_2074) <- cn
colnames(Pval_2075_2100) <- cn

# Convert matrices to data.tables
Pval_2015_2044_dt <- as.data.table(Pval_2015_2044)
Pval_2044_2074_dt <- as.data.table(Pval_2044_2074)
```

```
Pval_2075_2100_dt <- as.data.table(Pval_2075_2100)

# Define the output paths
output_path_2015_2044 <- "E:/MSc_final/FBN_Paper_v1/Significance test/Individual/Pval_SSp370_2015_2044.csv"
output_path_2044_2074 <- "E:/MSc_final/FBN_Paper_v1/Significance test/Individual/Pval_SSp370_2044_2074.csv"
output_path_2075_2100 <- "E:/MSc_final/FBN_Paper_v1/Significance test/Individual/Pval_SSp370_2075_2100.csv"

# Save the outputs as CSV files
fwrite(Pval_2015_2044_dt, output_path_2015_2044)
fwrite(Pval_2044_2074_dt, output_path_2044_2074)
fwrite(Pval_2075_2100_dt, output_path_2075_2100)
################################################################################
library(data.table)

Sig_2015_2044 <- NULL
Sig_2044_2074 <- NULL
Sig_2075_2100 <- NULL

for(bio in 1:19) {
 ind <- sprintf("%02d", bio)
 setwd("E:/MSc_final/FBN_Paper_v1/Significance test/Individual/Individual")

 # Load historical data
 fl <- list.files(pattern = paste("_bio", ind, "_SY1985EY2014", sep = ""))
 dat <- NULL
 for(i in 1:length(fl)) {
  dt <- data.frame(fread(fl[i]))
  dat[[i]] <- dt[, 2:31]
 }
 his <- Reduce("+", dat) / length(dat)

 # Load future data (2015-2100)
 fl <- list.files(pattern = paste("_ssp585_bio", ind, "_SY2015EY2100", sep = ""))
 dat <- NULL
 for(i in 1:length(fl)) {
```

```
  dt <- data.frame(fread(fl[i]))
  dat[[i]] <- dt[, 2:87]  # Columns 2 to 87 represent future data
}
fut <- Reduce("+", dat) / length(dat)

# Splitting the future data into the three periods
fut_2015_2044 <- fut[, 1:30]  # First 30 columns represent 2015-2044
fut_2044_2074 <- fut[, 31:60]  # Next 30 columns represent 2044-2074
fut_2075_2100 <- fut[, 61:86]  # Last columns represent 2075-2100

# Perform Wilcoxon tests for each period
options(scipen = 999)

# p-values for 2015-2044
pval_2015_2044 <- NULL
for(i in 1:nrow(his)) {
  pval_2015_2044 <- c(pval_2015_2044, wilcox.test(as.numeric(his[i,]),
as.numeric(fut_2015_2044[i,]), paired = F)[3]$p.value)
}
Sig_2015_2044[[bio]] <- pval_2015_2044

# p-values for 2044-2074
pval_2044_2074 <- NULL
for(i in 1:nrow(his)) {
  pval_2044_2074 <- c(pval_2044_2074, wilcox.test(as.numeric(his[i,]),
as.numeric(fut_2044_2074[i,]), paired = F)[3]$p.value)
}
Sig_2044_2074[[bio]] <- pval_2044_2074

# p-values for 2075-2100
pval_2075_2100 <- NULL
for(i in 1:nrow(his)) {
  pval_2075_2100 <- c(pval_2075_2100, wilcox.test(as.numeric(his[i,]),
as.numeric(fut_2075_2100[i,]), paired = F)[3]$p.value)
}
Sig_2075_2100[[bio]] <- pval_2075_2100

print(bio); flush.console()
```

```
}

# Combine p-values into matrices for each period
Pval_2015_2044 <- do.call(cbind, Sig_2015_2044)
Pval_2044_2074 <- do.call(cbind, Sig_2044_2074)
Pval_2075_2100 <- do.call(cbind, Sig_2075_2100)

cn <- paste("Bio", c(1:19), sep = "")
colnames(Pval_2015_2044) <- cn
colnames(Pval_2044_2074) <- cn
colnames(Pval_2075_2100) <- cn

# Convert matrices to data.tables
Pval_2015_2044_dt <- as.data.table(Pval_2015_2044)
Pval_2044_2074_dt <- as.data.table(Pval_2044_2074)
Pval_2075_2100_dt <- as.data.table(Pval_2075_2100)

# Define the output paths
output_path_2015_2044 <- "E:/MSc_final/FBN_Paper_v1/Significance test/Individual/Pval_SSp585_2015_2044.csv"
output_path_2044_2074 <- "E:/MSc_final/FBN_Paper_v1/Significance test/Individual/Pval_SSp585_2044_2074.csv"
output_path_2075_2100 <- "E:/MSc_final/FBN_Paper_v1/Significance test/Individual/Pval_SSp585_2075_2100.csv"

# Save the outputs as CSV files
fwrite(Pval_2015_2044_dt, output_path_2015_2044)
fwrite(Pval_2044_2074_dt, output_path_2044_2074)
fwrite(Pval_2075_2100_dt, output_path_2075_2100)
```

Appendix E: Projected Changes in Different Scenarios

Table E1: Projected Changes in Temperature and Precipitation Extremes Across Three SSP Scenarios (SSP1-2.6, SSP2-4.5, SSP5-8.5) for Near, Mid, and Far Future Periods Compared to the Baseline (1985–2014).

Index	Unit	Remarks	SSP1-2.6			SSP2-4.5			SSP5-8.5		
			Near future	Mid future	Far Future	Near future	Mid future	Far Future	Near future	Mid future	Far Future
TXx	°C	Maximum	1.05	2.01	2.26	0.78	1.95	3.12	0.89	2.89	5.12
		Minumum	0.47	0.94	1.01	0.13	0.92	1.42	0.22	1.51	2.99
TNx	°C	Maximum	1.09	1.92	1.96	0.86	2.07	2.80	0.94	2.89	5.08
		Minumum	0.58	1.05	1.10	0.54	1.21	1.62	0.55	1.73	3.15
TXn	°C	Maximum	0.90	1.55	1.70	0.86	1.96	2.51	0.83	2.48	4.50
		Minumum	0.39	0.72	0.75	0.25	0.89	1.12	0.16	1.21	2.10
TNn	°C	Maximum	1.05	1.61	1.71	0.96	1.95	2.72	1.03	2.85	5.49
		Minumum	0.44	0.91	0.94	0.51	1.22	1.62	0.39	1.76	2.99
TN10p	%	Maximum	0.98	1.75	1.93	0.86	2.18	2.93	0.88	3.06	5.44
		Minumum	0.44	0.84	0.95	0.42	0.99	1.36	0.35	1.65	3.10
TX10p	%	Maximum	0.75	1.31	1.36	0.69	1.59	2.15	0.71	2.30	4.04
		Minumum	0.33	0.60	0.67	0.19	0.84	1.19	0.17	1.17	2.43
TN90p	%	Maximum	0.86	1.47	1.53	0.79	1.75	2.22	0.93	2.46	4.01
		Minumum	0.45	0.75	0.76	0.45	1.04	1.43	0.51	1.51	2.87

TX90p	%	Maximum	1.10	1.83	1.96	0.59	1.81	2.92	0.95	2.64	5.13
		Minumum	0.28	0.56	0.59	0.10	0.74	1.07	0.15	1.09	2.29
SU	d	Maximum	18.70	34.04	34.47	14.70	39.13	52.93	15.24	53.83	84.00
		Minumum	6.74	13.85	15.11	3.56	15.36	19.29	2.80	18.87	24.83
TR	d	Maximum	14.34	26.39	27.42	13.44	32.16	42.56	14.32	44.40	76.57
		Minumum	5.60	12.97	13.60	6.53	17.64	22.87	5.81	23.42	28.22
DTR	°C	Maximum	0.21	0.18	0.18	-0.02	0.01	0.04	0.17	0.02	-0.12
		Minumum	-0.27	-0.34	-0.32	-0.38	-0.55	-0.63	-0.41	-0.71	-1.23
WSDI	d	Maximum	2.60	3.81	4.04	1.12	3.01	4.71	1.43	3.89	6.72
		Minumum	-0.15	-0.11	-0.13	-1.01	-1.41	-1.32	-1.03	-1.67	-2.22
CSDI	d	Maximum	1.52	2.35	1.78	1.29	2.38	3.34	2.23	3.06	4.34
		Minumum	0.10	-0.03	-0.20	0.05	0.04	0.66	0.18	-0.50	0.16